THE ROLE OF THE ATR-CHEK1 PATHWAY IN THERAPEUTIC RESISTANCE RESULTING FROM DISTAL 11Q LOSS IN CARCINOMA CELLS

by

Madhav Sankunny

B.Sc., SBM Jain College, Bangalore University, India, 2004

M.Sc., University of Madras, India, 2006

Submitted to the Graduate Faculty of

the Graduate School of Public Health in partial fulfillment

of the requirements for the degree of

Doctor of Philosophy

University of Pittsburgh

2013

UNIVERSITY OF PITTSBURGH

Graduate School of Public Health

This dissertation was presented

by

Madhav Sankunny

It was defended on

April 15, 2013

and approved by

Robert E. Ferrell, Ph.D.
Professor, Department of Human Genetics
Graduate School of Public Health
University of Pittsburgh

Zsolt Urban, Ph.D.
Professor, Department of Human Genetics
Graduate School of Public Health
University of Pittsburgh

Robert Nicholls, Ph.D.
Professor, Department of Paediatrics
School of Medicine
University of Pittsburgh

Dissertation Advisor
Susanne M. Gollin, Ph.D.
Professor, Department of Human Genetics
Graduate School of Public Health
University of Pittsburgh

Susanne M. Gollin, Ph.D.

THE ROLE OF THE ATR-CHEK1 PATHWAY IN THERAPEUTIC RESISTANCE RESULTING FROM DISTAL 11Q LOSS IN CARCINOMA CELLS

Madhav Sankunny, Ph.D.

University of Pittsburgh, 2013

One of the biggest public health problems worldwide is death from cancer as a result of tumor resistance to therapy. Our lab has determined that one form of therapeutic resistance results from distal 11q loss, a common chromosomal alteration in carcinomas. We observed loss of distal 11q with concomitant loss of critical DNA damage response (DDR) genes, including *ATM*, *MRE11A*, *H2AFX* and *CHEK1* in head and neck squamous cell carcinoma (HNSCC), non-small cell lung carcinoma (NSCLC) and ovarian carcinoma. Further, we showed that carcinoma cell lines with distal 11q loss have a diminished DNA damage response, decreased sensitivity to DNA damaging agents like ionizing radiation (IR), and decreased expression of genes on distal 11q. We hypothesized that the radioresistance observed in cells with distal 11q loss was due to upregulation of the compensatory ATR-CHEK1 pathway followed by G_2M arrest that halted the cells long enough to repair their DNA and progress through mitosis. Analysis of cells with distal 11q loss revealed an upregulated ATR-CHEK1 pathway and G_2M arrest. Knockdown of the ATR-CHEK1 pathway by siRNA or a targeted CHEK1 small molecule inhibitor (SMI) substantially decreased colony formation in response to IR exclusively in carcinoma cell lines with distal 11q loss. We also hypothesized that since gemcitabine-induced DNA damage leads to the activation of the ATR/CHEK1 pathway and S-phase arrest, that carcinoma cells with distal 11q loss would show decreased sensitivity to gemcitabine. We observed that biomarker-positive HNSCC and NSCLC cell lines also show ATR-CHEK1 upregulation and decreased sensitivity to

gemcitabine. Further, we observed that siRNA knockdown of the ATR-CHEK1 pathway and SMI inhibition of CHEK1 signaling in HNSCC and NSCLC cell lines increase their sensitivity to gemcitabine treatment. These results provide support for combining targeted therapies to the ATR-CHEK1 pathway with standard therapies in conjunction with an appropriate companion diagnostic biomarker, like distal 11q loss.

PUBLIC HEALTH SIGNIFICANCE: Our findings led to the development of a biomarker for loss of sensitivity to IR that may be useful as a prognostic marker that could be added to predictive personalized cancer genomic assays and used as a companion diagnostic for CHEK1 SMIs.

TABLE OF CONTENTS

ACKNOWLEDGMENTS ..... **XV**

PUBLIC HEALTH SIGNIFICANCE ..... **XVI**

1.0 INTRODUCTION **1**

1.1 OVERVIEW **1**

1.2 EPIDEMIOLOGY OF HNSCC, NSCLC AND OVARIAN CARCINOMAS **2**

1.3 CHARACTERISTICS OF CARCINOMAS **3**

1.3.1 Chromosomal Instability **3**

1.3.2 11q13 Amplification **4**

1.3.3 Distal 11q Loss **6**

1.4 DNA DAMAGE RESPONSE (DDR) PATHWAYS **9**

1.4.1 DDR Pathway Overview **9**

1.4.2 Double Strand Break (DSB) Response and Repair (ATM pathway) **12**

1.4.3 ATR-CHEK1 Pathway **15**

1.4.4 Cell Cycle Checkpoints in Cancer **18**

1.4.5 Gemcitabine-induced DNA Damage and Response **19**

1.5 CHEK1 INHIBITION AS A TARGETED CANCER THERAPY **22**

1.5.1 Targeted Cancer Therapy **22**

1.5.2 Synthetic Lethality **23**

1.5.3 CHEK1 Inhibition 24

2.0 MATERIAL AND METHODS 27

2.1 CELL CULTURE 27

2.1.1 HNSCC and Control Cell Lines 27

2.1.2 NSCLC Cell Lines 27

2.1.3 Ovarian Carcinoma (OvC) Cell Lines 28

2.2 FLUORESCENCE *IN SITU* HYBRIDIZATION (FISH) 28

2.3 CLONOGENIC SURVIVAL ASSAY 30

2.4 ASSESSMENT OF MITOTIC DEFECTS 31

2.5 QUANTITATIVE REAL TIME PCR (QRT-PCR) 31

2.6 IMMUNOBLOTTING 33

2.7 DENSITOMETRIC ANALYSIS OF PROTEIN BANDS 34

2.8 CELL CYCLE ANALYSIS BY FLOW CYTOMETRY 34

2.9 *CHEK1* KNOCKDOWN BY RNA INTERFERENCE 35

2.10 CHEK1 KNOCKDOWN BY SMALL MOLECULE INHIBITOR 36

3.0 RESULTS 37

3.1 LOSS OF DISTAL 11Q AND ITS CONSEQUENCES 37

3.1.1 Copy Number Loss in Genes within Distal 11q 37

3.1.2 Loss of Distal 11q is Associated with Reduced Sensitivity to IR 41

3.1.3 Loss of Distal 11q Results in Changes in Expression of *ATM* and *CHEK1* 45

3.1.4 Loss of Distal 11q is Associated with Increased Mitotic Defects in HNSCC but not NSCLC 48

3.2 UPREGULATED ATR-CHEK1 PATHWAY 50

3.2.1 The ATR-CHEK1 Pathway is Upregulated in HNSCC Cell Lines With Loss of Distal 11q 50

3.2.2 Increased ATR-dependent Phosphorylation of CHEK1 in Tumor Cells With Loss of Distal 11q..... 51

3.2.3 Increased Phosphorylation of CDC25C Due to an Upregulated ATR-CHEK1 Pathway 53

3.2.4 Distal 11q Loss is Associated with Increased S and G_2M checkpoint arrest after IR in HNSCC Cells, but not in NSCLC Cells..... 55

3.3 INHIBITION OF THE ATR-CHEK1 PATHWAY RESENSITIZES TUMOR CELLS WITH LOSS OF DISTAL 11Q TO IR..... 57

3.3.1 Knocking Down the ATR-CHEK1 Pathway Resensitizes Tumor Cells to DNA Damage Induced by IR 57

3.3.2 A CHEK1 SMI Resensitizes HNSCC Cells to DNA Damage Induced by IR 66

3.4 LOSS OF DISTAL 11Q AND GEMCITABINE RESISTANCE..... 71

3.4.1 Distal 11q Loss is Associated with Reduced Sensitivity to Gemcitabine .. 71

3.4.2 The ATR-CHEK1 Pathway is Upregulated in HNSCC and NSCLC Cell Lines.....74

3.4.3 Knockdown of the ATR-CHEK1 Pathway with siRNA/SMI Resensitizes Cells with Distal 11q Loss to Damage Induced by Gemcitabine 77

4.0 DISCUSSION 86

4.1 LOSS OF DISTAL 11Q IN CARCINOMA CELLS..... 86

4.2 UPREGULATION OF THE ATR-CHEK1 PATHWAY 90

4.3 DNA DSB REPAIR MECHANISMS 93

4.4 CHEK1 INHIBITION 96

4.5 LOSS OF DISTAL 11Q AND RESISTANCE TO GEMCITABINE 99

4.6 CONCLUSIONS 101

APPENDIX A : LIST OF BACTERIAL ARTIFICIAL CHROMOSOMES (BAC)..... 102

APPENDIX B : SEQUENCES FOR ATR AND CHEK1 SIRNA..... 103

APPENDIX C: LIST OF ANTIBODIES USED FOR IMMUNOBLOTTING..... 104

BIBLIOGRAPHY 105

LIST OF TABLES

Table 1. RT–PCR reagents..... 32

Table 2. Summary of interphase FISH for relative copy number loss[1] of *MRE11A*, *ATM*, *H2AFX* and *CHEK1* genes in HNSCC cell lines..... 38

Table 3. Summary of the interphase FISH for relative copy number loss[1] of *MRE11A*, *ATM*, *H2AFX* and *CHEK1* genes in NSCLC cell lines 39

Table 4. Summary of the interphase FISH for relative copy number loss[1] of MRE11A and ATM genes in OvC cell lines..... 40

Table 5. Relative expression of *ATM* and *CHEK1* in NSCLC cell lines..... 46

Table 6. Cell cycle analysis in NSCLC cells in response to IR..... 56

Table 7. Cell cycle analysis in OvC cells in response to IR 56

Table 8. p53 signaling status of HNSCC cell lines as determined by analyzing p53 and p21 expression after treatment with Adriamycin 67

LIST OF FIGURES

Figure 1. BFB mechanism resulting in distal 11q loss and 11q13 amplification (adapted from Reshmi *et al.* 2007) **6**

Figure 2. Ideogram of chromosome 11 with the locations of four DDR genes in relation to FRA11F site **7**

Figure 3. Schematic representation of the DNA damage and response pathway **10**

Figure 4. Schematic representation of DDR signal transduction pathway **11**

Figure 5. Schematic representation of the DSB response by the ATM-CHEK2 pathway ... **15**

Figure 6. FISH for *ATM* in HNSCC and NSCLC cell lines **40**

Figure 7. FISH for *CHEK1* in HNSCC and NSCLC cell lines **41**

Figure 8. Clonogenic survival assay of HNSCC cell lines in response to IR **42**

Figure 9. Clonogenic survival assay of NSCLC cell lines in response to IR **43**

Figure 10. Clonogenic survival assay of OvC cell lines in response to IR **44**

Figure 11. Clonogenic survival assay of NSCLC cell lines in response to 2 Gy treatment of IR five days per week for two weeks **45**

Figure 12. Relative expression of *ATM* and *CHEK1* in NSCLC cell lines **46**

Figure 13. Protein expression of CHEK1 and densitometric analysis of expression in HNSCC cell lines **47**

Figure 14. Frequency of mitotic defects in treated and untreated HNSCC cell lines..... 49

Figure 15. Frequency of mitotic defects in treated and untreated NSCLC cell lines 49

Figure 16. Total CHEK1 expression in response to IR in HNSCC cells..... 50

Figure 17. CHEK1 phosphorylation at ser345 in response to IR in HNSCC and NSCLC cells 52

Figure 18. CHEK1 phosphorylation at ser317 in response to IR in HNSCC cells 53

Figure 19. Densitometric analysis of CHEK1 phosphorylation at ser317 in response to IR in NSCLC cells..... 53

Figure 20. CDC25C phosphorylation at ser216 in response to IR in NSCLC cells 54

Figure 21. CHEK1 expression after siRNA-based knockdown in tumor cells..... 58

Figure 22. Clonogenic survival assay in response to IR after siRNA-based *CHEK1* knockdown in HNSCC cells 59

Figure 23. Clonogenic survival assay in response to IR after siRNA-based *ATR* knockdown in HNSCC cells with loss of distal 11q 60

Figure 24. Clonogenic survival assay in response to IR after siRNA-based *RAD9A* knockdown in HNSCC cells 61

Figure 25. Clonogenic survival assay in response to IR after siRNA-based *CHEK1* knockdown in NSCLC cells..... 62

Figure 26. Clonogenic survival assay in response to IR after siRNA-based *ATR* knockdown in NSCLC cells 63

Figure 27. Clonogenic survival assay in response to IR after siRNA-based RAD9A knockdwon in NSCLC cells..... 64

Figure 28. Clonogenic survival assay in response to IR after siRNA-based CHEK1 knockdown in OvC cells 65

Figure 29. Clonogenic survival assay determining appropriate timepoint for addition of SMI in relation to IR..... 68

Figure 30. Clonogenic survival assay in response to IR after SMI-based CHEK1 knockdown in HNSCC cells 69

Figure 31. Dose response curve to gemcitabine in NSCLC cells 71

Figure 32. Clonogenic survival assay of HNSCC cell lines in response to gemcitabine treatment..... 73

Figure 33. Clonogenic survival assay of NSCLC cell lines in response to gemcitabine treatment..... 73

Figure 34. Clonogenic survival assay of OvC cell lines in response to gemcitabine treatment 74

Figure 35. Total CHEK1 expression in response to gemcitabine in UPCI HNSCC cells..... 75

Figure 36. Total CHEK1 expression in response to gemcitabine in NSCLC cells..... 75

Figure 37. CHEK1 phosphorylation at ser345 and ser317 in response to gemcitabine in HNSCC cells 76

Figure 38. CHEK1 phosphorylation at ser345 and ser317 in response to gemcitabine in NSCLC cells..... 77

Figure 39. Clonogenic survival assay in response to gemcitabine after siRNA-based *CHEK1* knockdown in HNSCC cells with loss of distal 11q 79

Figure 40. Clonogenic survival assay in response to gemcitabine after siRNA-based *CHEK1* knockdown in NSCLC cells with loss of distal 11q..... 79

Figure 41. Clonogenic survival assay in response to gemcitabine after siRNA-based *CHEK1* knockdown in NSCLC cells without loss of distal 11q 80

Figure 42. Clonogenic survival assay in response to gemcitabine after siRNA-based *ATR* knockdown in HNSCC cells with loss of distal 11q 81

Figure 43. Clonogenic survival assay in response to gemcitabine after siRNA-based *ATR* knockdown in NSCLC cells with loss of distal 11q 82

Figure 44. Clonogenic survival assay in response to gemcitabine after siRNA-based *ATR* knockdown in NSCLC cells without loss of distal 11q 83

Figure 45. Clonogenic survival assay in response to gemcitabine after SMI-based CHEK1 knockdown in HNSCC cells 84

Figure 46. Clonogenic survival assay in response to gemcitabine after SMI-based CHEK1 knockdown in OvC cells 85

Figure 47. Model for resensitization of tumor cells to DNA damaging agents (adapted from Parikh et al. 2007) 98

ACKNOWLEDGMENTS

I am extremely grateful to my advisor, Dr. Susanne M. Gollin, for providing me the opportunity to work in her laboratory and for instilling in me the qualities of a good researcher and mentor. She has provided me constant support, encouragement and guidance through my time here. I thank her for her patience with me and for keeping me focused on my project. Her interest in my education, research and personal well-being has been encouraging. I am fortunate indeed to have done my dissertation work under her patient, yet strict guidance.

I thank the members of my thesis committee Dr. Robert Ferrell, Dr. Zsolt Urban and Dr. Robert Nicholls for their guidance and having time for me in spite of their busy schedules. I greatly appreciate the suggestions and help I received from Dr. William Saunders, Dr. Xin Huang and Dr. Rahul A. Parikh throughout my time here.

I would like to thank Mr. Dale Lewis, Ms. Jianhua Zhou and Dr. Brian Henson for their help and support with my project. I had a great experience, both at an educational and at a personal level working with different members of the Gollin laboratory. I would like to thank the past and present members of the Gollin laboratory for making my experience extremely rewarding.

I thank my parents and especially my fiancée, Kristine-Ann Buela, who were there when I needed them the most and for providing me constant support and encouragement.

PUBLIC HEALTH SIGNIFICANCE

Cancer remains the second leading cause of death in the United States of America, even in the wake of advances in diagnosis and treatment of this disease. Cancer incidence is also on the rise due to improvements in health care resulting in increased longevity. Tumor formation and progression involve a stepwise accumulation of genetic defects over a period of time, and these defects can be used as molecular biomarkers to differentiate tumor cells from normal cells. Our studies show that a novel biomarker, the loss of distal chromosome 11q is associated with decreased sensitivity to radiation therapy and gemcitabine, a cancer chemotherapeutic drug. This new biomarker may be useful in predicting response to conventional cancer therapy. Resistance to conventional therapy is a major cause of mortality in cancer patients. Our findings of an upregulated ATR-CHEK1 pathway in tumor cells with loss of distal 11q resulting in radioresistance and chemoresistance could explain one mechanism behind the failure of conventional therapy in some patients. Biomarkers can also be used as companion diagnostics to select the right therapy for the right patient. In this case, a patient with distal 11q loss in his or her tumor may respond best to a combination of conventional radiation therapy and ATR-CHEK1 pathway small molecule inhibitor therapy. Supplementing conventional therapy with a targeted small molecule inhibitor could improve survival, shorten treatment time, and substantially decrease the cost of care in a personalized genomic medicine strategy.

1.0 INTRODUCTION

1.1 OVERVIEW

Cancer is a critical public health problem accounting for one in four deaths in the U.S. and more worldwide in spite of advances in diagnosis and treatment (Heron, et al. 2009; Siegel, et al. 2013). Cancer consists of different conditions, with the predominant characteristic being one of uncontrolled and unregulated growth of cells in normal tissues with a tendency to spread to distant sites. Carcinomas are the most common form of cancer and arise from the epithelial lining of the body. These tissues tend to acquire a number of genetic insults over time helping the cancer evolve. Accumulation of genetic and epigenetic changes that range from large scale chromosomal rearrangements resulting in loss of tumor suppressor genes and gains or amplification of oncogenes, to point mutations that lead to altered gene function and/or regulation results in tumor formation and progression (Ha and Califano 2002). A large percentage of cancers are characterized by defects in DNA damage sensing and repair that makes them dependent on backup DNA repair pathways for survival. In some cases, these backup pathways give the cells a growth advantage in the presence of DNA damaging agents used as anti-cancer therapies. Conventional radiation and chemotherapeutic strategies prove to be ineffective in killing these cancer cells. Hence, novel inhibitors of these backup pathways capable of rendering cancer cells vulnerable to a combination of conventional and pathway

inhibitor therapy are being developed. Further, biomarkers that can be used to screen for cancers with specific characteristics that are indicative of reduced sensitivity to conventional treatment also need to be developed. In this study, we have characterized a biomarker, and identified the backup pathway helping some cancer cells survive conventional radiation therapy and chemotherapy in carcinomas of head and neck, lung, and ovaries.

1.2 EPIDEMIOLOGY OF HNSCC, NSCLC AND OVARIAN CARCINOMAS

Head and neck squamous cell carcinoma (HNSCC, including the oral cavity, larynx, and pharynx) is the eighth most common cancer in the U.S., accounting for an estimated 53,640 new cases (3.2%) in 2013 and 11,520 deaths (2%) (Siegel, et al. 2013). Worldwide, HNSCC (worldwide statistics include lip, oral cavity, larynx, and pharynx) was diagnosed in 550,319 new patients (4.4%) in 2008 and resulted in 305,096 deaths (4.0%) (Ferlay, et al. 2010; Jemal, et al. 2011; Bray, et al. 2013). If identified early, the prognosis of HNSCC is excellent. Over the past four decades, the 5-year relative survival rates have improved substantially for oropharyngeal SCC in both Caucasians (from 54 to 67%) and in African-Americans (from 36 to 45%). Of concern, these relative survival rates remain 22% lower in African Americans compared to Caucasians, possibly as a result of late diagnosis (Siegel, et al. 2012). Lung carcinomas are the third most common form of cancer in the U.S. and the most common cancer elsewhere in the world. Worldwide, lung carcinomas were diagnosed in 1,608,800 (12.7%) new patients and resulted in 1,378,400 (18.2%) deaths (Ferlay, et al. 2010; Jemal, et al. 2011; Bray, et al. 2013). The estimated number of new cases of lung carcinomas in the U.S. for 2013 is 228,190 (13.7%) and an estimated 159,480 (27.5%) deaths (Siegel, et al. 2013). Non-small cell lung carcinomas

(NSCLC) constitute 70-80% of all lung cancer. The relative 5-year survival rate for NSCLCs is roughly 15%. Ovarian cancers account for 22,240 (1.3%) new cases and 14,030 (2.4%) deaths in the U.S., and 225,000 (1.8%) new cases and 140,200 (1.8%) deaths worldwide (Ferlay, et al. 2010; Jemal, et al. 2011; Bray, et al. 2013; Siegel, et al. 2013). According to the American Society of Cancer, the mortality rate for ovarian cancer has not shown any marked improvement in the last forty years. The relative 5-year survival rate is approximately 44%. Even though lung and ovarian cancers do not show improvement in the overall 5-year survival rate, early diagnosis of these types of cancers markedly improves the survival rate. Therefore, there is a need to develop new biomarkers for early diagnosis and selection of the most effective therapeutic strategy for treatment.

1.3 CHARACTERISTICS OF CARCINOMAS

1.3.1 Chromosomal Instability

Chromosomal instability can be defined as gain and/or loss of entire or segments of chromosomes at a higher rate in a specific population of cells. Carcinomas, the most common form of cancer, are frequently characterized by chromosomal instability, resulting in loss of tumor suppressor genes and gain or amplification of oncogenes (Ha and Califano 2002). Carcinomas tend to have near-triploid or tetraploid chromosomal constitution composed of structural and numerical chromosomal abnormalities (Gollin 2001; Jin, et al. 2002). Structural abnormalities may result in further alteration of gene expression that can lead to chromosomal instability (Gollin 2005). Genetic alterations result in the inhibition of normal cellular function

leading to dysregulation of cell cycle, tipping the balance in favor of cell proliferation over cell death, and preventing the cells from responding properly to and repairing DNA damage (Cavenee and White 1995; Weinberg 1996; Lundberg and Weinberg 1999; Hanahan and Weinberg 2000; Gollin 2005; Shiloh 2006). As a result, tumor cells exhibit characteristics known as the 'hallmarks of cancer,' ranging from defects in cell growth and proliferation, evasion of apoptosis, genomic instability, sustained angiogenesis, invasion and metastasis (Hanahan and Weinberg 2000; Hanahan and Weinberg 2011). These characteristics help drive cancer growth and progression. Through its progression, the cancer genotype constantly evolves into one that is optimized for proliferation, spread and invasion into surrounding tissues. Thus, over a period of time, genetic alterations that confer a growth advantage are selected (Albertson, et al. 2003). Common genetic factors including chromosomal breakage and fusion of sister chromatids, gene amplifications, presence of fragile sites and DNA repair defects that are manifestations of chromosomal instability also help propagate it (Gollin 2001).

1.3.2 11q13 Amplification

Gene amplification, the increase in copy number of a localized region on a chromosome arm, is a common genetic defect in human tumors (Albertson 2006). Amplification and subsequent overexpression of critical genes have been shown to lead to dysregulation of the cell cycle, resulting in cellular proliferation and tumor formation and/or progression (Lundberg and Weinberg 1999). Chromosomal band 11q13, which harbors the locus for a key cell cycle regulatory gene, cyclin D1 (*CCND1*) and other neighboring genes, is one of the most frequently amplified segments in HNSCC, NSCLC and ovarian carcinomas (Akervall, et al. 1997; Shuster, et al. 2000; Gollin 2001; Huang, et al. 2002; Jin, et al. 2006; Gautschi, et al. 2007; Brown, et al.

2008). 11q13 amplification in the form of a homogenously staining region (hsr) is present in ~45% of HNSCC (Gollin 2001), ~30% of NSCLC (Gautschi, et al. 2007) and ~20% of other carcinomas including, breast, bladder, pancreatic, ovarian and esophageal cancers (Schraml, et al. 1999). Approximately 12 genes in the amplicon core are amplified, including *CCND1*, *EMS1* which encodes human cortactin, an actin binding protein possibly involved in the organization of the cytoskeleton and cell adhesion structures, *ORAOV1* which regulates cell growth by controlling apoptosis and cell cycle, *ANO1* which encodes a calcium dependent chloride channel, *FADD*, the FAS-associating protein with death domain gene, and *FGF3* and *FGF4* (fibroblast growth factors 3 and 4, also called *INT2* and *HSTF1*). *CCND1* was considered as the 'driver' (a gene whose overexpression due to amplification confers an growth advantage to the cancer cells) of the amplicon, but recent studies have shown that amplification of other genes could also provide an advantage to cancer cells (Huang, et al. 2002; Hsu, et al. 2006; Wilkerson and Reis-Filho 2013). The 11q13 amplicon consists of four distinct cores, each with a possible 'driver,' that can independently amplify (Wilkerson and Reis-Filho 2013).

11q13 amplification is reported to occur early in the pathogenesis of HNSCC and NSCLC (Izzo, et al. 1998; Gautschi, et al. 2007). Meta-analysis of molecular genetic studies of HNSCC in literature shows the presence of 11q13 amplification in 61% of carcinomas *in situ*, providing further evidence to support the early initiation of 11q13 amplification in HNSCC pathogenesis (Gollin 2001). 11q13 amplification is an independent prognostic factor that correlates with higher stage disease, lymph node involvement, shorter time to recurrence, and reduced overall survival (Akervall, et al. 1997; Fracchiolla, et al. 1997; Michalides, et al. 1997; Miyamoto, et al. 2003). Also, cyclin D1 overexpression is thought to alter sensitivity to ionizing radiation in breast and larynx cancer (Coco Martin, et al. 1999; Yoo, et al. 2000). 11q13

amplification in OSCC occurs by the breakage–fusion–bridge (BFB) mechanism and the first step in this process is the loss of a portion of the distal part of chromosome 11q, termed as 'distal 11q loss' (Reshmi, et al. 2007).

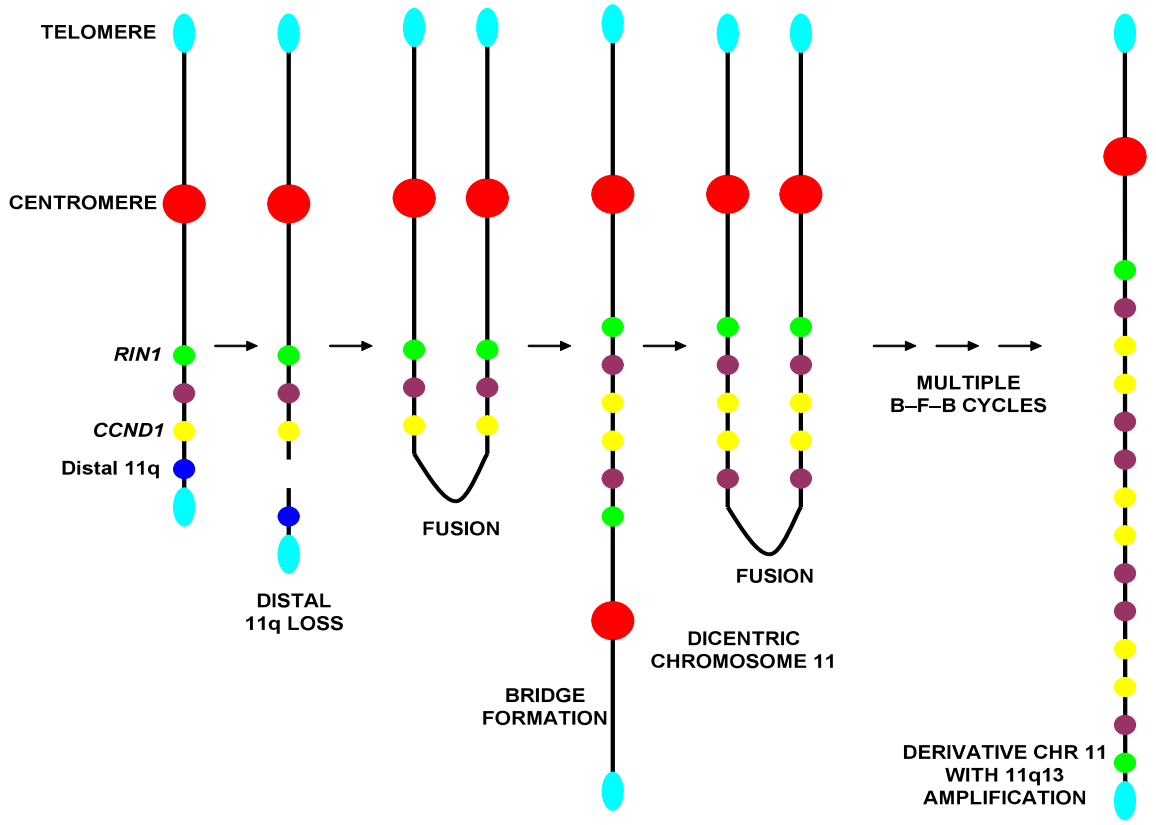

Figure 1. BFB cycle mechanism resulting in distal 11q loss and 11q13 amplification (adapted from Reshmi *et al.* 2007)

1.3.3 Distal 11q Loss

11q13 amplification results from breakage-fusion-bridge (BFB) cycles (Reshmi, et al. 2007) and/or chromosome breakage and rearrangement resulting from palindromic segmental duplications flanking 11q13 (Gibcus, et al. 2007). The first step in the BFB cycle is a chromosome break distal to the amplified region, possibly at the *FRA11F* chromosomal fragile site or as a result of rearrangement involving segmental duplications, resulting in loss of some or all of the distal segment of chromosome 11q (Shuster, et al. 2000; Reshmi, et al. 2007). Loss of

distal 11q and amplification of chromosomal band 11q13 have been suggested to contribute to the aggressiveness of HNSCC (Jin, et al. 1998; Jin, et al. 2006). Numerous investigators have identified copy number loss of distal 11q, from 11q14→11qter, centered primarily on 11q22→q23 (George, et al. 2007; Ambatipudi, et al. 2011; Swarts, et al. 2011; Edelmann, et al. 2012). The presence of distal 11q loss in primary HNSCC, lung, ovarian, and breast tumors was documented in our lab (Parikh, et al. 2007). Distal 11q contains four critical DNA damage response (DDR) genes, including *ATM* (11q22.3), *MRE11A* (11q21), *H2AFX* (11q23.3) and *CHEK1* (11q24.2). The cornerstone of the DDR to ionizing radiation (IR) is the *ATM* gene. We have shown that copy number loss of distal 11q, marked by the *ATM* gene, is associated with reduced sensitivity (resistance) to IR in HNSCC cell lines (Parikh, et al. 2007).

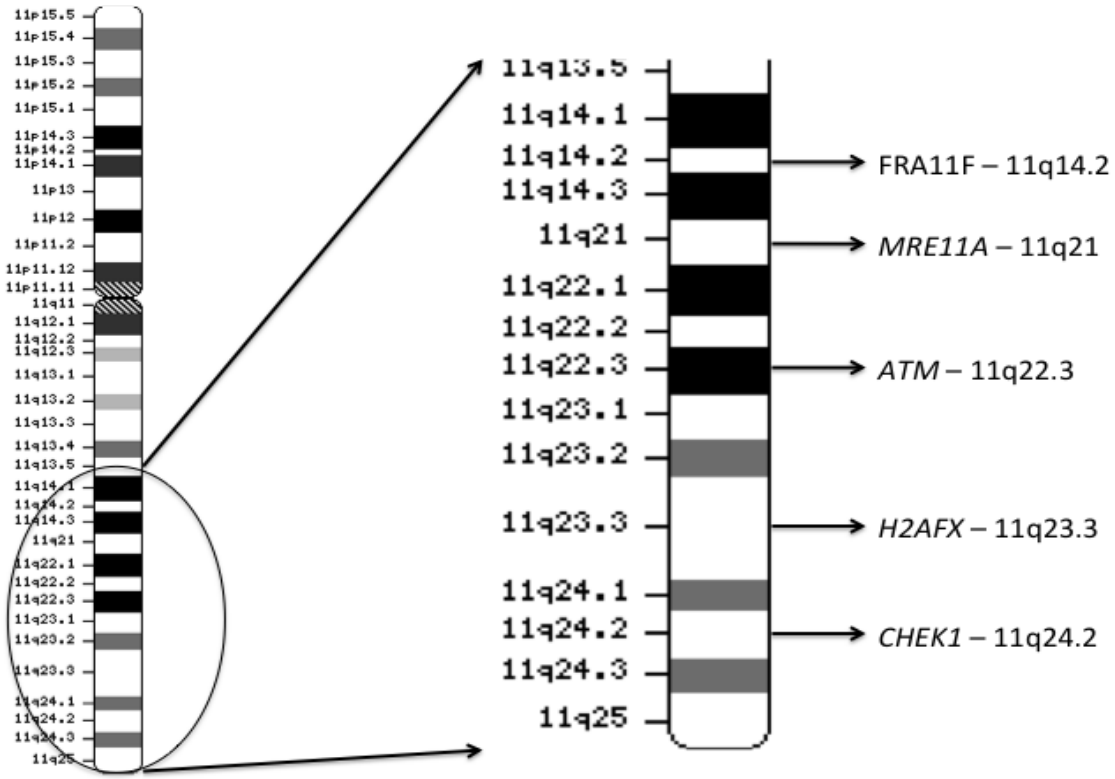

Figure 2. Ideogram of chromosome 11 with the locations of four DDR genes in relation to FRA11F site

In silico copy number analysis of the *ATM* gene on 11q shows that distal 11q loss is present in 21-25% of tumors. According to the Broad Institute *Tumorscape* website, "*ATM* is significantly focally deleted across the entire dataset of 3131 tumors and is located within a focal peak region of deletion containing 60 additional genes. ATM is significantly focally deleted in four of 14 independent subtypes analyzed in our dataset," including 20% of all cancers, ~ 45% of melanomas, breast cancers, and esophageal squamous carcinomas, 35-36% of head and neck, and prostate tumors, 28-29% of lung and ovarian tumors, and ~24% of medulloblastomas (Beroukhim, et al. 2010). Significant focal *ATM* loss at slightly different frequencies is also reported on the Broad Institute TCGA website (Mermel, et al. 2011) which indicates that "*ATM* is significantly focally deleted across the entire dataset of 6327 tumors and is located within a focal peak region of deletion containing 84 additional genes. ATM is significantly focally deleted in 10 of 20 independent cancer types analyzed in our dataset" including 25% of all cancers, ~55% of cervical squamous cell carcinomas and cutaneous melanomas, ~48% of invasive breast adenocarcinomas and HNSCC, 36% of bladder urothelial carcinomas, 32% of lung squamous cell carcinomas, 30% of ovarian serous cystadenocarcinomas, and between 18 and 28% of lung, stomach and rectal adenocarcinomas, colorectal cancers (Beroukhim, et al. 2010), and hepatocellular carcinomas. Thus, based on the American Cancer Society statistics (Siegel, et al. 2013) and the *Tumorscape* frequencies, at least 330,000 of the 1,660,290 new cancer cases expected in the U.S. in 2013 may have distal 11q loss.

1.4 DNA DAMAGE RESPONSE (DDR) PATHWAYS

1.4.1 DDR Pathway Overview

DNA damage caused either by exogenous or endogenous stress poses a serious risk for the maintenance of genomic integrity within cells (Shiloh 2006). DNA lesions that form as a result of such stress, if not effectively repaired, are either extremely cytotoxic or could lead to malignant transformation of the cells (Lord and Ashworth 2012). Hence, irregularities in the DDR pathway are directly responsible for and contribute to many of the classic characteristics observed in cancers (Hanahan and Weinberg 2011). DDR pathway functions are not limited to DNA repair, but also include cell cycle checkpoint regulation, transcriptional program activation and regulation of cell death mechanisms (Hoeijmakers 2009; Warmerdam and Kanaar 2010). These cellular functions are initiated by sensing the DNA damage and subsequent transduction of the damage signal to a cascade of downstream effector proteins that help in the initiation and regulation of the different pathways involved. The effective signaling of this pathway helps maintain a stable genome and maintain cellular homeostasis.

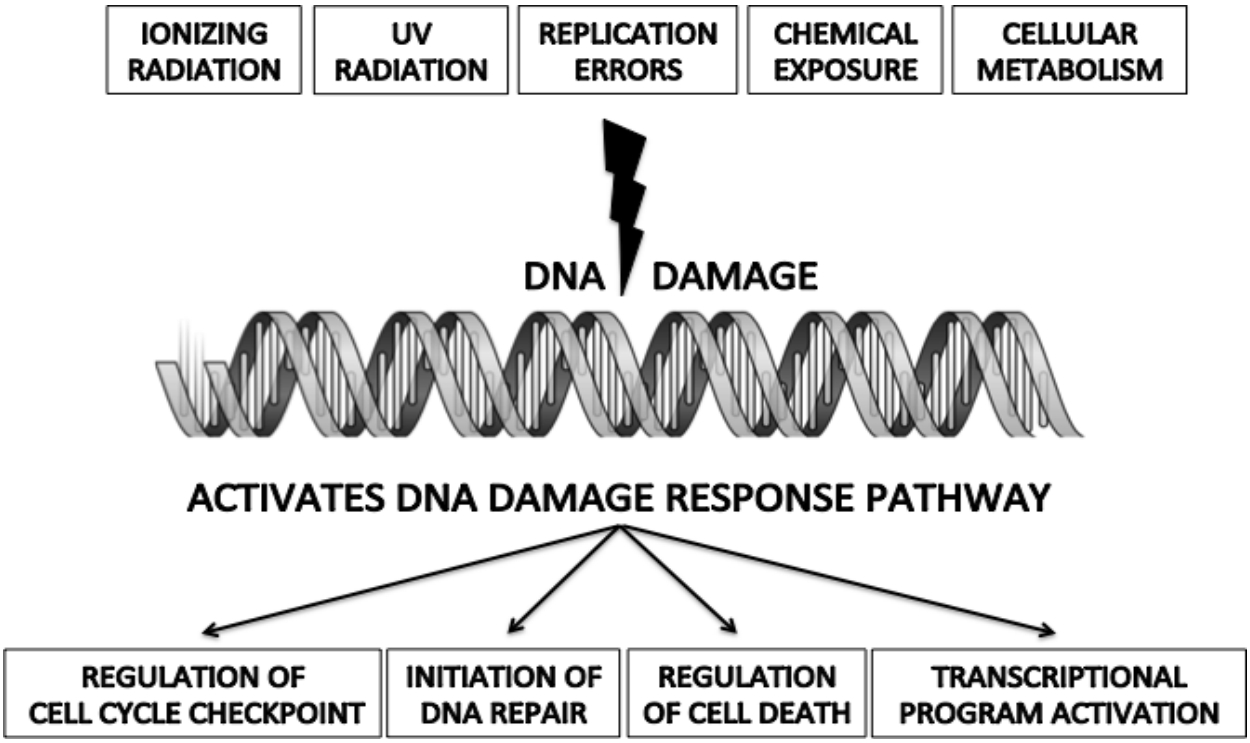

Figure 3. Schematic representation of the DNA damage and response pathway

The first step in the DDR pathway is the sensing of the DNA damage and/or chromatin alterations that occur after induction of damage by 'sensor' proteins. These are primary response proteins and are rapidly recruited to sites of DNA damage. These sensor molecules then signal to and recruit 'transducer' proteins to the sites of damage. The transducers in turn activate multiple 'effector' proteins that initiate and regulate the various cellular functions described earlier.

One family of transducers that play a critical role in DDR pathway is the phosphatidylinositol (PI) 3-kinase related kinases (PIKK). PIKK members are recognized as proximal response elements in stress induced signaling pathways (Abraham 2004; Lovejoy and Cortez 2009). They are a family of lipid/protein kinases that translate the stress induced damage into biochemical modifications that signal downstream targets to the presence of DNA damage resulting in DNA repair, cell cycle control and DNA recombinations (Keith and Schreiber 1995; Savitsky, et al. 1995; Abraham 2004; Lovejoy and Cortez 2009). Thus, they help maintain

genomic integrity and prevent the cycling of cells with DNA damage (Abraham 2004). The PIKK family consists of six members: ATM (ataxia telangiectasia mutated), ATR (ATM and Rad3 related), PRKDC (protein kinase, DNA-activated, catalytic polypeptide or DNA-PKc), MTOR (mammalian target of rapamycin), SMG1 (suppressor of morphogenesis in genitalia-1) and TRRAP (transformation/transcription domain-associated protein).

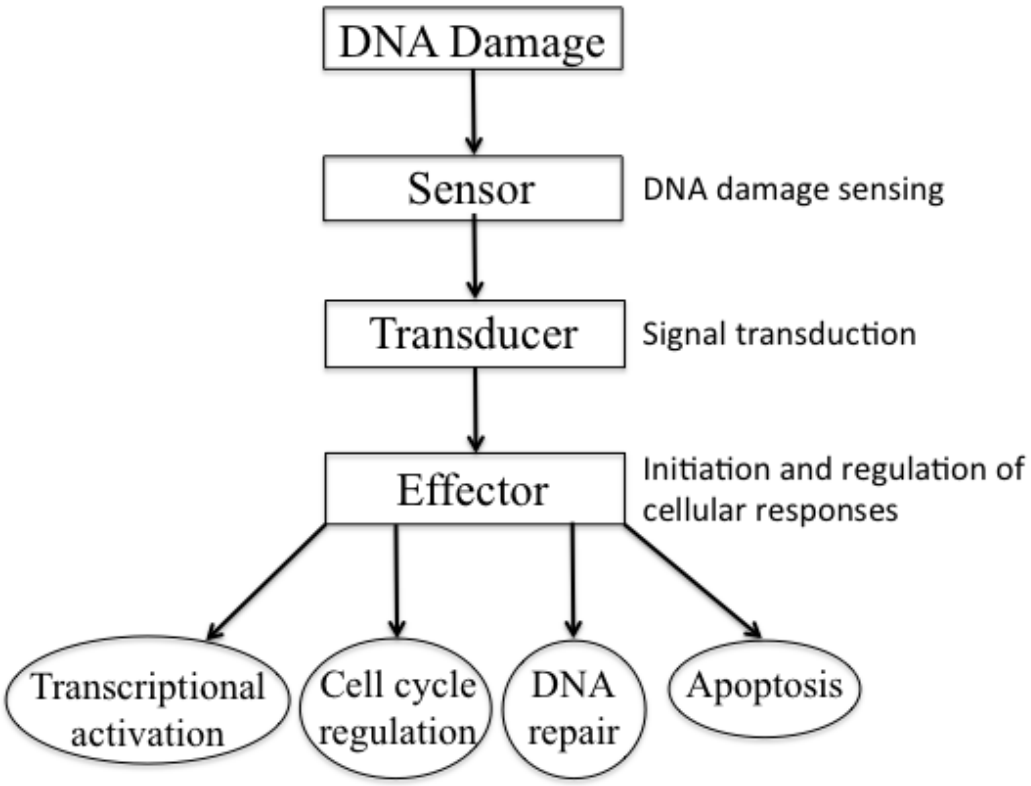

Figure 4. Schematic representation of DDR signal transduction pathway

Five of these six mammalian PIKKs are active protein kinases that take part in the stress induced signaling. ATM, ATR and PRKDC are primarily responsible for signaling DNA damage induced by exogenous and endogenous stress. SMG1 is involved in nonsense-mediated mRNA decay (NMD) and MTOR coordinates nutrient mediated signaling. TRRAP is the only member of the family with no known kinase activity (Abraham 2004; Lovejoy and Cortez 2009). Inhibition of these proteins using pharmacological drugs is being developed as potential anti-

cancer therapy. This is especially important, since cancer cells exhibit an altered DDR that might give them a growth advantage, and inhibition of these pathways involved in maintenance of integrity could increase efficiency of cancer therapies.

1.4.2 Double Strand Break (DSB) Response and Repair (ATM pathway)

A DNA lesion that is constantly generated throughout the lifespan of cells is the DSB. Unrepaired DSBs tend to leave the cell vulnerable to mutations and irreversible damage, and are extremely cytotoxic (Shiloh and Lehmann 2004; Lukas and Lukas 2013). DSBs are usually induced by ionizing radiation (IR), radiomimetic drugs, and oxygen radicals formed as a byproduct of normal metabolism, but can also be created as a consequence of stalled replication forks (Shiloh and Lehmann 2004). In our study, the main area of focus is on DSBs induced by IR and the DDR pathways involved in response and repair.

The nuclear protein, ATM, is primarily responsible for the IR-induced DDR. *ATM* is the gene mutated in the rare pleiotropic autosomal recessive disorder Ataxia telangiectasia (AT). The clinical manifestations of the disease include progressive cerebral ataxia, neuronal degeneration, hypersensitivity to ionizing radiation, premature aging, hypogonadism, growth retardation, immune deficiency, genomic instability, defective telomere metabolism and increased risk for cancer (Harnden 1994; Shiloh 1995; Lavin and Shiloh 1997; Morgan and Kastan 1997; Pandita, et al. 1999). Cell lines derived from AT patients tend to show defects in cell cycle regulation post-radiation, and this results in hypersensitivity to IR (Kastan, et al. 1992; Morgan and Kastan 1997). These same cell lines tend not to be affected by other genomic insults like UV damage (Rotman and Shiloh 1998). Since the repair of DNA damage induced by other agents such as UV

remains intact in AT cells, the ATM pathway is the primary response to DNA damage induced by IR (Shiloh 2003).

In response to IR-induced DSB, ATM undergoes rapid autophosphorylation of ser1981 resulting in the dissociation of the dimer and the subsequent phosphorylation of various other proteins involved in the regulation and repair of damage (Bakkenist and Kastan 2003; Kitagawa and Kastan 2005). Phospho-ser1981 ATM foci are visible within 10 minutes and phosphorylation of all cellular ATM is observed less than five minutes after irradiation (Kitagawa and Kastan 2005; Adams, et al. 2006). This rapid phosphorylation of ATM is facilitated by higher order chromatin structural changes that occur after formation of DSBs and does not require direct DNA binding (Bakkenist and Kastan 2003). Following IR, phospho-ATM is detected with a diffuse nuclear distribution within a few minutes and subsequently accumulates in foci, presumably at DSBs (Kitagawa and Kastan 2005). The MRE11A-RAD50-NBS1 (MRN) complex plays the role of a ‘sensor’ and is recruited rapidly to the site of damage in an ATM-dependent manner (Mirzoeva and Petrini 2003; Stracker, et al. 2004). It is also involved in the primary resection of the broken ends through its nuclease activity, resulting in secondary structures that are more amenable to repair and recruitment of other signaling molecules (D'Amours and Jackson 2002). The MRN complex is also necessary for maintenance of activation, proper phosphorylation of downstream targets, and also in the nuclear retention of the downstream targets after damage (Uziel, et al. 2003). Two critical downstream substrates of ATM are CHEK2 and p53. ATM phosphorylates CHEK2 and p53 at thr68 and ser15, respectively, after DSB formation (Canman, et al. 1998; Ward, et al. 2001). CHEK2 phosphorylation results in its immediate accumulation at sites of damage. Both of these proteins play significant roles in cell cycle control, DNA repair and apoptosis (Hirao, et al. 2002; Li, et al.

2010). Other downstream targets of ATM also play important roles in regulation of cell cycle checkpoints and DNA repair. Phosphorylation of CHEK2, p53 and MDM2 regulates the G_1 checkpoint. AT cells have a defective S phase checkpoint, and this has been attributed to the requirement of ATM for the phosphorylation of NBS1, FANCD2 and BRCA1 resulting in an effective S phase checkpoint. ATM signaling facilitates G_2M checkpoint activation through phosphorylation of CHEK2, RAD17 and BRCA1 (Kitagawa and Kastan 2005; Derheimer and Kastan 2010). ATM is known to accumulate and have enhanced kinase activity after IR in all phases of the cell cycle. This confirms its role as the protein required for a rapid response to DSBs independent of the cell cycle phase (Pandita, et al. 2000).

Another important substrate of ATM is the histone H2AX, a member of the histone H2A subfamily (Fernandez-Capetillo, et al. 2004). ATM activates H2AX at the DSB site, converting it into the phosphorylated form, γH2AX, which then anchors DNA damage response proteins to the sites of damage and initiates DNA repair (Stucki, et al. 2005; Kinner, et al. 2008). γH2AX foci are also seen in response to other forms of DNA damage suggesting that H2AX activation is regulated by other proteins like ATR (Gagou, et al. 2010). Cells lacking ATM show a persistence of γH2AX foci following IR, suggesting a direct role for ATM in DNA repair (Riballo, et al. 2004). The adapter protein, MDC1 is then recruited to the DSB site and phosphorylated by ATM. MDC1 binds to γH2AX, regulates retention of ATM at the site of DSB and also provides a target for DNA damage repair and signaling proteins to bind (Lukas, et al. 2004a; Stucki and Jackson 2004; Derheimer and Kastan 2010). ATM kinase activity has also been shown to be necessary for suppressing chromosomal instability (White, et al. 2008). Hence, ATM-mediated signaling is critical for the response to DNA damage in cells treated with IR.

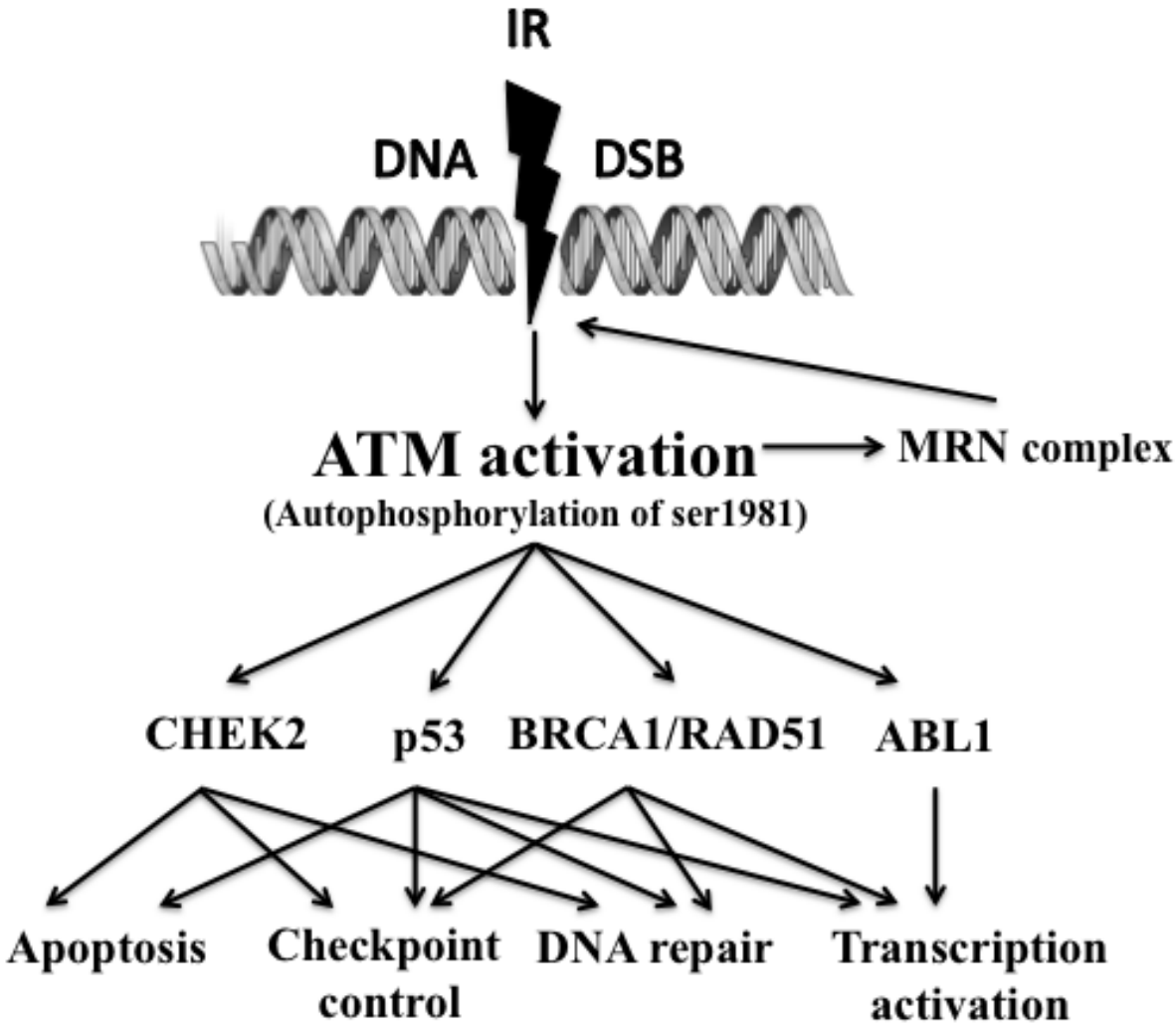

Figure 5. Schematic representation of the DSB response by the ATM-CHEK2 pathway

1.4.3 ATR-CHEK1 Pathway

ATR is another PI3K family protein involved primarily in signaling the presence of stalled replication forks and maintenance of genomic integrity during S phase, along with its partners, ATR interacting protein (ATRIP) and replication protein A (RPA) (Cortez, et al. 2001; Zou and Elledge 2003; Byun, et al. 2005). Unlike ATM and PRKDC, ATR signaling is critical in replicating cells (de Klein, et al. 2000; Cortez, et al. 2001; Brown and Baltimore 2003).

Homozygous deletion of ATR leads to early embryonic lethality in mammalian cells (Brown and Baltimore 2000; de Klein, et al. 2000). Partial loss of ATR activity causes the recessive disorder, Seckel syndrome in humans (O'Driscoll, et al. 2003).

The *ATR* gene maps to 3q23 and encodes a 302 kDa transducer protein. The canonical ATR signaling of stalled replication forks or other replication stress-induced lesions results in the generation of ssDNA. Even DNA DSBs are resected by nucleases to form ssDNA (Huertas 2010). This ssDNA is bound by the ssDNA binding protein RPA. RPA-bound ssDNA is then capable of independently recruiting ATR via ATRIP, and the checkpoint clamp, consisting of the RAD9-HUS1-RAD1 (9-1-1) complex and topoisomerase-binding protein 1 (TOPB1). Next, TOPB1 activates ATR and the signaling cascade is initiated (Nam and Cortez 2011). ATR phosphorylates its downstream effectors, CHEK1, BRCA1 and the Fanconi anemia (FANC) proteins. These effectors coordinate cell cycle progression and DNA repair (Parrilla-Castellar, et al. 2004). ATR also induces phosphorylation of H2AX, resulting in focus formation in response to replication stress (Ward and Chen 2001; Gagou, et al. 2010). In response to DNA damage, ATR phosphorylates CHEK1 at ser317 and ser345. Ser317 phosphorylation is required for subsequent ser345 phosphorylation in response to DNA damage (Wang, et al. 2012). Ser345 phosphorylation is necessary for activation of CHEK1, for a proper checkpoint response after DNA damage, and for nuclear retention of CHEK1 (Jiang, et al. 2003; Niida, et al. 2007). Early phosphorylation of ser345 in response to DNA damage is thought to occur in an ATR-dependent manner, whereas phosphorylation of ser317 in response to IR is reported to be dependent on ATM, NBS1 and ATR (Gatei, et al. 2003; Wang, et al. 2012). Targeted mutation of ser317 inhibits effective regulation of all cellular functions of CHEK1, but does not affect cell viability, whereas mutation of ser345 inhibits control of cellular functions of CHEK1 and also affects cell

viability (Wilsker, et al. 2008). Phosphorylated CHEK1 acts mainly during the S and G_2 phases of the cell cycle to activate cell cycle checkpoints (Liu, et al. 2000). CHEK1-induced S and G_2/M arrest is mediated through phosphorylation of the CDC25 phosphatases (Sanchez, et al. 1997; Uto, et al. 2004).

Although ATR plays a primary role in responding to ultraviolet light (UV) and chemotherapy-induced genomic insults and collapsed replication forks, it also appears to play a role in responding to IR-induced DNA damage (Adams, et al. 2006; Myers and Cortez 2006). The presence of ATR at nuclear foci after IR treatment is indicative of the recruitment of this kinase to sites of DNA damage; ATM is known to regulate the loading of ATR to sites of DNA DSB (Zou and Elledge 2003; Cuadrado, et al. 2006). Unlike the rapid phosphorylation of ATM post-IR treatment, ATR recruitment and activation is comparatively delayed, but also requires a functional MRN complex (Adams, et al. 2006). Further, the ATR-CHEK1 pathway is upregulated in IR-treated AT cells (Wang, et al. 2003). ATR kinase activity is also essential for the ser15 phosphorylation of p53 after IR or UV-induced damage (Tibbetts, et al. 1999). Although ATR signaling of stalled replication forks and maintenance of genomic integrity occurs during S phase, the role it plays in signaling IR-induced damage is not restricted to the S phase (Adams, et al. 2006). DSBs induced by radiation are processed into ssDNA, and the formation of ssDNA is responsible for the recruitment of ATR (Huertas 2010). Even though the ATM and ATR pathways are thought to respond primarily to different types of DNA damage, the two pathways appear to be intimately intertwined, especially since ATR signaling compensates for ATM when ATM is absent or if normal cells accumulate high levels of IR-induced damage (Abraham 2001; Golding, et al. 2009).

1.4.4 Cell Cycle Checkpoints in Cancer

The cell cycle is organized into a series of dependent events every cell traverses through prior to division into daughter cells. It is divided into four phases: G_1, S, G_2 and M. The purpose of the cell cycle is to maintain high fidelity during the replication of DNA and to assure the equal distribution of the genetic material between the two daughter cells. Therefore, the cell cycle is guarded by checkpoints that can delay the progression of cells in response to endogenous or exogenous stress. These checkpoints are at the G_1-S transition, within the S phase, and at the G_2-M transition. CDC25 phosphatase-mediated activation of cyclin-dependent kinase (CDK) complexes regulates progression of cells through the different checkpoints (Sorensen, et al. 2003; Kastan and Bartek 2004). Phosphorylation of CDC25 phosphatases creates a binding site for the 14-3-3 proteins. This binding sequesters the CDC25 phosphatases away from their substrates, thereby inhibiting their function (Boutros, et al. 2006). Defects in cell cycle checkpoints have been reported to contribute to genomic instability seen in various cancers (Kastan and Bartek 2004).

The G_1 checkpoint, the primary checkpoint that protects against genomic stress, is a p53-dependent pathway, which is initiated by ATM in response to DNA damage (Levine 1997; Lukas, et al. 2004b; Massague 2004). CHEK2, activated by ATM, in turn phosphorylates CDC25A and prevents activation of cyclin E/CDK2 (Mailand, et al. 2000). CHEK1 is also capable of phosphorylating CDC25A, and this CHEK1/CHEK2-CDC25A checkpoint is activated rapidly, independent of p53. A sustained G_1 arrest requires p53 mediation (Kastan and Bartek 2004). The G_1 checkpoint is frequently dysregulated in HNSCC (Michalides, et al. 2002). The S phase checkpoint is activated in response to DNA replication errors and DNA damage occurring during the S phase. CDC25A, phosphorylated by either of the two pathways, regulates

CDK2 activation, which controls S phase progression (Sorensen, et al. 2003). This checkpoint is independent of p53, but is under the control of the ATR/CHEK1 and ATM/CHEK2 kinases (Bartek, et al. 2004; Kastan and Bartek 2004). Abrogation of the S phase checkpoint in response to IR leads to premature mitosis, premature chromatin condensation (PCC), and mitotic apoptosis (Nghiem, et al. 2001). The aim of the G_2M checkpoint is to prevent cells, which have escaped the G_1 or S checkpoints with DNA damage or those with replication errors from entering mitosis. The Cyclin B/CDK1 complex that is regulated by the CDC25 phosphatases controls this checkpoint. Activation of CHEK1 by ATR results in the phosphorylation of the CDC25 (A, B, C) phosphatases, preventing the activation of the Cyclin B/CDK1 complex and G_2M arrest (Boutros, et al. 2006). Abrogation of the G_2M checkpoint is known to result in mitotic catastrophe (Hekmat-Nejad, et al. 2000). Since defects in the G_1 checkpoint are a common feature in most tumors, abrogation of the G_2M checkpoint by inhibition of ATM/ATR, CHEK1 or CDC25 resulting in cell death by mitotic catastrophe are being developed as potential anti-cancer therapies (Bucher and Britten 2008).

1.4.5 Gemcitabine-induced DNA Damage and Response

Gemcitabine or difluorodeoxycytidine (dFD-C) is a chemotherapeutic drug commonly used in the treatment of solid tumors (Carmichael 1998; Nabhan, et al. 2001). It is a deoxycytidine analog with two fluorine substitutions. Gemcitabine enters the cell through the nucleoside transporter pathway. Within the cell, it is phosphorylated into its mono-phosphorylated form, dFD-CMP by deoxycytidine kinase (dCK). The monophosphate form undergoes two further phosphorylations to form dFD-CDP and dFD-CTP by the action of monophosphate-pyrimidine kinase and diphospho-pyrimidine kinase, respectively. The activity of gemcitabine is dependent

on the formation of this triphosphate metabolite that can be incorporated into DNA. Gemcitabine is inactivated by either deamination into dFD-U (inactive metabolite) by cytidine deaminase (CDD) or dephosphorylation of dFD-CMP, thereby preventing the formation of the active form (Plunkett, et al. 1996; Galmarini, et al. 2002).

The active form of gemcitabine, dFD-CTP, is incorporated into the DNA during replication in the C sites of the growing strand. This dFD-CTP incorporated site is subsequently masked by the addition of a natural nucleoside, thereby preventing DNA repair by 3'-5' endonuclease activity. This masking stops the progress of the DNA polymerase by a process called masked DNA chain termination. The diphosphate metabolite, also an active form, has an indirect effect. This form inhibits ribonucleotide reductase (RNR), resulting in blocked *de novo* DNA synthesis. It also increases gemcitabine activity as a result of decreased intracellular levels of deoxynucleotide triphosphates. Gemcitabine is also capable of being incorporated into RNA, thereby inhibiting RNA synthesis (Galmarini, et al. 2002).

Resistance to treatment with gemcitabine has been observed in various tumor types, especially pancreatic cancers. There are many possible explanations for this lack of sensitivity. A low level of the active metabolite form of gemcitabine within the cells is one major reason. This can be as a result of breakdown of the pathway at various levels. The cell could have reduced expression of nucleoside transporter on the membrane resulting in inefficient uptake. Reduced levels of the activating enzyme, dCK and increased gemcitabine degradation could possibly lower the level of the active triphosphate metabolite (Galmarini, et al. 2002). Second, gemcitabine might have an altered interaction with intracellular targets. Thirdly, gemcitabine resistance could also result because of alteration of cell cycle and apoptosis-regulating genes like p53 (Chen, et al. 2000; Galmarini, et al. 2002). There are conflicting reports about the role of p53

signaling status in decreased sensitivity to gemcitabine. Some reports suggest that the lack of a functional p53 resulted in cell lines being considerably more resistant to DNA damaging agents like gemcitabine, mitomycin-C and doxorubicin. Although some reports also suggest that there is no difference in cytotoxicity of gemcitabine within cell lines of different tumor types based on p53 status (Merlin, et al. 1998; Rieger, et al. 1999; Chen, et al. 2000; Galmarini, et al. 2002).

Sensitivity to gemcitabine can also be modified by alteration of the DDR and repair pathways in tumor cells. The DDR to gemcitabine-induced stalled replication forks activates the ATR-CHEK1 pathway and results in S-phase arrest in leukemia cell lines (Shi, et al. 2001). Cells lacking RAD9, ATR and/or CHEK1 have been observed to be more sensitive to gemcitabine (Karnitz, et al. 2005). Inhibition of the ATR-CHEK1 pathway in pancreatic cancer cells resulting in gemcitabine sensitization was shown not to be due to abrogation of the S or G_2M phase checkpoints. CHEK1 inhibition resulted in inhibition of RAD51-mediated DDR and this signaling from CHEK1 to RAD51 was important for the DDR to gemcitabine-induced replication stress (Parsels, et al. 2009). DDR to gemcitabine-induced damage also requires functional ATM and the MRN complex, and deficiency of these proteins increased the sensitivity of cells to gemcitabine (Ewald, et al. 2008). H2AX phosphorylation and focus formation marked stalled replication forks after treatment with gemcitabine. The role of ATM in this phosphorylation was proven when chemical inhibition of ATM blocked H2AX phosphorylation (Ewald, et al. 2007). Previous studies have also shown a lack of effect of gemcitabine in cells deficient in homologous recombination repair (HRR) (Crul, et al. 2003).

1.5 CHEK1 INHIBITION AS A TARGETED CANCER THERAPY

1.5.1 Targeted Cancer Therapy

Cancer drug development in the current research setting is focused on the identification of therapeutic targets. The emergence of molecular cancer therapeutics has put further focus on target identification as an initial step in the development of novel anti-cancer drugs. Most tumors during their development accumulate mutations or genetic/epigenetic lesions that help with the progression of carcinogenesis (Hanahan and Weinberg 2011). These mutations are classified into two categories - driver mutations and passenger mutations. Target identification has been focused on driver mutations, as they are essential for malignant growth (Greenman, et al. 2006). These targets of molecular cancer therapeutics can be classified into three types based on the different approaches used. The first class was focused on critical signaling proteins that acquired driver mutations. Inhibition of the BCR-ABL1 fusion protein by Imatinib, the mutant or amplified EGF receptor by Gefitinib or Erlotinib, the mutated *BRAF* gene by PLX-4032 or the *EML4-ALK* fusion oncogenes by ALK inhibitor (Druker, et al. 1996; Sharma, et al. 2007; Janku, et al. 2010; Maemondo, et al. 2010; Smalley 2010). Most mutated genes are not amenable to easy inhibition by pharmacologic drugs. So even though targeting these mutations is an obvious approach, it is not feasible in all cases. The second approach under development focused on complete pathways. *KRAS* is a commonly mutated gene and is not easily targeted by small molecular inhibitors (Saxena, et al. 2008). *MEK* and *BRAF*, two downstream effectors of *KRAS*, that are themselves not mutated, but are targeted in a pathway-focused approach and this inhibition has shown considerable anti-tumor effect in preclinical studies (Solit, et al. 2006; Garon, et al. 2010). The third approach focuses on screening for synthetic lethal genes. Synthetic

lethality refers to the interaction of two genes, when the singular mutation of the genes is compatible with viability, but the combined mutation is lethal. Therefore, synthetic lethal interactions can be targeted by a wider array of molecular therapeutics.

1.5.2 Synthetic Lethality

The concept of synthetic lethality is based on the original use of the term in yeast mutation screens, wherein mutations in two or more genes results in cell death, although one or the other does not kill the cells. Cell viability is compromised by the additive negative effect of the two synthetic lethal mutations on a critical cellular function. A specific gene mutation in cancer can sensitize it to drug-based inhibition of its synthetic lethal partner. This therapeutic strategy has the added advantage that it would not affect normal cells and therefore, is selective for tumor cells. Also, this treatment strategy could be used to target both loss-of-function and gain-of-function mutations (Ferrari, et al. 2010). In the context of cancer, synthetic lethality takes advantage of the necessity for cancer cells to repair their DNA due to the inherent genomic and chromosomal instability and frequent DNA damage in these cells (Shaheen, et al. 2011a). Relating this concept to the cell cycle checkpoints defined above, cancer cells with DNA damage must stop at a major cell cycle checkpoint to repair their DNA lest they replicate or distribute to their daughter cells increasingly damaged genomes. As discussed above, most cancer cells lack an effective G_1 checkpoint. Thus, after DNA damage caused by IR or chemotherapy, cancer cells must arrest at the G_2M checkpoint to repair their genomes prior to cell division. Knocking out the G_2M checkpoint using targeted CHEK1 inhibition would be ‘synthetic lethal’ because these cells would enter mitosis with damaged genomes and undergo mitotic catastrophe (MC) (Origanti, et al. 2013). Knocking out the G_2M checkpoint would not be expected to damage

normal cells, as they would have a normal G_1 checkpoint, which protects them against DNA damage-induced cell death.

1.5.3 CHEK1 Inhibition

CHEK1 inhibition resulting in synthetic lethality appears to be a very promising targeted therapy for several reasons. Many tumor cells lack a G_1 checkpoint as a result of defective p53, p16, or pRB1 signaling; cells lacking a G_1 checkpoint are selectively affected by CHEK1 inhibition, which abrogates the G_2M cell cycle checkpoint, sending cells with DNA damage into mitotic catastrophe/apoptosis (Merry, et al. 2010; Morgan, et al. 2010; Furgason and Bahassi el 2013; Origanti, et al. 2013). Studies have shown that the p53 mutant HCT116 (human colon cancer cell line) is more sensitive to CHEK1 knockdown than p53 wild-type cells (Pan, et al. 2009). The advantage of this strategy is that somatic cells with normal checkpoint signaling are not thought to be affected deleteriously by CHEK1 inhibitors, since they are protected by functioning cell cycle checkpoints that enable them to repair DNA damage or undergo apoptosis in response to irreparable damage (Furgason and Bahassi el 2013). ATR inhibition is also reported to selectively sensitize cells deficient in the G_1 checkpoint to premature chromatin condensation (Nghiem, et al. 2001; Reaper, et al. 2011). NU6027, an ATR inhibitor, sensitized MCF7 (a human breast cancer cell line) cells to IR, temozolomide, cisplatin, camptothecin, doxorubicin and hydroxyurea (Peasland, et al. 2011). CHEK1 inhibitors have been combined with DNA damaging agents in both *in vitro* and *in vivo* studies. This combination increased the efficacy of agents such as ionizing radiation in a variety of carcinomas (Riesterer, et al. 2011; Borst, et al. 2012a; Ma, et al. 2012), cisplatin in colon cancer, gemcitabine in pancreatic cancer (Venkatesha, et al. 2012), and cytarabine in acute myelogenous leukemia (Karp, et al. 2012a; Schenk, et al.

2012a), among others. Increased efficacy enables decreased dosages of IR or these relatively toxic chemotherapies (Bennett, et al. 2012). UCN-01 is one of the earliest CHEK1 inhibitors used in preclinical studies that caused a complete disruption of the G_2 checkpoint in response to ionizing radiation (Busby, et al. 2000). AZD7762, a CHEK1 inhibitor from AstraZeneca, when combined with gemcitabine was shown to target pancreatic cancer stem-like cells that are otherwise resistant to standard therapy (Venkatesha, et al. 2012). This inhibitor also potentiated the effect of other DNA damaging agents like camptothecin and irinotecan (Zabludoff, et al. 2008). PF00477736, a Pfizer CHEK1 inhibitor, potentiated the effect of gemcitabine and camptothecin in CA46 (a p53-mutated lymphoma) and HeLa (HPV18-positive human cervical cancer) cells by abrogating DNA damage-induced S-phase and G_2M-phase arrest (Blasina, et al. 2008). CHEK1 inhibition combined with inhibition of the DNA repair enzyme poly(ADP-ribose) polymerase (PARP) resulted in synthetic lethality in a panel of human breast and pancreatic cell lines (Mitchell, et al. 2010).

The present study is expected to show that cells with distal 11q loss tend to be resistant to doses of IR and gemcitabine that are considered lethal in cancer cells without this loss. It will also provide evidence that the ATR-CHEK1 pathway is responsible for the radioresistance and also gemcitabine resistance in cancer cells with distal 11q loss. Our study is significant in providing a possible explanation for the unresponsiveness of tumor cells impaired by distal 11q loss to treatment with either radiation or gemcitabine therapy and the reason that these tumors tend to relapse and lead to a poor prognosis for patients, although this will not be examined in the study. The study also has translational value since the genetic basis for loss of sensitivity to IR and gemcitabine could be used as a biomarker for predicting response to therapy. The ability

to sensitize cells to IR and gemcitabine by the inhibition of ATR-CHEK1 pathway can be used to increase the success of radiation therapy and gemcitabine-based chemotherapy.

2.0 MATERIAL AND METHODS

2.1 CELL CULTURE

2.1.1 HNSCC and Control Cell Lines

The UPCI:SCC HNSCC cell lines developed in the Gollin laboratory (White, et al. 2007) were cultured in M10 medium comprised of Minimal Essential Medium (MEM) supplemented with 1% non-essential amino acids (NEAA), 1% L-glutamine, 0.05 mg/ml gentamicin and 10% fetal bovine serum (FBS) (all from GIBCO Invitrogen, Grand Island, NY). *TERT*-transfected human keratinocytes (OKF6/TERT-1 cells, a gift of James Rheinwald, Brigham and Women's Hospital, Harvard Institutes of Medicine (Dickson, et al. 2000)) were cultured in Keratinocyte-SFM supplemented with 25 μg/ml bovine pituitary extract, 0.2 ng/ml EGF, 0.3 mM $CaCl_2$, and penicillin-streptomycin (GIBCO Invitrogen).

2.1.2 NSCLC Cell Lines

Most NSCLC cell lines were cultured in Basal Medium Eagle (BME) (Gibco Invitrogen) supplemented with 0.05 mg/ml penicillin-streptomycin with 1% L-glutamine (PSG) (Gibco Invitrogen) and 10% fetal bovine serum (FBS). A549 cells were cultured in Dulbecco's Modified Eagles Medium (DMEM) (Gibco Invitrogen), supplemented with 1% NEAA, PSG and 10%

FBS. H1299 cells were cultured in RPMI-1640 medium (Gibco Invitrogen) supplemented with 1% NEAA, 0.05mg/ml gentamicin and 10% FBS. Examination of lung cancer cell lines was a collaboration with Dr. Jill Siegfried.

2.1.3 Ovarian Carcinoma (OvC) Cell Lines

OvC cancer cell lines were cultured in either DMEM supplemented with 1% NEAA, PSG and 10% FBS or RPMI-1640 medium supplemented with 1% NEAA, 0.05mg/ml gentamicin and 10% FBS. Examination of ovarian cancer was a collaboration with Drs. Anda Vlad and Robert Edwards.

2.2 FLUORESCENCE *IN SITU* HYBRIDIZATION (FISH)

Molecular cytogenetic analysis was carried out to determine the relative copy numbers of *ATM*, *MRE11A*, *H2AFX* and *CHEK1* in HNSCC cell lines compared to the chromosome 11 centromere (CEP11/D11Z1, Abbott Molecular Inc., Des Plaines, IL). Cytogenetic analyses were carried out in the University of Pittsburgh Cell Culture and Cytogenetics Facility. Metaphase and interphase cells were prepared from the cell lines using standard cytogenetic techniques. Briefly, cells were harvested following 2-5 h treatment with 0.01μg/ml Colcemid^{TM} (Irvine Scientific, Santa Ana, CA), hypotonic KCl (0.075 M) treatment for 30 min at 37°C, followed by fixation and washes in 3:1 acetone-free methanol:glacial acetic acid.

Slides for FISH analysis were prepared from the harvested cell lines by dropping the cell suspension onto microscope slides and air dried. Following pretreatment with 2xSSC (saline-

sodium citrate), the slides were dehydrated using a graded series of ethanol (70%, 80%, and 100%). Chromatin was denatured with 70% formamide at 75ºC, and the slides were dehydrated in a cold (-20°C) graded series of ethanol. The FISH probes were prepared from DNA isolated from BAC clones purchased from Children's Hospital of Oakland Research Institute (CHORI, Oakland, CA; http://www.chori.org/bacpac). The BAC clones used were: RP11-241D13 (*ATM* gene), RP11-685N10 (*MRE11A* gene), RP11-892K21 (*H2AFX* gene) and RP11-712D22 (*CHEK1* gene). BAC DNA was labeled with Spectrum Orange™ using a nick translation kit (Abbott Molecular Inc.). For each BAC probe, the labeled DNA was precipitated with ethanol, resuspended in hybridization buffer, combined with a Spectrum Green™-labeled CEP11 probe (D11Z1, Abbott Molecular Inc.), denatured for 5 min at 75°C, and preannealed for 15-30 min at 37°C. The probes were applied to each slide, covered with a 22x22 mm coverslip, sealed with rubber cement, and co-hybridized on the slide for 16 h at 37°C. The slides were washed first with 0.4xSSC/0.3% Tween-20 at 73ºC, next in 2xSSC/0.1% Tween-20 at room temperature, counterstained with 4',6-diamidino-2-phenylindole (DAPI, 160 ng/ml 2xSSC), and mounted with antifade (comprised of 1 mg/ml 1,4-phenylene-diamine (Sigma-Aldrich, St. Louis, MO) in 86% glycerol/PBS at pH 8.0) prior to analysis. All FISH analyses were carried out using an Olympus BX-61 epifluorescence microscope (Olympus Microscopes, Melville, NY). An Applied Imaging CytoVision workstation with Genus v3.6 software was used for image capture and analysis (Leica Microsystems, San Jose, CA). Copy number gain or loss of genes was determined by the relative ratio of the BAC probe to centromere 11. A ratio of <1.0 was considered to have relative gene copy loss, a ratio of 1 = equal, a ratio between 1 and 2.5 = gain, and a ratio ≥ 2.5 = amplified with respect to CEP11. The percentage of cells with relative loss, gain, or amplification was determined after counting at least 200 cells per slide. Results were reported as

a percentage of cells with an altered copy number of the gene relative to the copy number of chromosome 11 in that cell.

2.3 CLONOGENIC SURVIVAL ASSAY

Clonogenic (also called colony) survival assays were carried out to determine cell survival in response to treatment as described earlier (Parikh, et al. 2007). Two thousand cells from a single cell suspension of each cell line were seeded into 60 mm Petri dishes and incubated overnight to facilitate attachment. For IR-induced damage studies, cells were then treated with 2.5, 5, or 10 Gy doses of γ-irradiation from a Gammacell 1,000 Elite irradiator (Nordion International, Ottawa, Canada) with a ^{137}Cs source at a dose rate of 2.83 Gy/min. For gemcitabine-induced damage studies, cells were treated with 5 or 10 nM of gemcitabine. Cell culture medium in all dishes was changed seven days after treatment. Untreated cells, also seeded at the same density, were used as controls to determine relative plating efficiency. After 12-14 days, 70% ethanol was used to fix the colonies in all culture dishes. The fixed colonies were then stained with Giemsa (Sigma) and counted. A colony was defined as a cluster of >50 cells, assuming that it had originated from a single cell. All experiments were performed in triplicate. Results were reported as a 'Surviving fraction', which is the ratio of the number of colonies observed at a particular dose to that observed in the untreated control, represented as a percentage. It is calculated using the formulae below.

Plating efficiency, PE = colonies counted in untreated / cells seeded

Surviving Fraction, SF = colonies counted in treated / (cells seeded * PE/100)

2.4 ASSESSMENT OF MITOTIC DEFECTS

We analyzed mitotic defects in HNSCC cell lines grown on coverslips. Cells were either untreated or treated with IR and then grown for 18 and 36 hours. At the end of 18 and 36 hours, the cells were fixed with 100% methanol, dried, and stained with DAPI. Coverslips were mounted onto slides with antifade. The slides were coded and 1000 cells were analyzed from each cell line. The frequencies of anaphase and interphase bridges and micronuclei were recorded. The values for cell lines were averaged and grouped into two categories, 'Distal 11q loss' and 'No distal 11q loss.'

2.5 QUANTITATIVE REAL TIME PCR (QRT-PCR)

QRT-PCR was carried out to assess the relative *ATR* and *CHEK1* expression in untreated cell lines and those treated with IR or transfected with *CHEK1* siRNA. RNA extraction for real-time PCR was performed using TRIzol reagent (Gibco Invitrogen) according to the manufacturer's instructions. The extracted RNA was purified using the RNeasy Mini kit (QIAGEN, Germantown, MD) and resuspended in 100 µl RNase free water. The RNA samples were purified of contaminating DNA using a DNA–free DNase kit (Ambion, Austin, TX) according to the manufacturer's instructions. RNA concentrations were assessed using the SmartSpec 3000 (Bio-Rad Laboratories, Hercules, CA) and normalized to 40 ng/µl. Reverse transcription (RT) - PCR was carried with three inputs for each sample: 400 ng of total RNA, 100 ng of total RNA and a negative control with no reverse transcriptase. The RT set up is described in the table below:

Table 1. RT–PCR reagents

Reagent	Company	Input		
		400 ng	**100 ng**	**No reverse transcriptase**
10X PCR Buffer II	Applied Biosystems	10 ml	10 ml	10 ml
$MgCl_2$ (25 mM)	Applied Biosystems	30 ml	30 ml	30 ml
dNTP (25 mM)	Roche Molecular Biochemicals	4 ml	4 ml	4 ml
MMLV (10 U/ml)	Ambion	1 ml	1 ml	1 ml
RNase Inhibitor (40 U/ml)	Applied Biosystems	1 ml	1 ml	1 ml
Hex Primer (500 mM)	Applied Biosystems	2.5 ml	2.5 ml	2.5 ml
Nuclease Free Water	Ambion	41.5 ml	49 ml	42.5 ml
RNA		10 ml	2.5 ml	10 ml

The thermocycler conditions were set up as: 25 ^{o}C for 10 min, 48 ^{o}C for 40 min, 95 ^{o}C for 5 min and hold at 10 ^{o}C. The cDNA was diluted 2.5 times to yield working concentrations of 1.6 ng/μl and 0.4 ng/μl.

QRT-PCR of cDNA obtained after reverse transcription was carried out on the 7300 Real-Time PCR System (Applied Biosystems), and analysis was done using the relative quantitation method as in Huang et al. (Huang, et al. 2002). The final concentrations of the QRT-PCR reaction components were as follows: 1X Taqman Gene Expression Master Mix and 1X Taqman Gene Expression Assays (Probe/Primer mix for *ATR*, *CHEK1* and 18s RNA) (Applied Biosystems). Thermocycler conditions for QRT-PCR were as follows: 95°C for 10 min, 40 cycles of 95°C for 15 s and 60°C for 60 s using the (Applied Biosystems). The RNA expression levels were quantified relative to Universal Reference cDNA obtained from Clontech (Mountain View, CA).

2.6 IMMUNOBLOTTING

Immunoblotting was utilized to evaluate expression of ATR-CHEK1 pathway proteins like ATR, CHEK1 and pCDC25C and to study the function of p53 in our cell lines by analyzing p53 and p21 protein expression after Adriamycin treatment (0.4 μg/ml of medium for 4-5 h at 37°C). First, cells were removed by trypsinization, washed with ice cold PBS, and lysed on ice with a solution containing 50 mM Tris, 1% Triton X-100 (Sigma), 0.1% sodium dodecyl sulfate (Bio-Rad Laboratories, Hercules, CA), 150 mM NaCl (Fisher Chemicals, Fairlawn, NJ), 1 mM dithiothreitol (DTT) (Fisher Scientific, Inc., Hampton, NH), 10 μg/ml leupeptin (Roche Applied Science, Indianapolis, IN), 10 μg/ml pepstatin (Roche Applied Science) and 1 nM phenyl methyl sulfonyl fluoride (PMSF) (Santa Cruz Biotechnology, Inc., Santa Cruz, CA). The soluble cell lysate was centrifuged at 13,148 xg for 15 min and the supernatant was transferred to a clean microfuge tube. Protein concentrations were determined using the Bio-Rad Quick Start Bradford Protein Assay Kit and the SmartSpec 3000 (Bio-Rad Laboratories). Normalized lysates were resolved by sodium dodecyl sulfate polyacrylamide gel electrophoresis (SDS-PAGE) and transferred to Immobilon-P membrane (Millipore Corporation, Billerica, MA). After blocking with 5% non-fat dry milk (NFDM) for 1 h, the membrane was incubated overnight with primary antibodies for specific DNA damage response proteins. The primary antibodies used were: ATR (Affinity Bioreagents, Golden, CO, 1:1000 dilution), CHEK1 (Cell Signaling, Danvers, MA, 1:1000 dilution), pCHEK1 ser 345 (Cell Signaling, 1:1000 dilution), pCHEK1 ser 317 (Cell Signaling, 1:1000 dilution), pCDC25C (Cell Signaling, 1:1000 dilution), p53 (Santa Cruz Biotechnology, Inc., 1:750 dilution) and p21 (Santa Cruz Biotechnology, Inc., 1:750 dilution). The membrane was then incubated with the appropriate secondary antibody (Santa Cruz Biotechnology, Inc., 1:5000 dilution) for 1 h and target proteins were visualized using the

Western Lightning™ Chemiluminescence Reagent Plus kit (PerkinElmer Life Sciences, Boston, MA) according to the manufacturer's instructions. To verify equal protein loading in the gels, membranes were stripped and re-probed with antibodies against β-actin (Sigma Immunochemicals, St. Louis, MO, 1:1000 dilution) or α-Actinin (Santa Cruz Biotechnology, Inc., 1:1000 dilution).

2.7 DENSITOMETRIC ANALYSIS OF PROTEIN BANDS

Image J software from NIH was used for analyzing densities of protein bands in western blots. Relative optical densities were calculated for specific protein of interest and loading control for all lanes using one of the lanes as a reference. Adjusted densities were then calculated for each sample by normalizing the relative density of the protein of interest to the loading control for the same.

2.8 CELL CYCLE ANALYSIS BY FLOW CYTOMETRY

For cell cycle analysis, cells were seeded in 35 mm or 60 mm dishes and allowed to attach overnight. Following the relevant treatments, mock or IR, floating and adherent cells were collected at the end of 24 h, washed with phosphate-buffered saline (PBS), and fixed with 70% ethanol. The cells were then treated with 80 µg/ml RNase A and 50 µg/ml propidium iodide (Invitrogen-Molecular Probes, Carlsbad, CA) for 45 min at 37^{o}C. The stained cells were analyzed using a Coulter Epics XL Flow Cytometer in the UPCI Flow Cytometry Facility.

2.9 *CHEK1* KNOCKDOWN BY RNA INTERFERENCE

Small interfering RNAs (siRNA) are 21-25 nucleotide long double stranded RNAs, complimentary to a known target mRNA (Elbashir, et al. 2001). Usually a pool of two or more siRNA duplexes is used to specifically bind to and degrade the target mRNA. RNA interference to *CHEK1*, *ATR* and *RAD9A* was performed using Smartpool duplexes obtained from Dharmacon (Lafayette, CO). Nonspecific (scrambled) control duplexes (Dharmacon) were used as controls. The duplexes were reconstituted in DNA–free RNA resuspension buffer provided by Dharmacon according to the manufacturer's instructions. For transfection, the carcinoma cell lines were seeded in 60 mm dishes or T25 flasks and transfected with siRNA duplexes using Lipofectamine 2000 (Invitrogen) according to the manufacturer's instructions. The final working siRNA concentration ranged from 90-100 nM. We examined cells treated without vector (untreated controls), cells transfected with the nonspecific (scrambled) control siRNA (mock-transfected controls), and cells transfected with specific smartpool siRNA duplexes (siRNA transfected) for all of our siRNA experiments. Peak siRNA transfection was seen at the end of 24-96 h as assessed by RT-PCR and immunoblotting. At 72 h post-transfection, cells were seeded for clonogenic survival assay.

2.10 CHEK1 KNOCKDOWN BY SMALL MOLECULE INHIBITOR

PF-00477736, a potent, specific CHEK1 small molecule inhibitor (SMI) was a gift from Pfizer, Inc. (Groton, CT). PF-00477736 selectively inhibits enzymatic activity of CHEK1, abrogates DNA damage-induced cell cycle arrest, and increases the cytotoxic effect of DNA damaging agents (Blasina, et al. 2008). PF-00477736 is only effective in p53-defective cell lines (Blasina, et al. 2008). Dose-response curves for the SMI, assessment of the optimal time for addition of the SMI in relation to IR treatment, and the effects of monotherapy with the drug or combined treatment with IR were determined using clonogenic survival assays.

3.0 RESULTS

3.1 LOSS OF DISTAL 11Q AND ITS CONSEQUENCES

3.1.1 Copy Number Loss in Genes within Distal 11q

Dual-color FISH with BAC probes to the *ATM, MRE11A, H2AFX* or *CHEK1* genes was carried out to compare copy number of the test probe with a centromere 11 enumeration probe (CEP11). Table 2 summarizes our FISH results determining the relative copy number of the *ATM, MRE11A, H2AFX,* and *CHEK1* genes. Relative copy number loss (~haploinsufficiency) of one or more of these genes (specifically including *ATM* loss) is defined as 'distal 11q loss' (Figs. 6 and 7). Five of the 17 cell lines lost all four genes in more than 90% of cells. One of the 17 and six of the17 cell lines lost three and two genes, respectively in more than 70% of cells. Four of the 17 cell lines lost one or no genes on distal 11q. Thus, our results suggest that copy number loss of genes on distal 11q is observed in a substantial frequency of HNSCC cell lines.

Table 2. Summary of interphase FISH for relative copy number loss[1] of *MRE11A*, *ATM*, *H2AFX* and *CHEK1* genes in HNSCC cell lines

		Percentage of Cells with Loss of[2]			
Tumor Site	**Cell Line**	***MRE11A*[3] 11q21 (94150466 - 94227040)**	***ATM*[3] 11q22-q23 (108093559 - 108239826)**	***H2AFX*[3] 11q23.3 (118964584 - 118966177)**	***CHEK1*[3] 11q24.2 (125495031-125546150)**
Head and neck squamous cell carcinoma (HNSCC)	UPCI:SCC029B	90	92	97	99
	UPCI:SCC040	100	99	99	99
	UPCI:SCC084	95	93	98	97
	UPCI:SCC131	98	92	96	98
	UPCI:SCC136	99	92	91	96
	UPCI:SCC172	96	98	79	64
	UPCI:SCC099	91	11	5	77
	UPCI:SCC103	20	91	96	63
	UPCI:SCC104	1	98	96	1
	UPCI:SCC105	10	70	77	5
	UPCI:SCC122	54	98	87	50
	UPCI:SCC142	1	94	60	92
	UPCI:SCC081	8	22	97	4
	UPCI:SCC066	20	3	13	15
	UPCI:SCC090	15	2	2	0
	UPCI:SCC116	14	15	16	10
	UPCI:SCC125	30	54	44	50

[1] The results are displayed in terms of variation in copy number of a gene in relation to the ploidy of each cell line as determined by chromosome 11 centromere enumeration.
[2] The numerical value represents the percentage of cells with copy number loss of specific gene.
[3] *ATM*, *MRE11A*, *H2AFX* and *CHEK1* genes are all located in the distal segment of the long arm of chromosome 11.

We also observed copy number loss of genes on distal 11q in NSCLC and OvC cell lines studied (Figs. 6 and 7). In NSCLC, three of eight cell lines lost all four genes in more than 80 % of cells (Table 3). One of eight had loss in two genes and four of eight did not have loss of any genes tested on distal 11q loss. In OvC, FISH to determine relative copy number was carried out for *MRE11A* and *ATM* genes. Three of five cell lines had loss in both genes (Table 4). One each of five cell lines had loss of one gene or loss of none. Thus, our results suggest that relative copy number loss of genes in the distal 11q region is present in multiple tumor types.

Table 3. Summary of the interphase FISH for relative copy number loss[1] of *MRE11A*, *ATM*, *H2AFX* and *CHEK1* genes in NSCLC cell lines

		Percentage of Cells with Loss of[2]			
Tumor Site	**Cell Line**	***MRE11A*[3] 11q21 (94150466 - 94227040)**	***ATM*[3] 11q22-q23 (108093559 - 108239826)**	***H2AFX*[3] 11q23.3 (118964584 - 118966177)**	***CHEK1*[3] 11q24.2 (125495031- 125546150)**
Non-small cell lung carcinoma (NSCLC)	A549	100	91	99	89
	253T	88	93	98	81
	101-87T	100	95	75	80
	84T	97	87	50	68
	CALU-1	8	11	0	3
	H1299	2	4	0	1
	54T	14	4	0	4
	201T	0	13	0	5

[1] The results are displayed in terms of variation in copy number of a gene in relation to the ploidy of each cell line as determined by chromosome 11 centromere enumeration.
[2] The numerical value represents the percentage of cells with copy number loss of specific gene.
[3] *ATM*, *MRE11A*, *H2AFX* and *CHEK1* genes are all located in the distal segment of the long arm of chromosome 11.

Table 4. Summary of the interphase FISH for relative copy number loss[1] of MRE11A and ATM genes in OvC cell lines

		Percentage of Cells with Loss of[2]	
Tumor Site	**Cell Line**	***MRE11A*[3] 11q21 (94150466 - 94227040)**	***ATM*[3] 11q22-q23 (108093559 - 108239826)**
Ovarian carcinoma (OvC)	SKOV-3	100	100
	OVCAR-3	100	100
	CP70	99	70
	ES-2	0	95
	A2780	1	0

[1] The results are displayed in terms of variation in copy number of a gene in relation to the ploidy of each cell line as determined by chromosome 11 centromere enumeration.
[2] The numerical value represents the percentage of cells with copy number loss of specific gene.
[3] *ATM* and *MRE11A* genes are located in the distal segment of the long arm of chromosome 11.

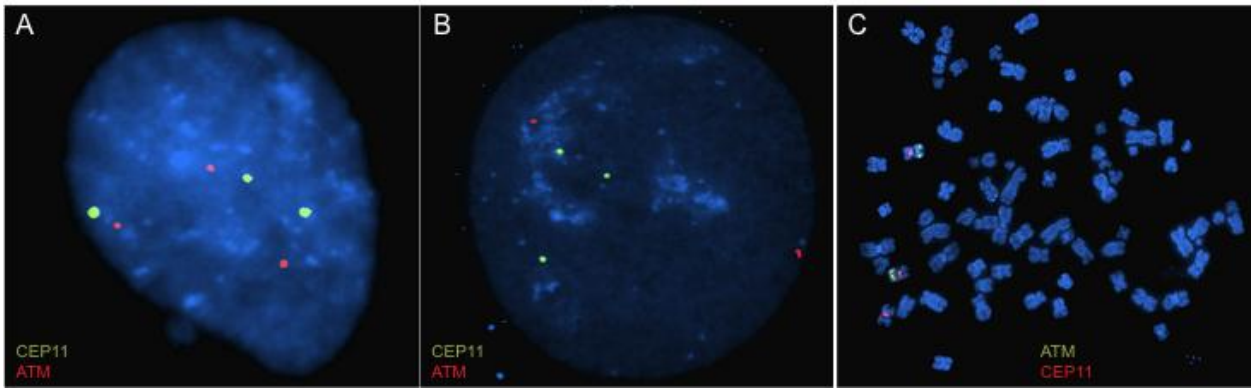

Figure 6. FISH for *ATM* in HNSCC and NSCLC cell lines

(A) demonstrates normal copy number of *ATM* compared to CEP11, (B) and (C) demonstrates loss of *ATM* copy number compared to CEP11.

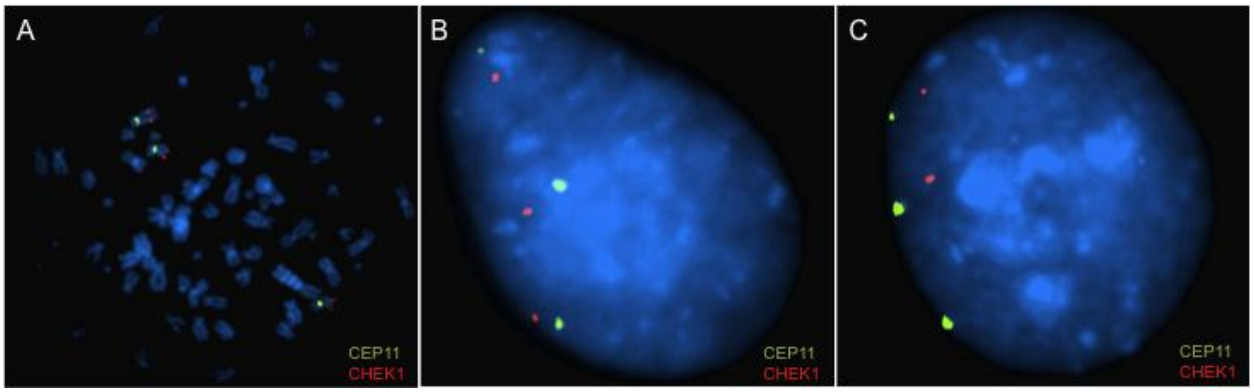

Figure 7. FISH for *CHEK1* in HNSCC and NSCLC cell lines

(A) and (B) demonstrates relative normal copy number of *CHEK1* compared to CEP11, and (C) demonstrates loss of *CHEK1* copy number compared to CEP11.

3.1.2 Loss of Distal 11q is Associated with Reduced Sensitivity to IR

The sensitivity of HNSCC, NSCLC and OvC cells to IR was assessed by clonogenic survival assay. The cell lines were divided into two groups: 'distal 11q loss' and 'no distal 11q loss.' Based on previous studies in our lab and discussions with our Radiation Oncologists, the appropriate IR doses used for our experiments were 2.5 Gy and 5 Gy. Results were reported as plots of 'Surviving Fraction' vs. radiation dose. HNSCC cell lines in the 'distal 11q loss' group (UPCI:SCC029B, 040 and 131) showed 64 ± 2% and 18 ± 1% survival at 2.5 and 5 Gy of IR, respectively, whereas cell lines in the 'no distal 11q loss' group (UPCI:SCC066, 081 and 116) showed 24 ± 2% and 2 ± 0.1% survival respectively at the same two doses (Fig. 8). These results translated to three-fold higher survival at 2.5 Gy and eight-fold higher survival at 5 Gy IR in the HNSCC cell lines with 'distal 11q loss' compared to the 'no distal 11q loss' HNSCC cell lines. Similar to our previous results (Parikh, et al. 2007), these results showed clear evidence of radioresistance (or increased survival) in HNSCC cell lines with 'distal 11q loss' cells compared to 'no distal 11q loss' HNSCC cell lines at both radiation doses tested. Hence, radioresistance appears to be associated with copy number loss of genes on distal 11q.

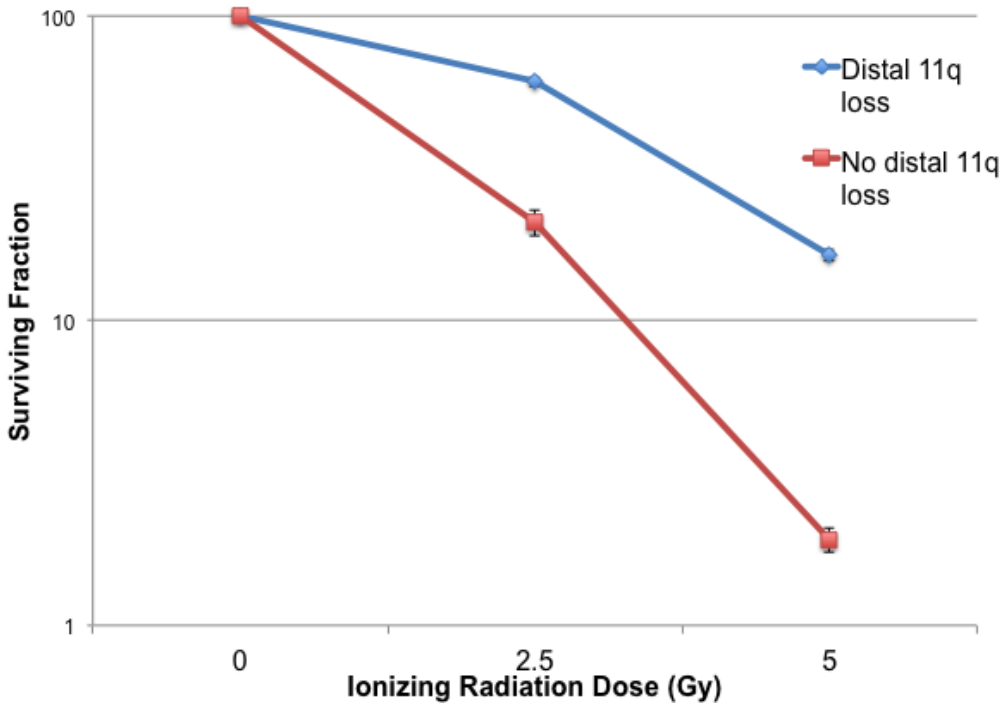

Figure 8. Clonogenic survival assay of HNSCC cell lines in response to IR

The surviving fraction of cells at specific IR doses is plotted with error bars (± SEM) on a logarithmic scale. Carcinoma cells in the "distal 11q loss" group (UPCI:SCC029B, 040 and 131) showed three-fold higher survival at 2.5 Gy and eight-fold higher survival at 5 Gy compared to cells in the "no distal 11q loss" group (UPCI:SCC066, 081 and 116).

In NSCLC cell lines, the 'distal 11q loss' group (A549, 84T, 253T and 101-87T) showed 49 ± 4% and 15 ± 2% survival at 2.5 and 5 Gy, respectively (Fig. 9). At the same two doses, the 'no distal 11q loss' group (CALU-1, H1299, 54T and 201T) showed 18 ± 2% and 4 ± 1% survival, respectively. The distal 11q loss cell lines had approximately a three-fold higher survival compared to the no loss cell lines, both at 2.5 and 5 Gy IR. Similar results were also observed in the OvC cell lines. The 'distal 11q loss' group (ES-2 and OVCAR-3) showed 70 ± 0.1% and 29 ± 2% survival at 2.5 and 5 Gy respectively, whereas A2780 (no distal 11q loss) had 24 ± 3% and 2 ± 1% survival at the same doses (Fig. 10). A three-fold higher survival was observed in the 'distal 11q loss' group at 2.5 Gy and a 17-fold higher survival at 5 Gy. Based on our findings, the reduced sensitivity to IR and loss of distal 11q seem to be strongly correlated in HNSCC, NSCLC and OvC cell lines.

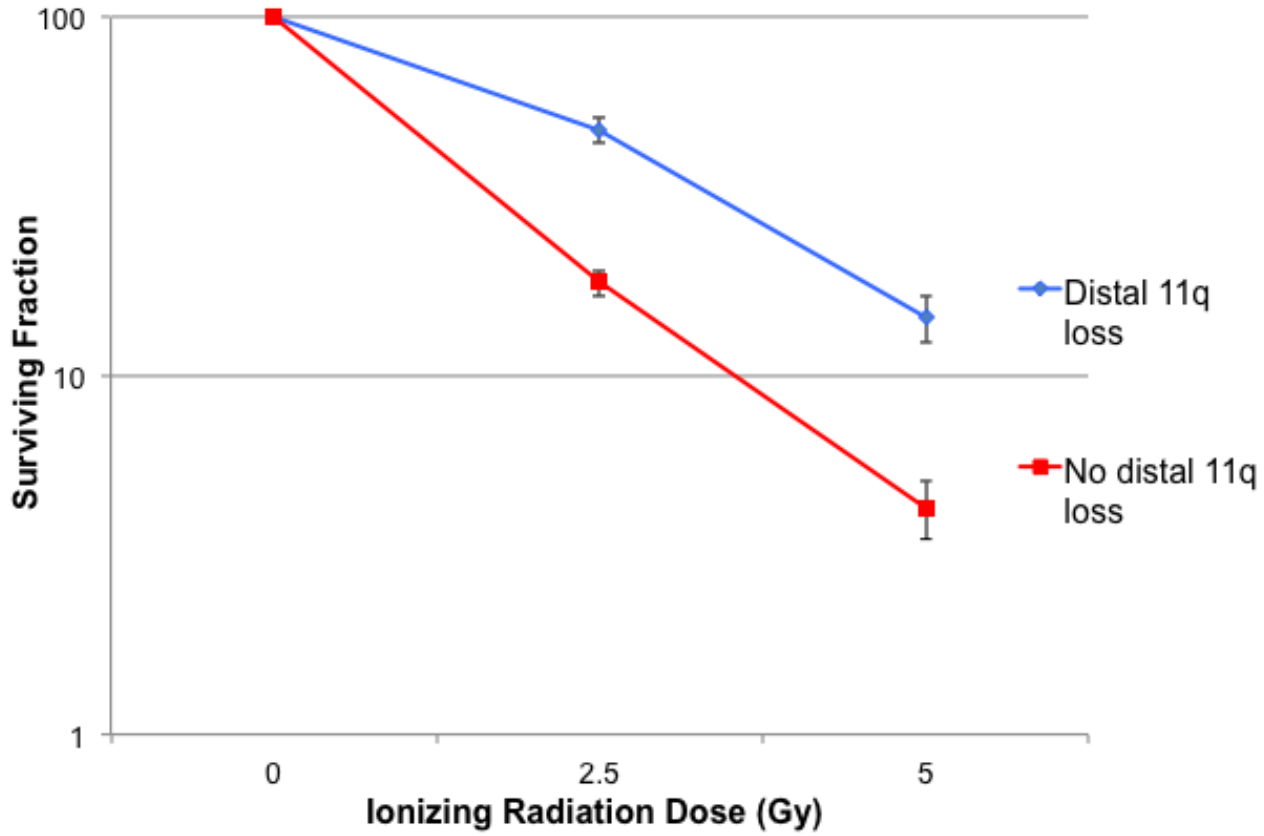

Figure 9. Clonogenic survival assay of NSCLC cell lines in response to IR

The surviving fraction of cells at specific IR doses is plotted with error bars (± SEM) on a logarithmic scale. Carcinoma cells in the "distal 11q loss" group (A549, 84T, 101-87T, 253T) showed three-fold higher survival at 2.5 and 5 Gy compared to cells in the "no distal 11q loss" group (CALU-1, H1299, 54T, 201T).

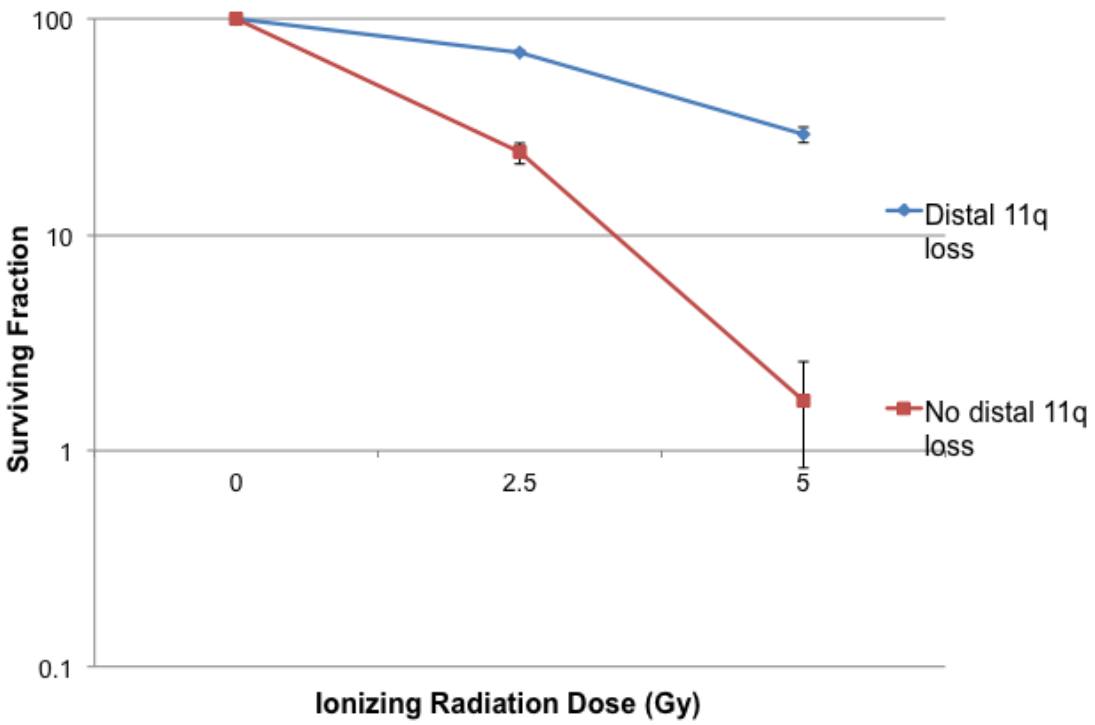

Figure 10. Clonogenic survival assay of OvC cell lines in response to IR

The surviving fraction of cells at specific IR doses is plotted with error bars (± SEM) on a logarithmic scale. Carcinoma cells in the "distal 11q loss" group (ES-2, OVCAR-3) showed three-fold higher survival at 2.5 Gy and 17-fold higher survival at 5 Gy compared to cells in the "no distal 11q loss" group (A2780).

Further, in an effort to replicate *in vivo* therapeutic strategy, in which patients get multiple low doses (2 Gy) of IR over a period up to seven weeks, we irradiated our cells plated for clonogenic survival assays with 2 Gy of IR for five days per week over a period of two weeks. Growing the cells for one rather than two weeks facilitated colony formation. In NSCLC cell lines with 'distal 11q loss,' the observed survival rate was 12 ± 2%, whereas the 'no distal 11q loss' group had a survival rate of 0.5 ± 0.2% (Fig. 11). The highest observed survival in the 'no distal 11q loss' group was in the 54T cell line, and the value was less than 1%. Therefore, the 2 Gy daily treatments were lethal in the 'no distal 11q loss' cells. These results provide further support for the correlation between loss of distal 11q and decreased sensitivity to IR.

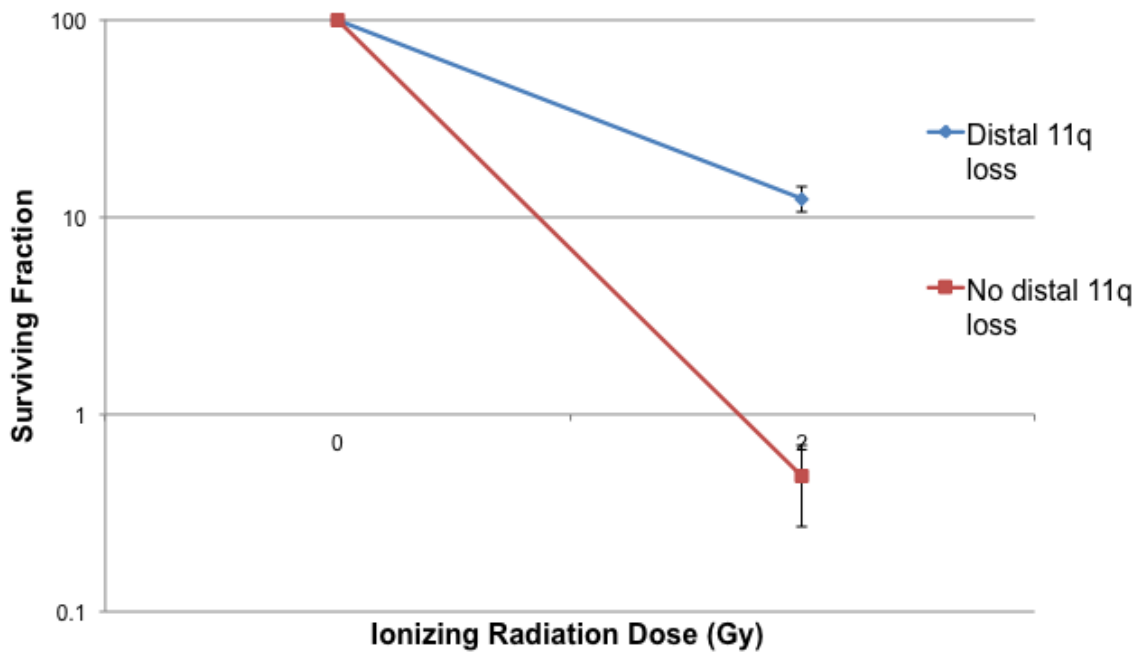

Figure 11. Clonogenic survival assay of NSCLC cell lines in response to 2 Gy treatment of IR five days per week for two weeks

The surviving fraction of cells at 2 Gy IR is plotted with error bars (± SEM) on a logarithmic scale. Carcinoma cells in the "distal 11q loss" group (A549, 101-87T, 253T) showed twice as much survival as cells in the "no distal 11q loss" group (CALU-1, 54T, 201T).

3.1.3 Loss of Distal 11q Results in Changes in Expression of *ATM* and *CHEK1*

ATM and *CHEK1* gene expression was assessed by QRT-PCR to determine whether loss of one or more copies of these genes translates into a reduction in their expression. HNSCC cell lines with distal 11q loss have been reported to exhibit a reduction in *ATM* and *H2AFX* expression relative to a control NHOK cell line and cell lines without distal 11q loss (Parikh, et al. 2007). In NSCLC, cell lines with distal 11q loss exhibited a similar decrease in expression of *ATM* and *CHEK1* compared to tumor cells without distal 11q loss (Table 5, Fig. 12).

Table 5. Relative expression of *ATM* and *CHEK1* in NSCLC cell lines

Loss of distal 11q status	Cell line	Relative *ATM* Expression	Relative *CHEK1* Expression
No loss	54T	2.24	1.75
	201T	3.69	4.69
	273T	5.11	5.65
Loss	84T	1.8	1.99
	253T	2.08	1.26
	A549	2.31	1.75

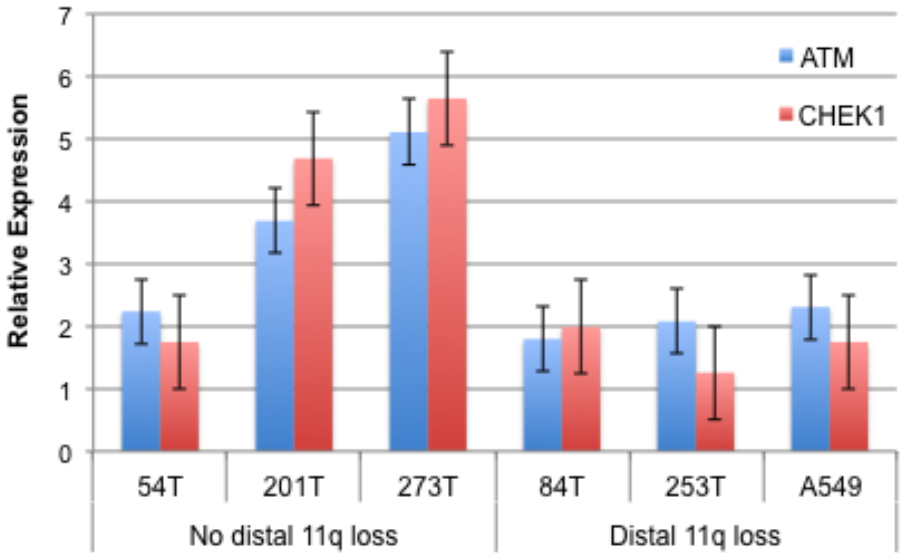

Figure 12. Relative expression of *ATM* and *CHEK1* in NSCLC cell lines

QRT-PCR was carried out for *ATM* and *CHEK1* genes. Loss of copy number of these two genes resulted in relatively lowered expression of *ATM* and *CHEK1* in cells compared to expression levels in cells without loss of distal 11q.

Immunoblotting for CHEK1 protein revealed that in untreated HNSCC and NSCLC cells, there was no strong correlation observed between CHEK1 protein expression and distal 11q loss as was seen between *CHEK1* gene expression and distal 11q loss. HNSCC cell lines with loss of distal 11q (UPCI:SCC029B, 040, 104, 131) showed relatively lower CHEK1 expression compared to HNSCC cell lines without loss of distal 11q (UPCI:SCC066, 081, 116) (Fig. 13). Another cell line, UPCI:SCC136 (loss of distal 11q), had a higher CHEK1 expression than

UPCI:SCC116. Similarly, NSCLC cell lines with loss of distal 11q (A549, 101-87T, 253T) also showed relatively reduced CHEK1 expression compared to tumor cell lines without loss of distal 11q (54T, CALU-1 and H1299).

Thus, copy number loss of distal 11q leads to relatively reduced RNA expression of *ATM*, and relative reduced RNA and protein expression of CHEK1 in HNSCC and NSCLC cell lines.

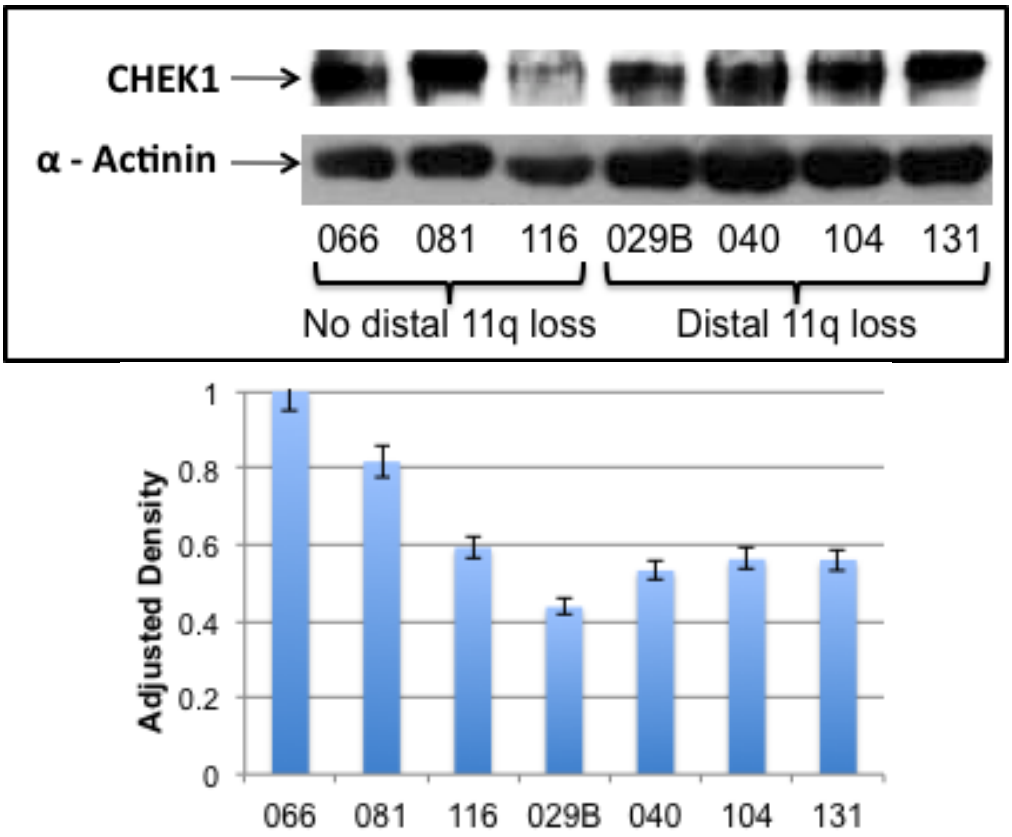

Figure 13. Protein expression of CHEK1 and densitometric analysis of expression in HNSCC cell lines

CHEK1 expression assessed by immunoblotting showed that cells with loss of distal 11q had a relative lower expression of CHEK1 compared to cells without loss of distal 11q.

3.1.4 Loss of Distal 11q is Associated with Increased Mitotic Defects in HNSCC but not NSCLC

To assess mitotic defects in HNSCC and NSCLC cell lines after treatment with IR, we measured the frequency of micronuclei, and anaphase and interphase bridges. Micronuclei and interphase bridges are manifestations of anaphase bridges and are markers of genotoxic stress and chromosomal instability. The presence of these defects suggests misrepaired or unrepaired DNA breaks (Acilan, et al. 2007; Fenech, et al. 2011). The frequency of each aberration type with and without IR treatment is represented in Figures 11 and 12. Our results show that in HNSCC cells with loss of distal 11q, there is a greater than two-fold increase in micronuclei and a 10-fold increase in interphase bridges 18 and 36 h post-irradiation compared to tumor cells without distal 11q loss (Fig. 14). No significant accumulation of anaphase bridges was observed in either group of cell lines. In NSCLC cell lines, there was no significant difference in the frequency of measured mitotic defects (Fig. 15). Hence, HNSCC cells but not NSCLC cells with loss of distal 11q have defective or diminished DDR to damage induced by IR compared to tumor cells without 11q loss.

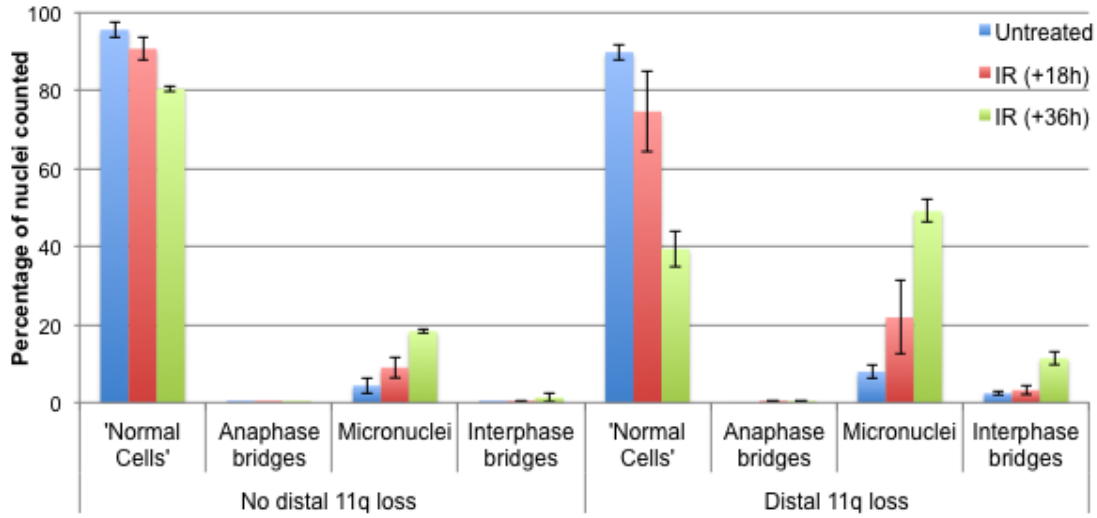

Figure 14. Frequency of mitotic defects in treated and untreated HNSCC cell lines

Presence of mitotic defects was assessed in two HNSCC cell lines each, with and without distal 11q loss. Cells with distal 11q loss showed an increased accumulation of micronuclei and interphase bridges after IR-induced damage compared to cells without distal 11q loss.

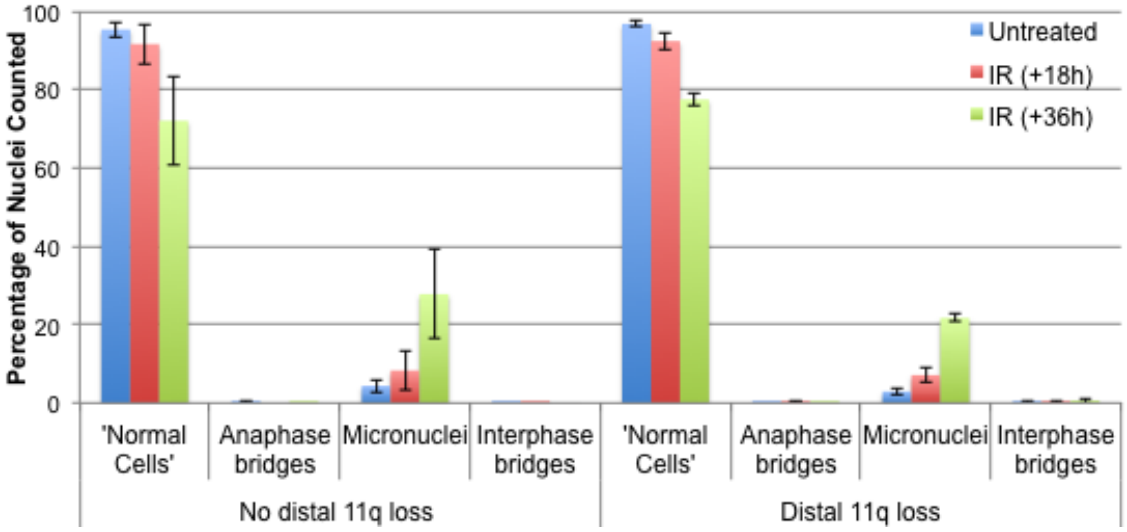

Figure 15. Frequency of mitotic defects in treated and untreated NSCLC cell lines

Presence of mitotic defects was assessed in two NSCLC cell lines each, with and without distal 11q loss. Cells with distal 11q loss did not show a significant difference in accumulation of micronuclei and interphase bridges after IR-induced damage compared to cells without distal 11q loss.

3.2 UPREGULATED ATR-CHEK1 PATHWAY

3.2.1 The ATR-CHEK1 Pathway is Upregulated in HNSCC Cell Lines With Loss of Distal 11q

Copy number loss of *MRE11A, ATM, H2AFX*, and *CHEK1* on distal 11q resulted in decreased expression of these genes and their proteins (Parikh, et al. 2007). This observation combined with the radioresistant phenotype suggests that a decrease in the ATM pathway results in increased activity of a compensatory pathway in the cells with distal 11q loss. We evaluated the activity of the related ATR-CHEK1 pathway by examining the protein expression of CHEK1 in response to IR. HNSCC cell lines with distal 11q loss, when treated with IR showed an increase in CHEK1 expression 6 h after radiation compared to cell lines without distal 11q loss (Fig. 16). This suggests upregulation of the ATR-CHEK1 pathway after irradiation in HNSCC cells with loss of distal 11q.

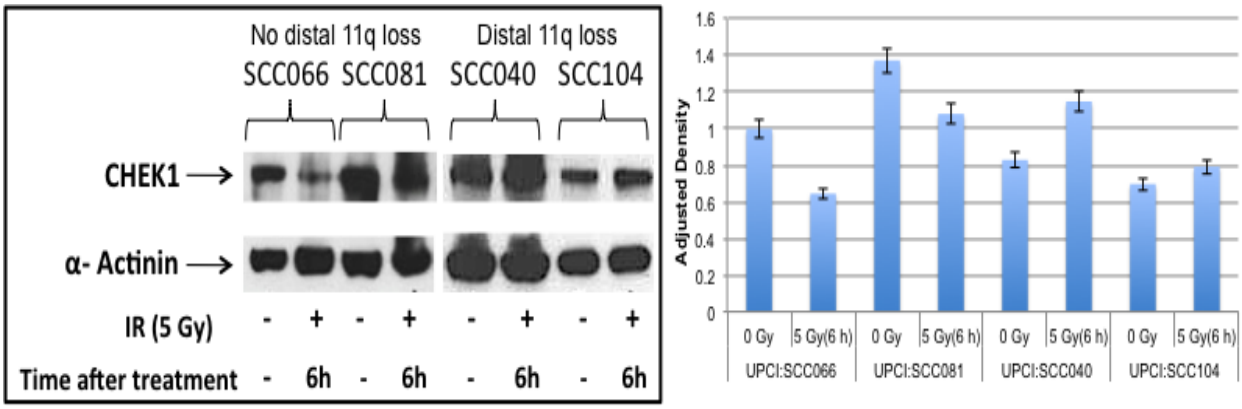

Figure 16. Total CHEK1 expression in response to IR in HNSCC cells

Total CHEK1 expression assessed by immunoblotting showed that CHEK1 expression in response to IR was increased in HNSCC cells with loss of distal 11q compared to HNSCC cells without distal 11q loss.

3.2.2 Increased ATR-dependent Phosphorylation of CHEK1 in Tumor Cells With Loss of Distal 11q

The phosphorylation status of CHEK1 was examined using antibodies against the phosphorylation sites ser345 and ser317 to confirm upregulation of the ATR-CHEK1 pathway. Ser345 phosphorylation is necessary for CHEK1 activation and a proper checkpoint response after DNA damage. This phosphorylation also promotes nuclear retention of CHEK1 (Jiang, et al. 2003; Niida, et al. 2007). Ser317 phosphorylation is required for subsequent ser345 phosphorylation in response to DNA damage (Wang, et al. 2012). Early phosphorylation of ser345 is thought to occur in an ATR-dependent manner, whereas phosphorylation of ser317 in response to IR is reported to be dependent on ATM and NBS1 (Gatei, et al. 2003; Wang, et al. 2012). As predicted, HNSCC and NSCLC cells with loss of distal 11q showed an increase in CHEK1 ser345 phosphorylation after IR, which was absent in the cells without distal 11q loss (Fig. 17). In HNSCC and NSCLC cells without loss of distal 11q, ATM appears to be primarily responsible for the DDR and hence, the phosphorylation of CHEK1 ser317 was increased in these cells. There was also an observable increase in ser317 phosphorylation in tumor cells with distal 11q loss, since they retain some ATM expression (Figs. 18 and 19). Densitometric analysis of expression did not show a significant correlation between the level of phosphorylation and loss of distal 11q. All cell lines have a base line level of protein expression that varies considerably, and therefore, an absolute number for protein expression cannot be used as a marker for identifying increased activity of the ATR-CHEK1 pathway. Increased phosphorylation of ser345 exclusively in tumor cells with loss of distal 11q confirms increased activity of the ATR-CHEK1 pathway in response to IR in these cells compared to those without loss of distal 11q. Increased phosphorylation of ser317 in tumor cells with and without distal 11q

loss suggests that in response to IR ATM is activated in all cell lines. Hence, this upregulated ATR-CHEK1 pathway might be responsible for the radioresistant phenotype observed in tumor cells with loss of distal 11q.

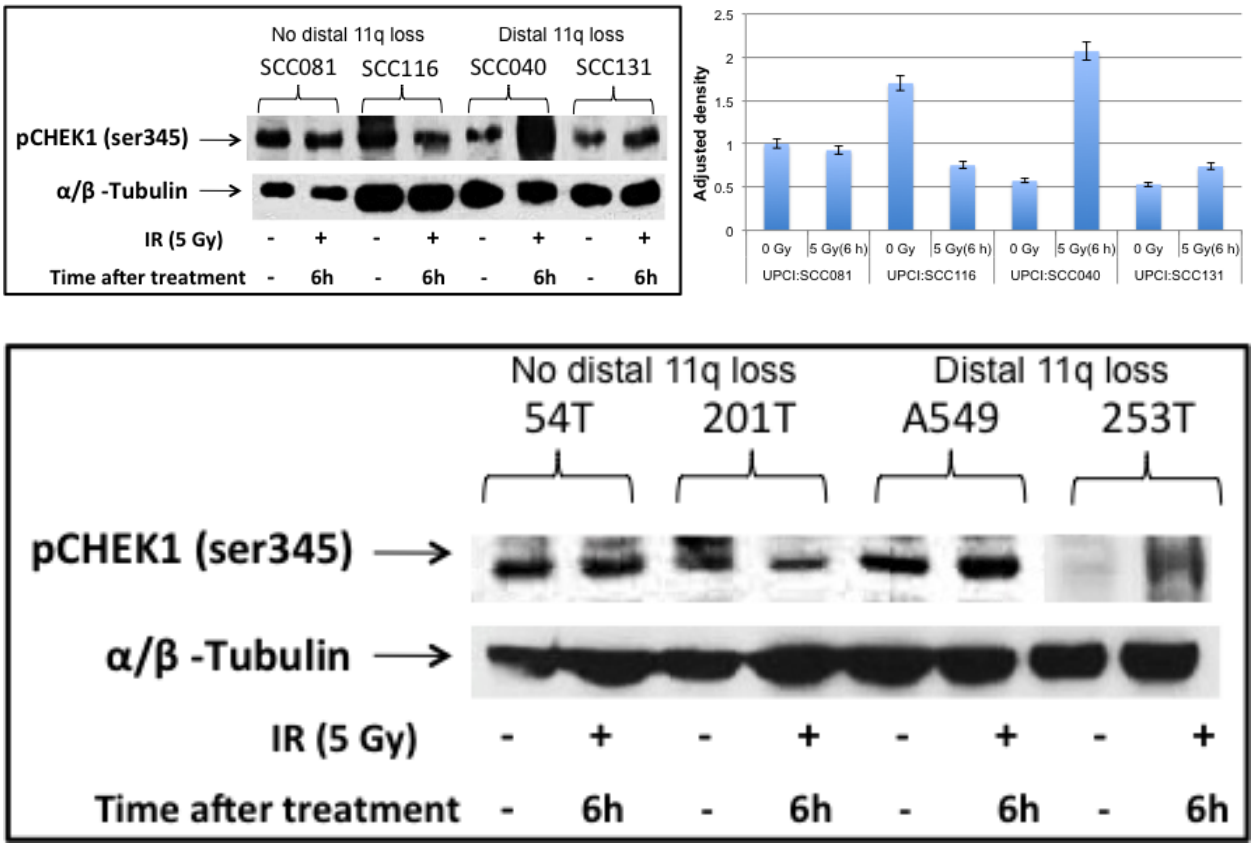

Figure 17. CHEK1 phosphorylation at ser345 in response to IR in HNSCC and NSCLC cells

Immunoblotting for phosphorylated CHEK1 6 h post-IR treatment demonstrates increased phosphorylation of CHEK1 at ser345 at this timepoint only in HNSCC and NSCLC cells with loss of distal 11q.

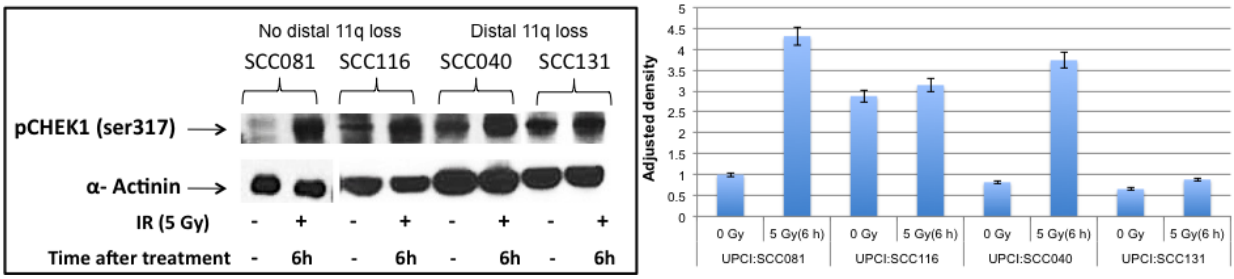

Figure 18. CHEK1 phosphorylation at ser317 in response to IR in HNSCC cells

Immunoblotting for phosphorylated CHEK1 6 h post-IR treatment demonstrates increased phosphorylation of CHEK1 at ser317 at this timepoint in HNSCC cells with and without loss of distal 11q.

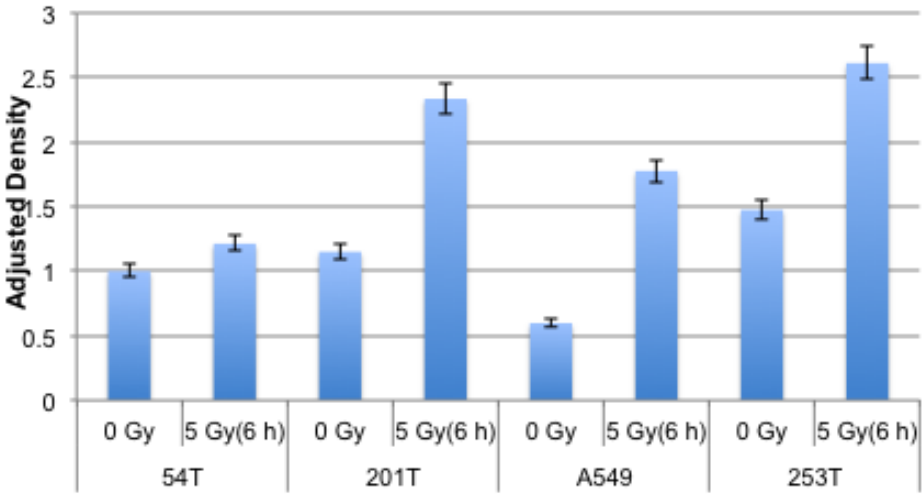

Figure 19. Densitometric analysis of CHEK1 phosphorylation at ser317 in response to IR in NSCLC cells

Densitometric analysis of phosphorylated CHEK1 expression 6 h post-IR treatment demonstrates increased phosphorylation of CHEK1 at ser317 at this timepoint in NSCLC cells with and without loss of distal 11q.

3.2.3 Increased Phosphorylation of CDC25C Due to an Upregulated ATR-CHEK1 Pathway

We also evaluated the downstream signaling efficiency of the ATR-CHEK1 pathway by assessing the phosphorylation status of CDC25C on ser216 in response to 5 Gy IR treatment.

Phosphorylation of CDC25C is thought to prevent the activation of Cyclin B/CDK1 complex and G_2 arrest. Increased phosphorylation of CDC25C was previously reported in UPCI:SCC104 (distal 11q loss) compared to UPCI:SCC066 (no distal 11q loss) (unpublished data). In NSCLC cell lines, 84T (loss of distal 11q) cells showed an increase in ser216 phosphorylation within one hour of IR treatment, and this phosphorylation was maintained for eight hours post-treatment (Fig. 20). At 16 hours after IR treatment, these cells showed a decrease in phosphorylation. In an NSCLC cell line without loss of distal 11q (201T), CDC25C was not phosphorylated at ser216 at either of the two early timepoints (1 or 8 h) after IR. There was an increase in phosphorylation at 16 h after IR in these cells. This is consistent with our earlier results and confirms the increased early activation and upregulation of the ATR-CHEK1 pathway in tumor cells with distal 11q loss.

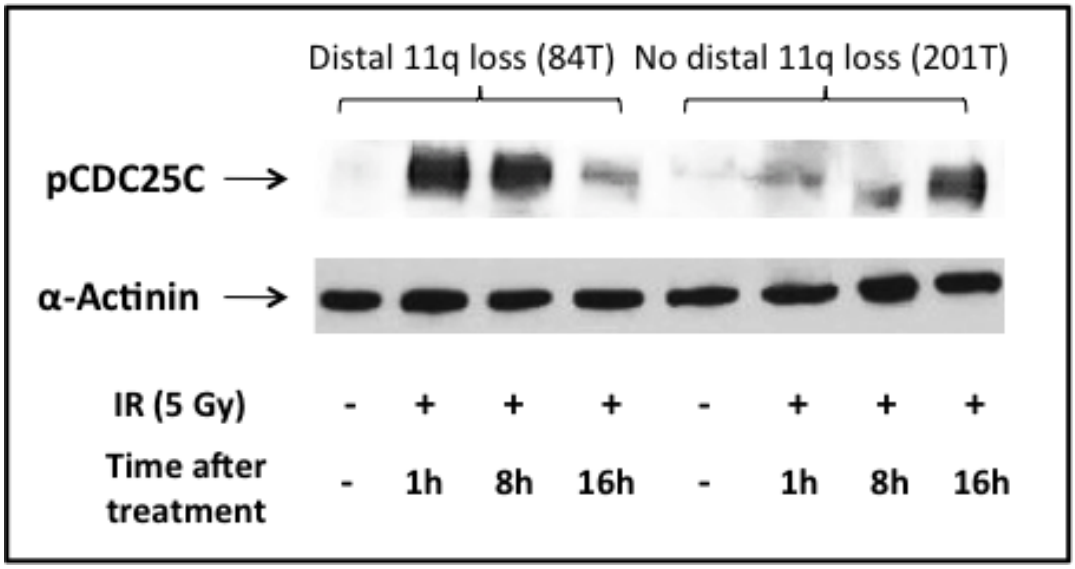

Figure 20. CDC25C phosphorylation at ser216 in response to IR in NSCLC cells

Immunoblotting for phosphorylated CDC25C after IR treatment demonstrates increased phosphorylation of CDC25C at ser216 at two and eight hours post-IR in NSCLC cells with loss of distal 11q. In NSCLC cells without loss of distal 11q, there was a delayed (16 h post-IR) increase of CDC25C phosphorylation.

3.2.4 Distal 11q Loss is Associated with Increased S and G_2M checkpoint arrest after IR in HNSCC Cells, but not in NSCLC Cells

To study the cell cycle profiles of HNSCC, NSCLC and OvC cells in response to DNA damaging agents, flow cytometry was carried out on cell lines treated with 5 Gy IR (Tables 6 and 7). Dr. Rahul Parikh reported a loss of the G_1 checkpoint and increased G_2M accumulation after treatment with IR in five of eight cell lines tested. Each of these five cell lines also had distal 11q loss (unpublished data). In NSCLC cells, tumor cells with loss of distal 11q (A549, 101-87T, 253T) did not accumulate in the G_2M phase after treatment with IR. There was no observed loss of the G_1 checkpoint either. Two of three NSCLC cells without distal 11q loss (54T, CALU-1) did show a loss of the G_1 checkpoint and G_2M accumulation after treatment with IR. A third cell line without distal 11q loss did not show either of the two characteristics. Cell cycle profile after treatment with IR was also tested in two OvC cell lines, one each with and without loss of distal 11q. ES-2 (distal 11q loss) cells showed loss of the G_1 checkpoint and G_2M accumulation, similar to HNSCC cells with distal 11q loss. A2780 (no distal 11q loss) cells did not show a significant loss of the G_1 checkpoint or G_2M accumulation. The ATR-CHEK1 pathway is known to control the S and G_2M checkpoints, and upregulation of this pathway in the HNSCC and OvC cells with distal 11q loss might contribute to the accumulation of cells at the G_2M checkpoint in response to DNA damage induced by IR. Unlike in HNSCC cells with distal 11q loss, G_2M checkpoint arrest may not contribute to the radioresistant phenotype in NSCLC cells with distal 11q loss and an upregulated ATR-CHEK1 pathway.

Table 6. Cell cycle analysis in NSCLC cells in response to IR

Cell lines	Distal 11q loss status	Untreated			5 Gy IR (24 h)		
		G0/G1	S	G2/M	G0/G1	S	G2/M
54T	No loss	64	19	16	34	25	40
CALU-1	No loss	66	11	22	33	10	57
201T	No loss	73	14	7	70	15	11
101-87T	Loss	80	8	12	80	4	16
253T	Loss	86	6	5	90	4	4
A549	Loss	78	8	11	77	7	14

Table 7. Cell cycle analysis in OvC cells in response to IR

Cell lines	Distal 11q loss status	Untreated			5 Gy IR (24 h)		
		G0/G1	S	G2/M	G0/G1	S	G2/M
A2780	No loss	71	13	14	59	13	25
ES-2	Loss	79	10	10	35	26	38

3.3 INHIBITION OF THE ATR-CHEK1 PATHWAY RESENSITIZES TUMOR CELLS WITH LOSS OF DISTAL 11Q TO IR

3.3.1 Knocking Down the ATR-CHEK1 Pathway Resensitizes Tumor Cells to DNA Damage Induced by IR

We have shown that the ATR-CHEK1 pathway is associated with the radioresistant phenotype observed in our cell lines with distal 11q loss. To confirm the role of the ATR-CHEK1 pathway in radioresistance in cells with distal 11q loss, we used siRNA specific to *ATR*, *CHEK1* and *RAD9A* to knock down their expression in cell lines and assess the effect of this knockdown on resistance. RAD9A is a part of the 9-1-1 complex that is involved in sensing DNA damage and signaling to the ATR-CHEK1 pathway. Hence, *RAD9A* inhibition was also carried out with *ATR* and *CHEK1* inhibition to assess the effect of knockdown at all three levels of the DDR (sensing, transduction and effector functions). CHEK1 expression was inhibited to a high level (~ 90%) after knockdown using siRNA specific to *CHEK1*, while a scrambled non–specific siRNA did not inhibit CHEK1 expression after 72 h, assessed by QRT-PCR and immunoblotting (Fig. 21). Similarly, *ATR* and *RAD9* knockdown also resulted in high levels of inhibition of the expression of these two genes. The effect of inhibiting the ATR-CHEK1 pathway on sensitivity to IR was assessed by clonogenic survival assays. Cells in the clonogenic survival assay were divided into three groups – 'Untreated,' 'Mock-transfected,' and 'siRNA-transfected.' The 'Mock-transfected' group represents the average survival values for the two controls, one a control treated with transfection reagent, Lipofectamine 2000, and the other control treated with a pool of non-specific siRNA. To maximize siRNA-based knockdown, cells were plated for clonogenic survival assay 48-72 hours post-transfection and treated with IR 72-96 h post-transfection.

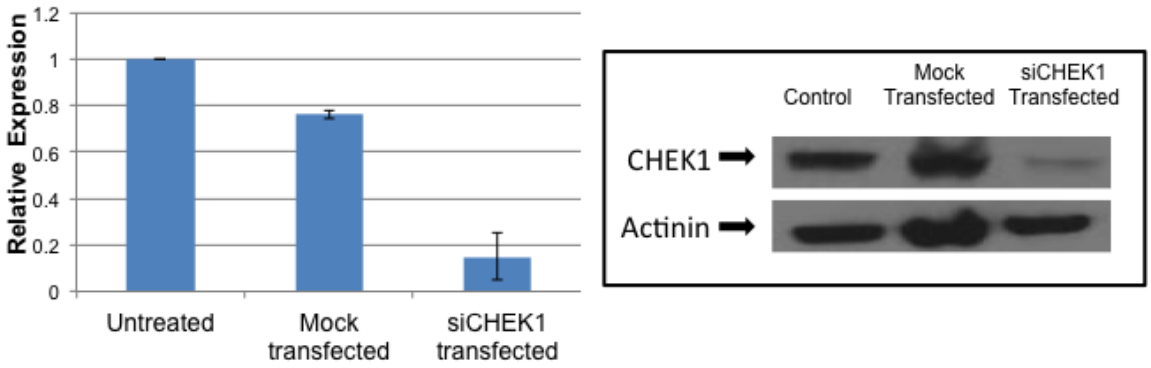

Figure 21. CHEK1 expression after siRNA-based knockdown in tumor cells

QRT-PCR and Western blotting to assess CHEK1 expression after siRNA-based knockdown demonstrates that tumor cells did have a stable knockdown of CHEK1 gene and protein expression 72 h after transfection with siRNA.

The survival of 'Untreated' HNSCC cells from the 'Distal 11q loss' group (UPCI:SCC040, UPCI:SCC029B and UPCI:SCC131) was 66 ± 0.2% and 19 ± 0.1% at 2.5 and 5 Gy of IR, respectively (Fig. 22). 'Mock-transfected' cells showed a slight, but not statistically significant decrease in survival compared to the 'Untreated' cells. The survival of 'si*CHEK1*-transfected' cells was 30 ± 6% and 6 ± 2% at 2.5 and 5 Gy of IR, respectively. The results show that half as many HNSCC cells with distal 11q loss survived an IR dose of 2.5 Gy after transfection with *CHEK1* siRNA compared to cells without 11q loss. Radiation treatment of 5 Gy resulted in three-fold lowered survival in CHEK1 siRNA transfected cells with distal 11q loss compared to untreated and mock-transfected cells. No significant difference in survival was observed between the three treatment conditions in tumor cells without distal 11q loss. Similarly, *ATR* and *RAD9A* knockdown resulted in resensitization exclusively of tumor cells with distal 11q loss to radiation treatment. *ATR* inhibition in HNSCC cells with loss of distal 11q (UPCI:SCC029B, 040 and 131) showed a four-fold decrease in survival at 2.5 Gy and a 10-fold decrease at 10 Gy (Fig. 23). *RAD9A* inhibition showed a two-fold decrease in survival at 2.5 Gy in tumor cell line with loss of distal 11q (UPCI:SCC029B) (Fig. 24). HNSCC cells without loss of distal 11q (UPCI:SCC116) did not show a significant difference in survival after *ATR* or

RAD9A inhibition. The knockdown of *ATR*, *CHEK1* and *RAD9A* expression by siRNA transfection showed that inhibiting the activity of the ATR-CHEK1 pathway can reverse the radioresistance phenotype in HNSCC cells.

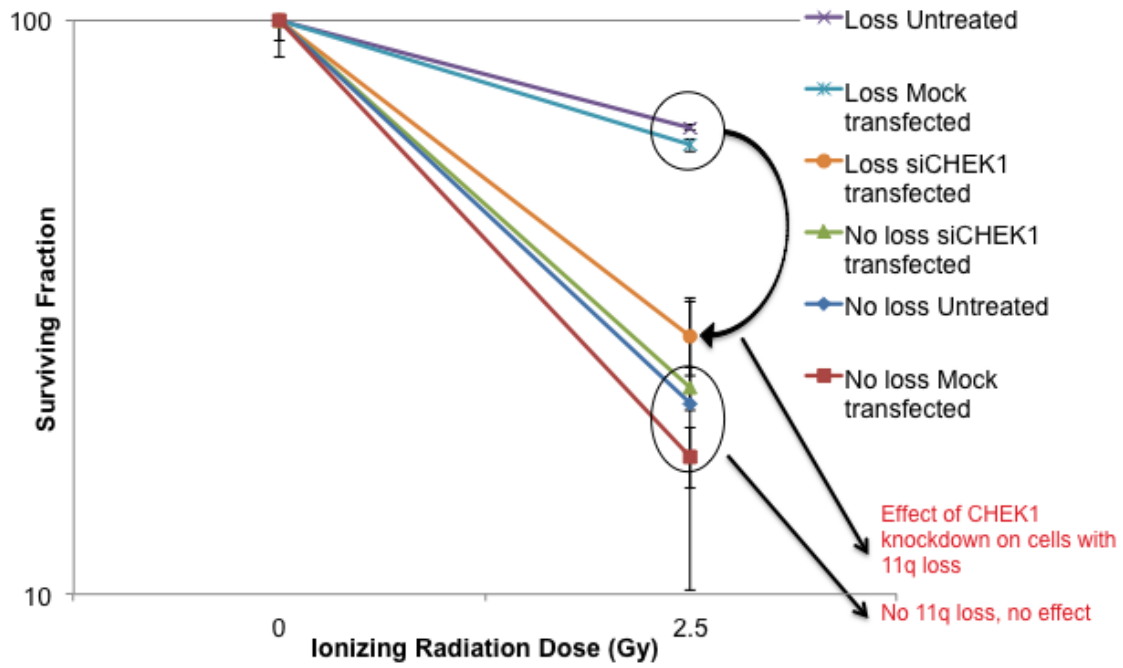

Figure 22. Clonogenic survival assay in response to IR after siRNA-based *CHEK1* knockdown in HNSCC cells

The surviving fraction of cells at 0 and 2.5 Gy IR for the three conditions (untreated, mock-transfected and si*CHEK1*-transfected) is plotted with error bars (± SEM) on a logarithmic scale. HNSCC cells transfected with si*CHEK1* in the 'distal 11q loss' group (UPCI:SCC029B, 040, 131) showed two-fold decrease in survival compared to the untreated and mock-transfected cells. Cells without distal 11q loss (UPCI:SCC116) did not show any significant difference in survival between the three conditions.

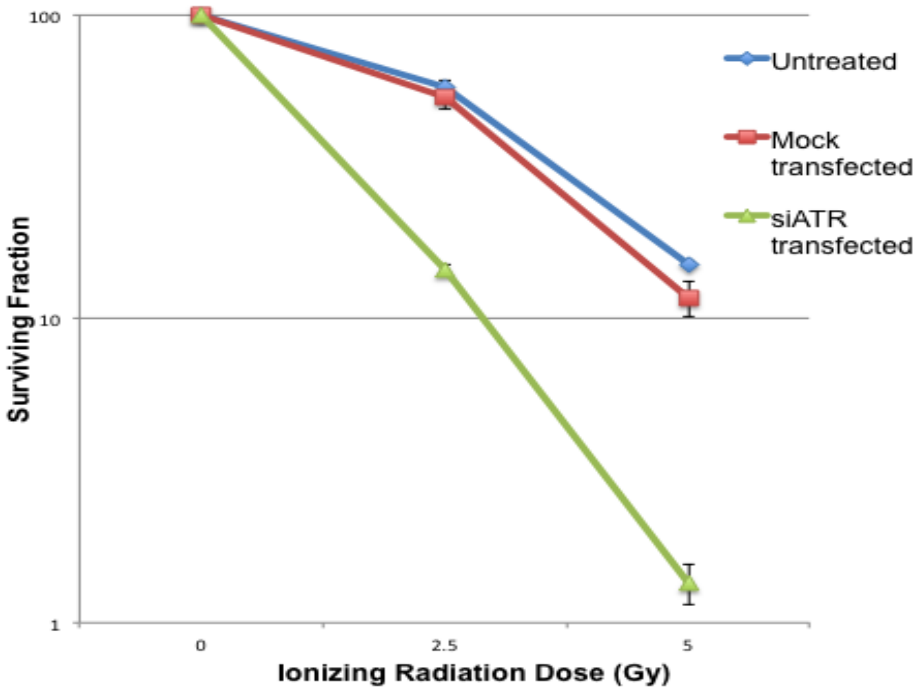

Figure 23. Clonogenic survival assay in response to IR after siRNA-based *ATR* knockdown in HNSCC cells with loss of distal 11q

The surviving fraction of cells at 0, 2.5 and 5 Gy IR for the three conditions (untreated, mock-transfected and si*ATR*-transfected) is plotted with error bars (± SEM) on a logarithmic scale. HNSCC cells transfected with si*ATR* in the 'distal 11q loss' group (UPCI:SCC029B, 040, 131) showed four-fold decrease in survival at 2.5 Gy and 10-fold decrease at 5 Gy compared to the untreated and mock-transfected cells.

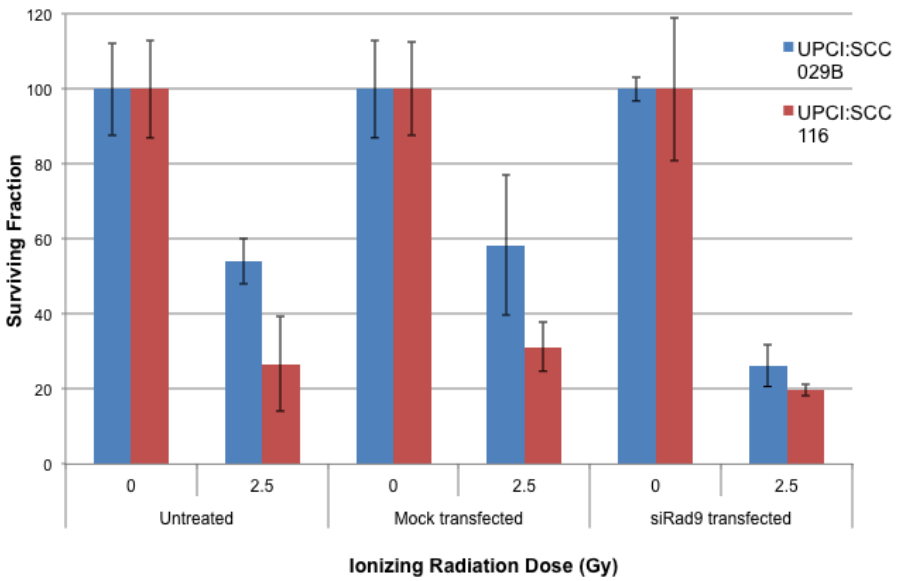

Figure 24. Clonogenic survival assay in response to IR after siRNA-based *RAD9A* knockdown in HNSCC cells

The surviving fraction of cells at 0 and 2.5 Gy IR for the three conditions (untreated, mock-transfected and si*RAD9A*-transfected) is plotted with error bars (± SEM). HNSCC cell line with distal 11q loss (UPCI:SCC029B) transfected with si*RAD9A* showed two-fold decrease in survival at 2.5 Gy compared to the untreated and mock-transfected cells. Cells without distal 11q loss (UPCI:SCC116) did not show any significant difference in survival between the three conditions.

Similar results were observed in NSCLC cell lines. 'Untreated' cells from the 'Distal 11q loss' group (A549, 101-87T, 253T, 84T) survived 46 ± 3% and 13 ± 0.5% at 2.5 and 5 Gy of IR, respectively. The 'Mock-transfected' group did show a slight, but not significant reduction in survival rate. 'si*CHEK1*-transfected' group survived 14 ± 1% and 2 ± 0.6% at 2.5 and 5 Gy of IR, respectively (Fig. 25). This translates to a three-fold decrease in survival at 2.5 Gy and six-fold decrease in survival at 5 Gy after transfection. Cells without distal 11q loss (54T, 201T, CALU-1) did not show any significant difference in survival between the three experimental categories (Fig. 25). *ATR* knockdown in NSCLC cells with distal 11q loss resulted in a two-fold decrease in survival at 2.5 Gy and a three-fold decrease in survival at 5 Gy (Fig. 26). This inhibition did not result in a significant difference in survival after IR in NSCLC cells without

loss of distal 11q (CALU-1, 201T, 54T). *RAD9A* inhibition also resulted in a two-fold decrease in survival at 2.5 Gy in NSCLC cell line with loss of distal 11q (253T), whereas tumor cell line without loss of distal 11q (54T) did not show a significant difference in survival after IR (Fig. 27).

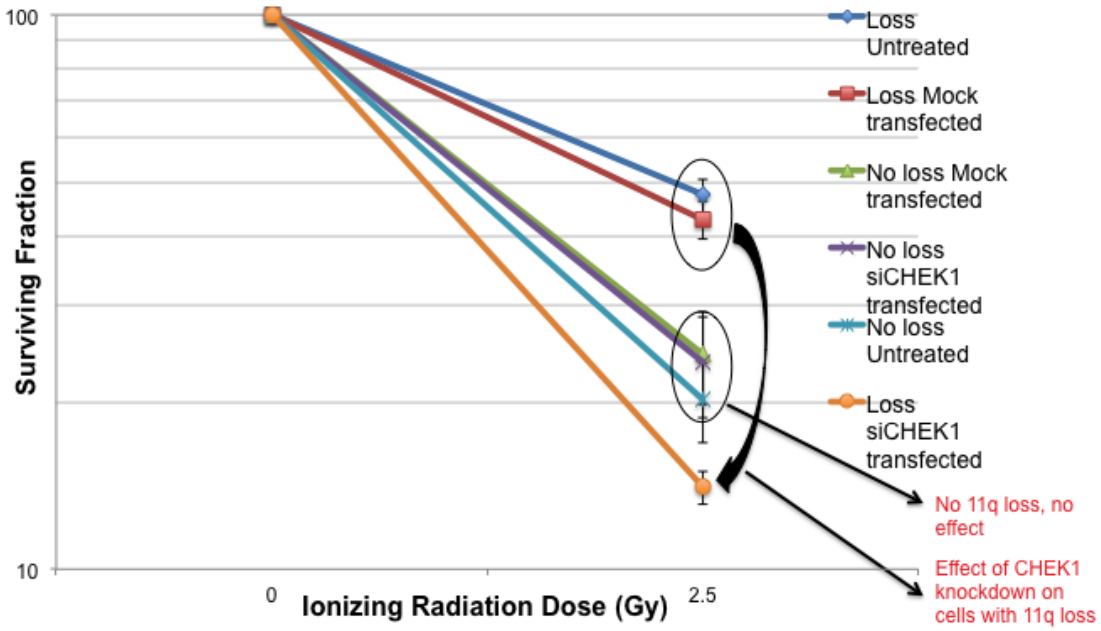

Figure 25. Clonogenic survival assay in response to IR after siRNA-based *CHEK1* knockdown in NSCLC cells

The surviving fraction of cells at 0 and 2.5 Gy IR for the three conditions (untreated, mock-transfected and si*CHEK1*-transfected) is plotted with error bars (± SEM) on a logarithmic scale. NSCLC cells transfected with si*CHEK1* in the 'distal 11q loss' group (A549, 84T, 101-87T, 253T) showed three-fold decrease in survival compared to the untreated and mock-transfected cells. NSCLC cells without distal 11q loss (CALU-1, 54T, 201T) did not show any significant difference in survival between the three conditions.

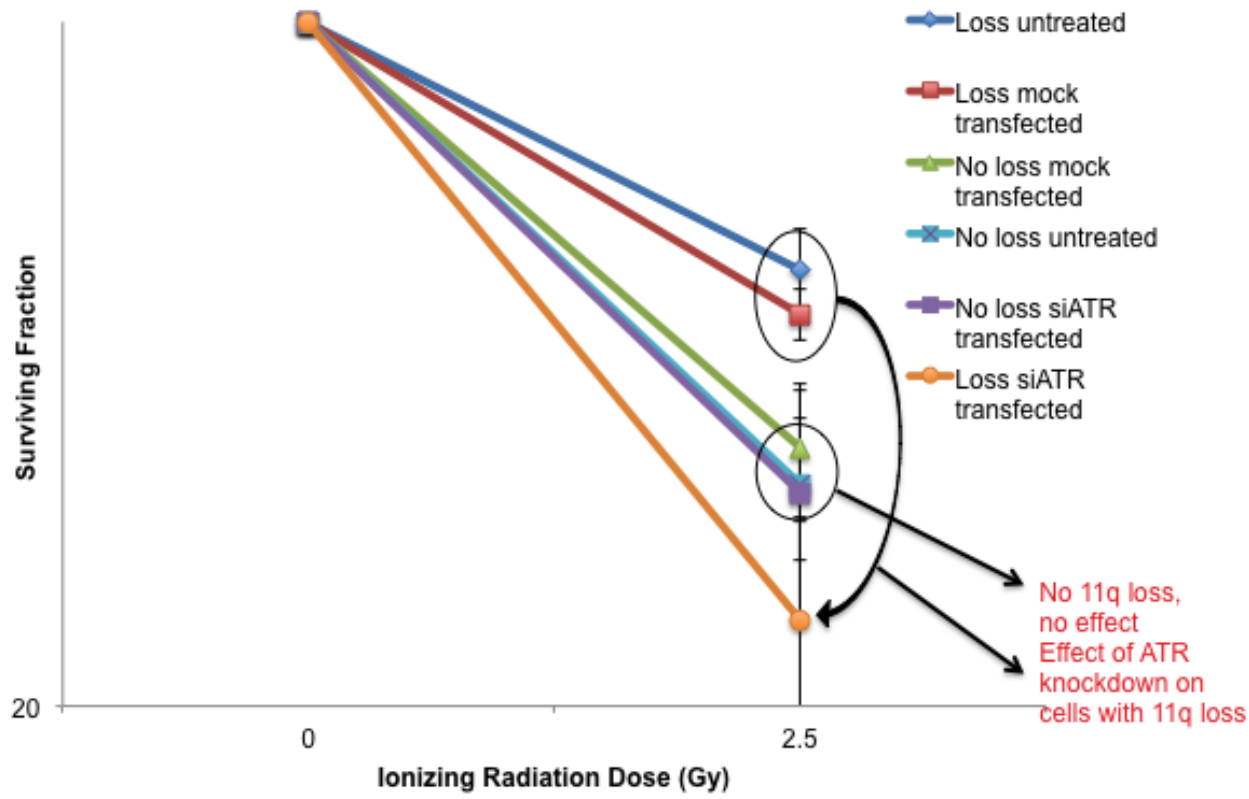

Figure 26. Clonogenic survival assay in response to IR after siRNA-based *ATR* knockdown in NSCLC cells

The surviving fraction of cells at 0, 2.5 and 5 Gy IR for the three conditions (untreated, mock-transfected and si*ATR*-transfected) is plotted with error bars (± SEM) on a logarithmic scale. NSCLC cells transfected with si*ATR* in the 'distal 11q loss' group (A549, 101-87T, 253T) showed two-fold decrease in survival at 2.5 Gy and three-fold decrease at 5 Gy compared to the untreated and mock-transfected cells. NSCLC cells without distal 11q loss (CALU-1, 54T, 201T) did not show any significant difference in survival between the three conditions.

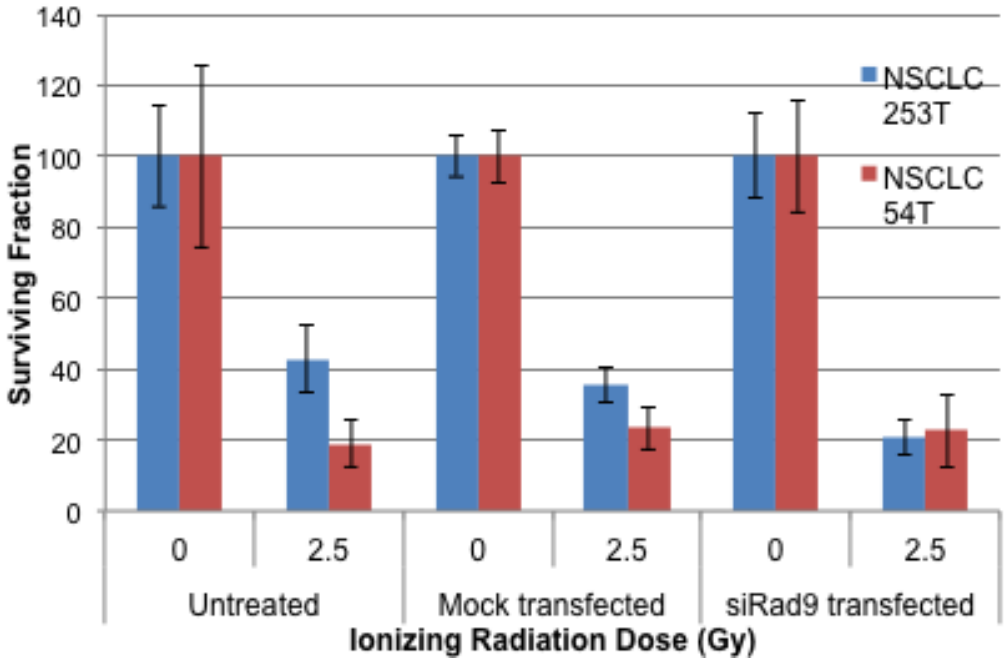

Figure 27. Clonogenic survival assay in response to IR after siRNA-based RAD9A knockdwon in NSCLC cells

The surviving fraction of cells at 0 and 2.5 Gy IR for the three conditions (untreated, mock-transfected and si*RAD9A*-transfected) is plotted with error bars (± SEM). NSCLC cells with distal 11q loss (253T) transfected with si*RAD9A* showed four-fold decrease in survival at 2.5 Gy and 10-fold decrease at 5 Gy compared to the untreated and mock-transfected cells. Cells without distal 11q loss (54T) did not show any significant difference in survival between the three conditions.

Clonogenic survival assay in response to IR after *CHEK1* knockdown was also done in OvC cell lines. OvC cell line, ES2 (Distal 11q loss), also was resensitized to IR after *CHEK1* knockdown. When treated with 2.5 Gy IR, si*CHEK1*-transfected ES2 cells (13 ± 4%) showed a four-fold decrease in survival when compared to the untreated cells (58 ± 6%) and mock-transfected cells (49 ± 4%) (Fig. 28). Similar to the HNSCC and NSCLC cell lines, OvC cell line, A2780 (No distal 11q loss) did not exhibit any significant reduction in survival after transfection. CHEK1 knockdown resulted in increased sensitivity to IR in NSCLC and OvC tumor cells with loss of distal 11q.

Since inhibition of the ATR-CHEK1 pathway resulted exclusively in resensitization of tumor cells with loss of distal 11q to radiation treatment, these results suggest that upregulation

of the ATR-CHEK1 pathway plays a direct role in the radioresistance phenotype observed in HNSCC, NSCLC and OvC cells with loss of distal 11q.

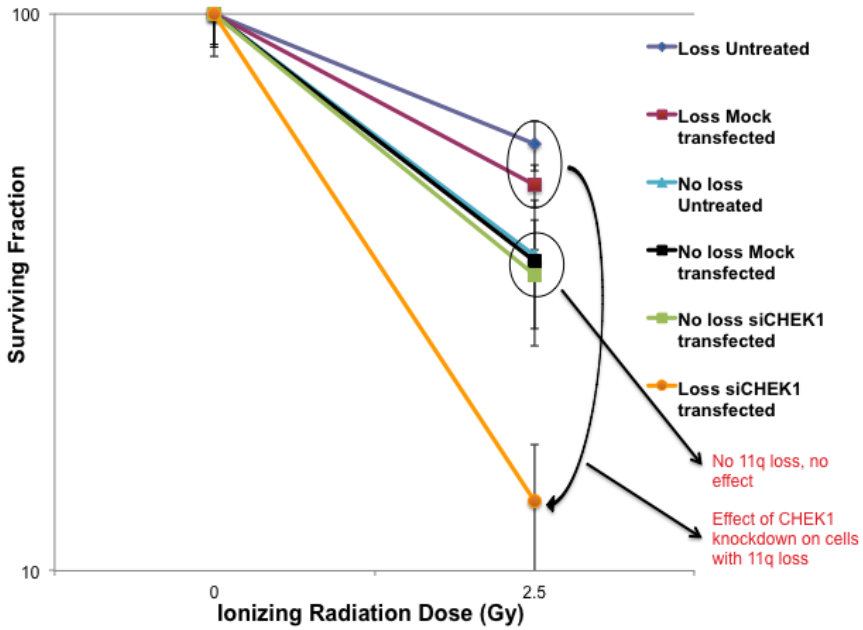

Figure 28. Clonogenic survival assay in response to IR after siRNA-based CHEK1 knockdown in OvC cells

The surviving fraction of cells at 0 and 2.5 Gy IR for the three conditions (untreated, mock-transfected and si*CHEK1*-transfected) is plotted with error bars (± SEM) on a logarithmic scale. OvC cell line, ES-2 (distal 11q loss) transfected with si*CHEK1* showed four-fold decrease in survival compared to the untreated and mock-transfected cells. OvC cell line, A2780 (without distal 11q loss) did not show any significant difference in survival between the three conditions.

3.3.2 A CHEK1 SMI Resensitizes HNSCC Cells to DNA Damage Induced by IR

To advance these studies towards the clinic, we used a potent and specific targeted CHEK1 small molecule inhibitor (SMI), PF-00477736, to inhibit the enzymatic activity of CHEK1 and then assessed the effect of this inhibition on survival. CHEK1 inhibitors are reported to selectively increase the efficacy of IR and other DNA damaging agents in cells with defective G_1 checkpoints (e.g., as a result of defective p53 signaling) while producing minimal damage in cells without G_1 checkpoint defects (Blasina, et al. 2008). Prior to SMI treatment, we tested our cell lines for p53 functionality by treating the cells with the chemotherapeutic agent, Adriamycin and then assessing the protein expression of p53 and its downstream target, p21 by immunoblotting. We identified HNSCC cell lines with loss of distal 11q and defective p53 signaling for our SMI experiments (Table 8). All NSCLC cell lines with loss of distal 11q had effective p53 signaling. Knocking down p53 in these cell lines using siRNA did not produce stable inhibition of p53 signaling and therefore, combined treatment of the SMI and IR could not be assessed in NSCLC cells.

Table 8. p53 signaling status of HNSCC cell lines as determined by analyzing p53 and p21 expression after treatment with Adriamycin

Tumor type	Cell Line	Distal 11q status	p53 signaling status
HNSCC	UPCI:SCC**016**	Loss	+
	UPCI:SCC**029B**	Loss	-
	UPCI:SCC**040**	Loss	-
	UPCI:SCC**066**	No loss	-
	UPCI:SCC**075**	No loss	-
	UPCI:SCC**081**	No loss	+
	UPCI:SCC**084**	Loss	+
	UPCI:SCC**104**	Loss	-
	UPCI:SCC**105**	Loss	-
	UPCI:SCC**114**	Loss	-
	UPCI:SCC**116**	No loss	-
	UPCI:SCC**122**	Loss	+
	UPCI:SCC**125**	Heterogeneous loss	-
	UPCI:SCC**131**	Loss	-
	UPCI:SCC**136**	Loss	+
	UPCI:SCC**142**	Loss	-
	UPCI:SCC**154**	Loss	-
	UPCI:SCC**172**	Loss	-
	UPCI:SCC**182**	No loss	+

PF-00477736 dose response curves generated in HNSCC cell lines in our lab and previous reports (Blasina, et al. 2008) have shown that the optimal dose range required to achieve maximum effect is between 360 and 540 nM. To determine the best time to add the SMI, clonogenic survival assays were carried out after adding the SMI at varying timepoints around the radiation therapy. Addition of the SMI 8h prior to irradiation was determined to have the maximum effect on cell kill (Fig. 29).

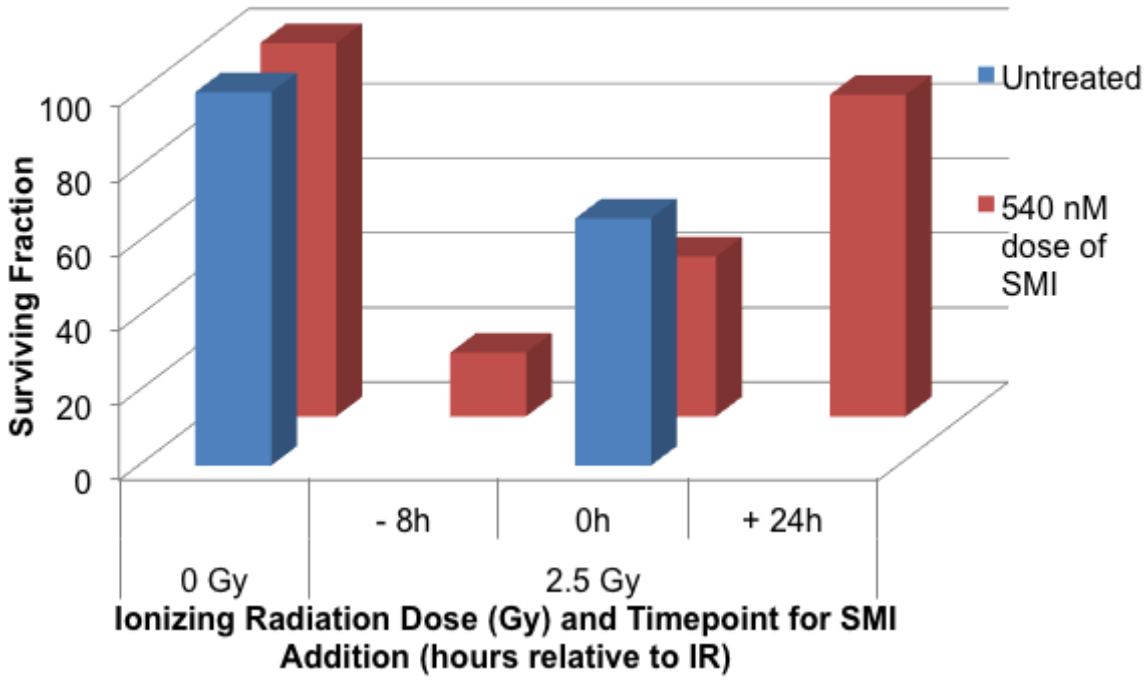

Figure 29. Clonogenic survival assay determining appropriate timepoint for addition of SMI in relation to IR

The surviving fraction of HNSCC cells with distal 11q loss (UPCI:SCC040, 131) treated with 540 nM PF-00477736 at various time-points in relation to IR is plotted. The addition of SMI 8 h prior to IR was found to be most effective.

HNSCC cell lines UPCI:SCC040 and UPCI:SCC131 (both with distal 11q loss and defective p53 signaling) when treated with 540 nM SMI in combination with IR resulted in a two-fold reduction in survival at 2.5 Gy and >four-fold reduction in survival at 5 Gy as compared to cells treated with IR alone (Fig. 30). UPCI:SCC116 (no distal 11q loss and defective p53 signaling) when treated with the same dose of SMI combined with IR showed no difference in survival between the untreated and SMI-treated at 2.5 or 5 Gy. The SMI alone did not have any effect on these cells, but was lethal at 360 nM in UPCI:SCC066 (no distal 11q loss and defective p53 signaling) and hTERT-transfected human OKF6 cells (OKF6-hTERT). Our results indicate that the CHEK1 SMI, PF-00477736 mirrored the effect of the siRNA-based knockdown in HNSCC cell lines.

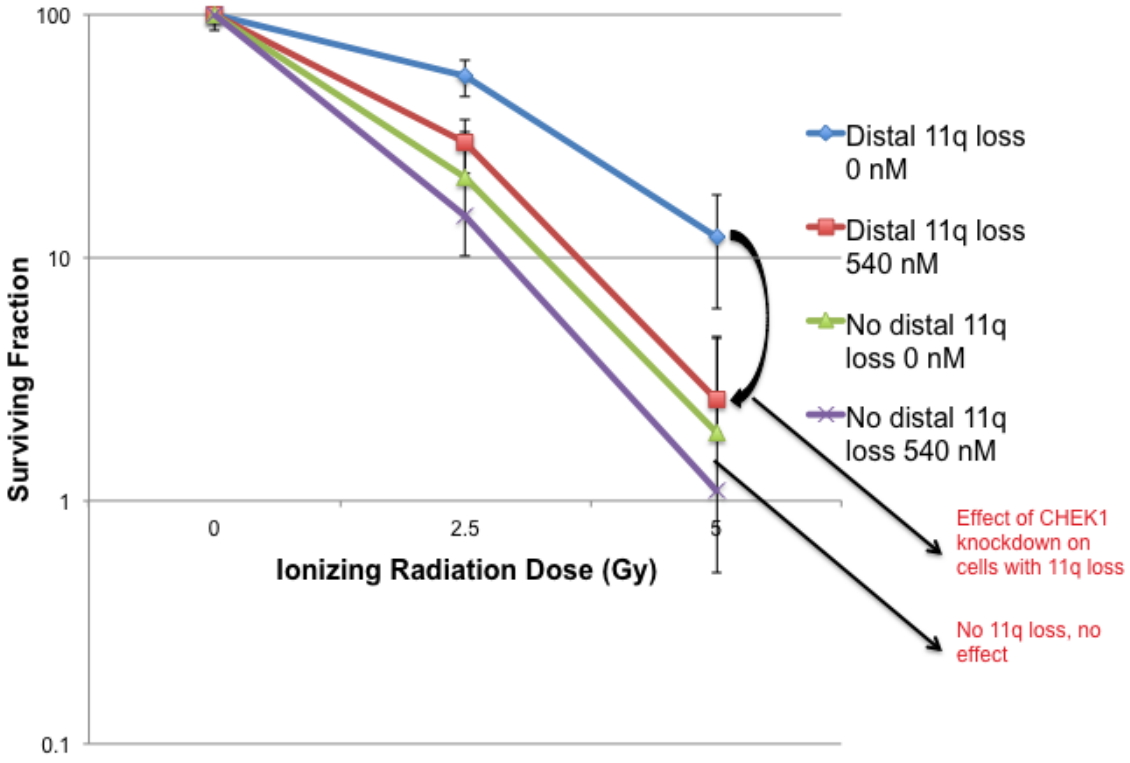

Figure 30. Clonogenic survival assay in response to IR after SMI-based CHEK1 knockdown in HNSCC cells

The surviving fraction of cells at 0 and 2.5 Gy IR for untreated and CHEK1 SMI treated is plotted with error bars (± SEM) on a logarithmic scale. Combined treatment of the SMI and IR in cells with distal 11q loss (UPCI:SCC131 and UPCI:SCC040) showed two-fold decrease in survival at 2.5 Gy and four-fold decrease at 5 Gy compared to cell treated only with IR. In cells without loss of distal 11q (UPCI:SCC116), there was no significant difference in survival at 2.5 or 5 Gy between the combined treatment of SMI and IR, and IR treatment alone.

To assess the effect of active p53 signaling on the efficiency of the SMI, NSCLC cells with loss of distal 11q and effective p53 signaling were treated with 540 nM SMI. There was no observable difference in survival at 2.5 Gy of IR between the untreated and SMI-treated cells. In OvC cell lines, treatment with SMI alone killed 70-80% of cells irrespective of their distal 11q copy number. Due to the lack of NSCLC cell lines with distal 11q loss and defective p53 signaling, and the sensitivity of OvC cell lines to the SMI, conclusive assessment of the relation between loss of distal 11q and SMI-based CHEK1 knockdown could not be made in the cell

lines of these two tumor types. From these studies, we conclude that in HNSCC cells with distal 11q loss the combination of IR and CHEK1 SMI increases the efficacy of IR treatment.

3.4 LOSS OF DISTAL 11Q AND GEMCITABINE RESISTANCE

3.4.1 Distal 11q Loss is Associated with Reduced Sensitivity to Gemcitabine

Sensitivity of the NSCLC, HNSCC and OvC cell lines to the DNA damaging agent, gemcitabine was determined using clonogenic survival assays. The assays were done in triplicate for each cell line and the results were grouped into two: 'Distal 11q loss' and 'No distal 11q loss' as in our IR studies. We generated dose response curves to determine the appropriate dose of gemcitabine to be used. Based on these results, it was determined that 5 and 10 nM doses of gemcitabine were best, as the 25 nM and 50 nM doses killed all cells without distal 11q loss (Fig. 31).

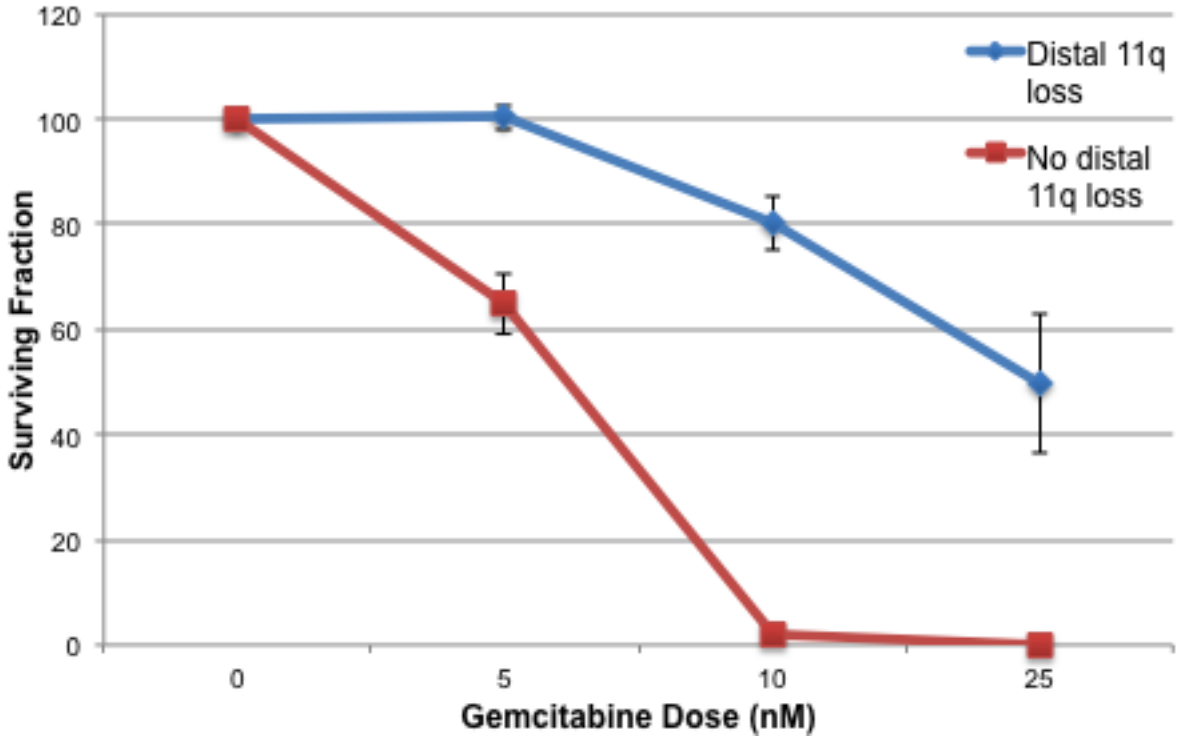

Figure 31. Dose response curve to gemcitabine in NSCLC cells

The surviving fraction of cells at 0, 5 and 10 nM gemcitabine is plotted with error bars (± SEM) on a logarithmic scale. In NSCLC cells without distal 11q loss (CALU-1, 54T, 201T) gemcitabine doses of 10 and 25 nM were lethal.

HNSCC cells in the ‘distal 11q loss’ group (UPCI:SCC029B, 040, 131, 136) showed 97 ± 5% and 82 ± 6% survival at 5 and 10 nM gemcitabine, respectively. HNSCC cells in the ‘no distal 11q loss’ group (UPCI:SCC066, 081, 116) showed 70 ± 6% and 51 ± 10% survival at the same two doses (Fig. 32). NSCLC cells in the ‘distal 11q loss’ group (A549, 101-87T, 253T) showed 99 ± 2% and 75 ± 4% survival at 5 and 10 nM, respectively. The ‘no distal 11q loss’ group (CALU-1, 54T, 201T) showed 54 ± 1% and 21 ± 11% survival at the same two doses (Fig. 33). H1299, an NSCLC cell line without 11q loss showed a high survival rate (57.3%) at 10 nM gemcitabine and therefore, wasn’t included in the earlier results. Three OvC cell lines, A2780 (no distal 11q loss), ES-2 and OVCA432 (both with distal 11q loss) were tested for gemcitabine sensitivity. There was no significant difference observed between the three cell lines at 5 nM (Fig. 34). At 10 nM, OVCA432 showed a much higher survival compared to the other two cell lines. Hence, resistance to gemcitabine treatment seems to be associated with copy number loss of distal 11q genes in HNSCC and NSCLC cell lines, but not in OvC cell lines.

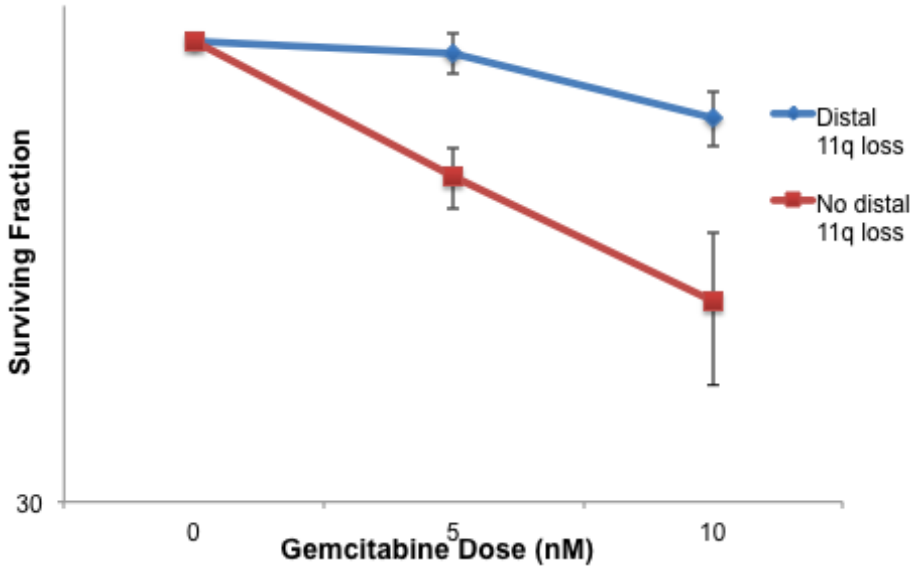

Figure 32. Clonogenic survival assay of HNSCC cell lines in response to gemcitabine treatment

The surviving fraction of cells at specific gemcitabine doses is plotted with error bars (± SEM) on a logarithmic scale. Carcinoma cells in the "distal 11q loss" group (UPCI:SCC029B, 040 and 131) showed increased survival compared to cells in the "no distal 11q loss" group (UPCI:SCC066, 081 and 116).

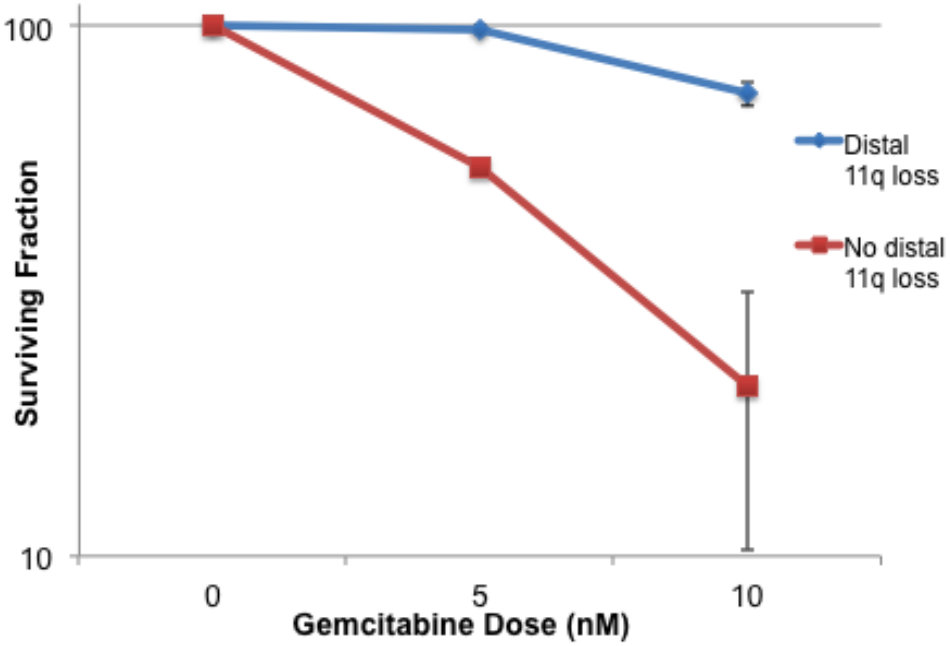

Figure 33. Clonogenic survival assay of NSCLC cell lines in response to gemcitabine treatment

The surviving fraction of cells at specific gemcitabine doses is plotted with error bars (± SEM) on a logarithmic scale. Carcinoma cells in the "distal 11q loss" group (A549, 101-87T, 253T) showed increased survival compared to cells in the "no distal 11q loss" group (CALU-1, 54T, 201T).

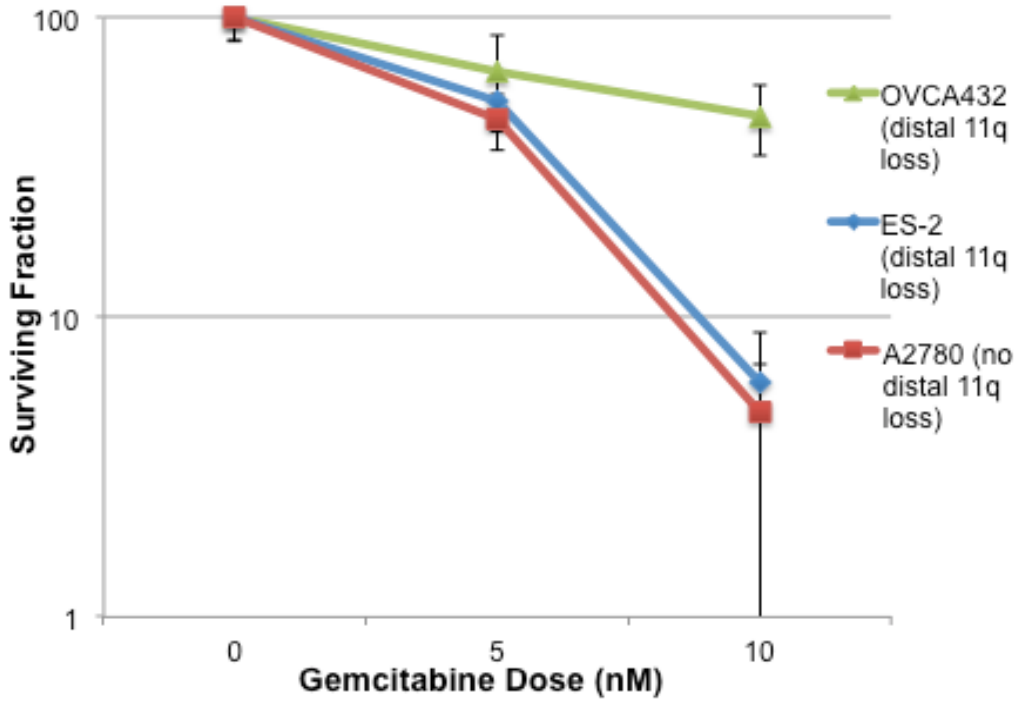

Figure 34. Clonogenic survival assay of OvC cell lines in response to gemcitabine treatment

The surviving fraction of cells at specific gemcitabine doses is plotted with error bars (± SEM) on a logarithmic scale. There was no significant difference in survival between cells with and without distal 11q loss.

3.4.2 The ATR-CHEK1 Pathway is Upregulated in HNSCC and NSCLC Cell Lines

The primary pathway responsible for the DDR to gemcitabine-induced damage is the ATR-CHEK1 pathway (Shi, et al. 2001; Karnitz, et al. 2005). The activity of this pathway was evaluated by examining the protein expression of CHEK1 in response to gemcitabine. The phosphorylation status of ser317 and ser345 on CHEK1 was also examined to assess the efficiency of signaling of the ATR-CHEK1 pathway. HNSCC and NSCLC cell lines, with and without distal 11q loss, when treated with 10 nM gemcitabine showed increased CHEK1 expression 6 h after treatment (Figs. 35 and 36). These results are consistent with reports that the ATR-CHEK1 pathway initiates the DDR to gemcitabine-induced damage in tumor cells.

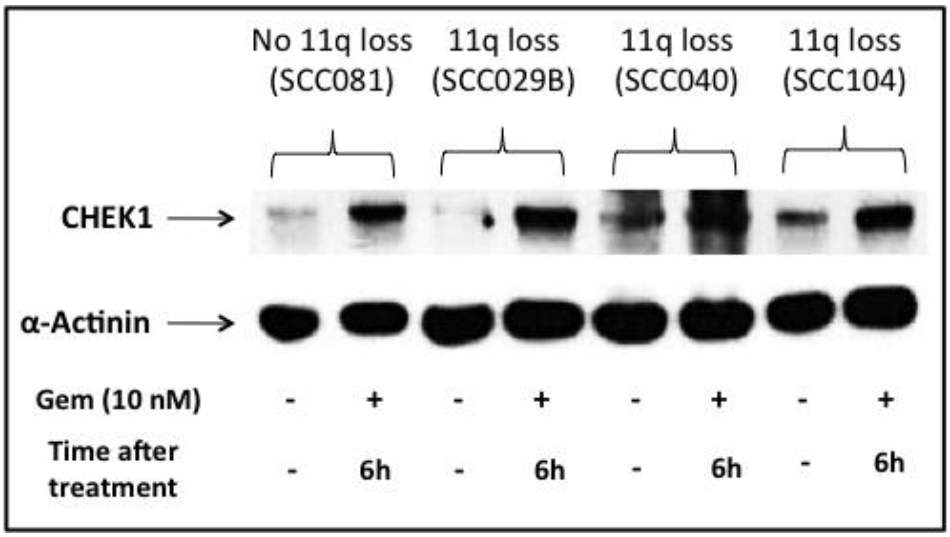

Figure 35. Total CHEK1 expression in response to gemcitabine in UPCI HNSCC cells

Total CHEK1 expression assessed by immunoblotting showed that CHEK1 expression after gemcitabine treatment was increased in HNSCC cells with and without distal 11q loss.

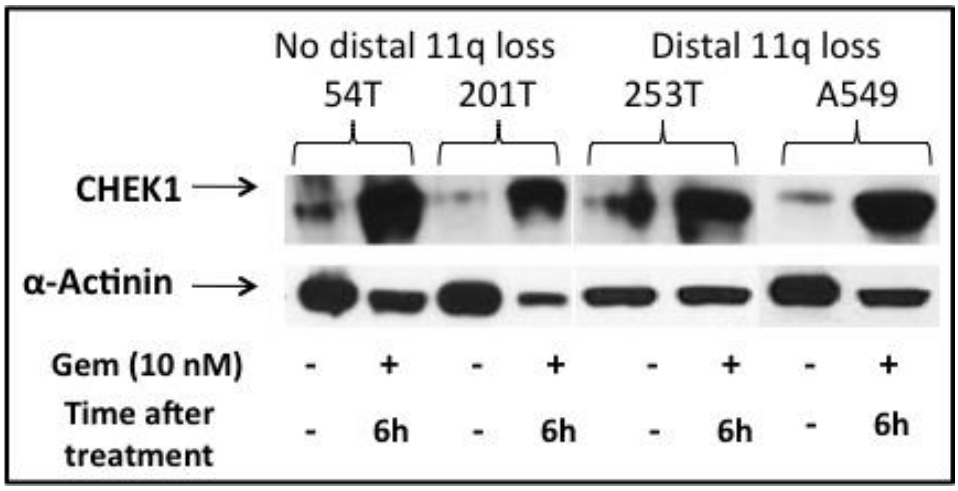

Figure 36. Total CHEK1 expression in response to gemcitabine in NSCLC cells

Total CHEK1 expression assessed by immunoblotting showed that CHEK1 expression after gemcitabine treatment was increased in NSCLC cells with and without distal 11q loss.

To further assess the DDR signaling to gemcitabine by the ATR-CHEK1 pathway, the phosphorylation status of CHEK1 was examined using antibodies against the phosphorylation sites ser345 and ser317. As predicted, HNSCC and NSCLC cells with and without loss of distal 11q showed increased phosphorylation of both ser345 and ser317 sites on CHEK1 after a 6 h treatment with 10 nM gemcitabine (Figs. 37 and 38). There was no significant difference in the

level of phosphorylation between tumor cells with and without loss of distal 11q. These results confirm increased activity of the ATR-CHEK1 pathway in tumor cells with and without loss of distal 11q in response to gemcitabine induced damage. These results suggest that altered ATR-CHEK1 pathway activation is not responsible for the decreased sensitivity to gemcitabine that was observed in tumor cells with distal 11q loss.

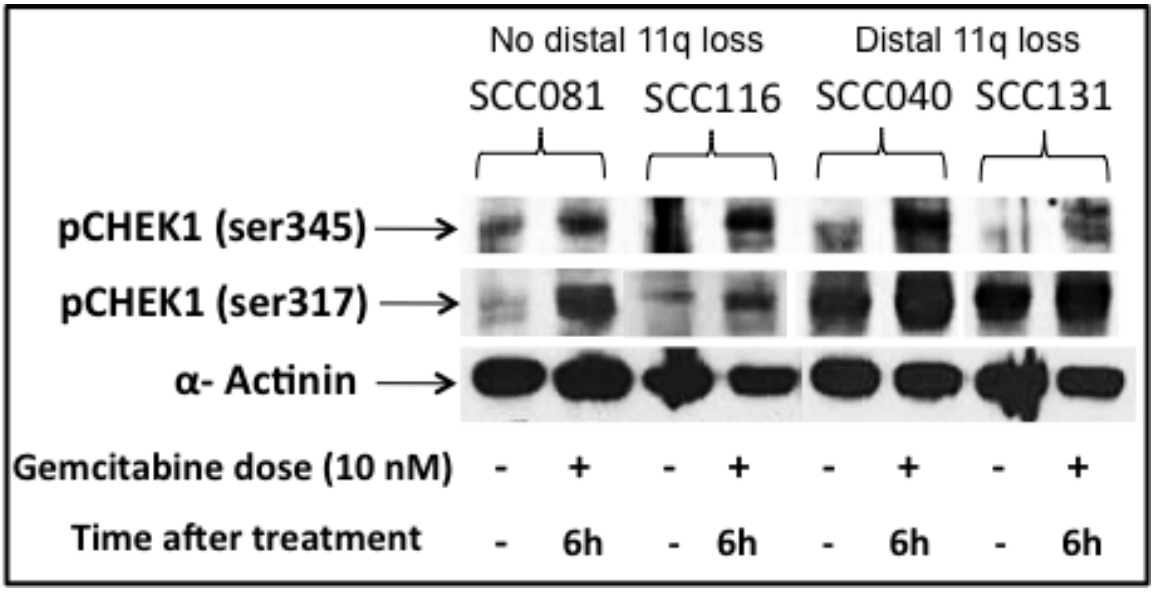

Figure 37. CHEK1 phosphorylation at ser345 and ser317 in response to gemcitabine in HNSCC cells

Immunoblotting for phosphorylated CHEK1 6 h after treatment with 10 nM gemcitabine demonstrates increased phosphorylation of CHEK1 at ser345 at this timepoint in HNSCC and NSCLC cells with and without loss of distal 11q.

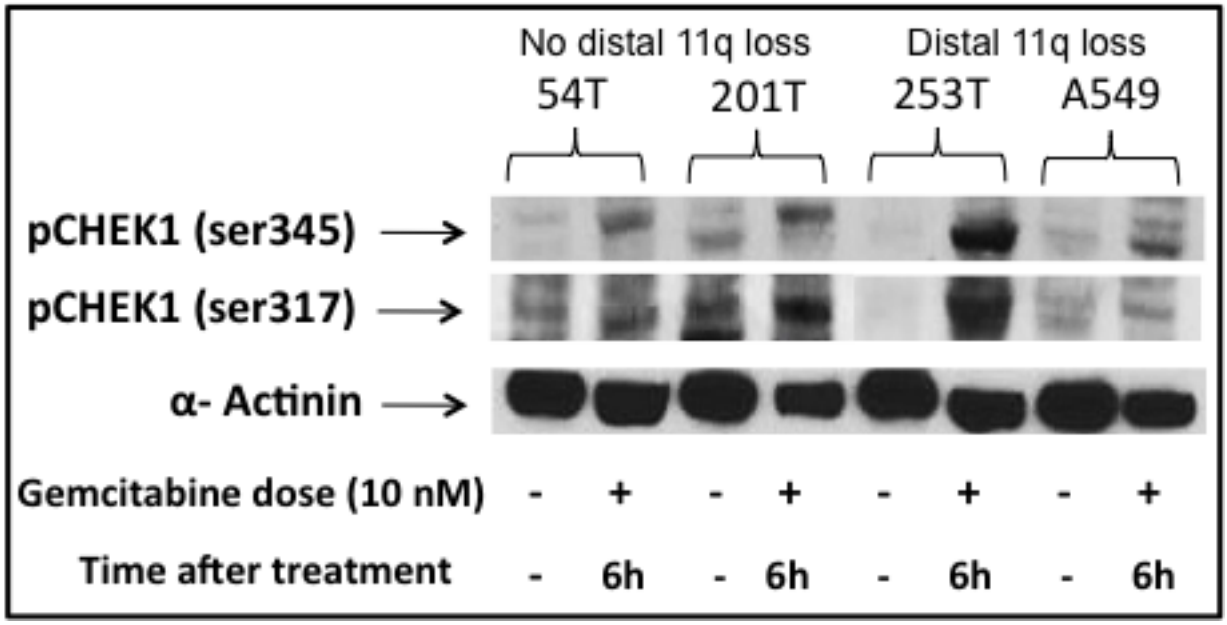

Figure 38. CHEK1 phosphorylation at ser345 and ser317 in response to gemcitabine in NSCLC cells

Immunoblotting for phosphorylated CHEK1 6 h after treatment with 10 nM gemcitabine demonstrates increased phosphorylation of CHEK1 at ser317 at this timepoint in HNSCC and NSCLC cells with and without loss of distal 11q.

3.4.3 Knockdown of the ATR-CHEK1 Pathway with siRNA/SMI Resensitizes Cells with Distal 11q Loss to Damage Induced by Gemcitabine

The effect of *CHEK1* inhibition using siRNA or SMI on resistance to gemcitabine was assessed using clonogenic survival assays. *CHEK1* knockdown with siRNA or SMI in combination with gemcitabine treatment was carried out in a similar to the knockdown experiments with IR. HNSCC cells with loss of distal 11q (UPCI:SCC029B, 040, 131) when treated with siRNA against *CHEK1*, showed decreased survival in response to gemcitabine as compared to 'Untreated' or 'Mock-transfected' cells. Cells in the latter two groups showed a survival of 90 ± 5% and 81 ± 7%, and 92 ± 4% and 82 ± 5% at 5 and 10 nM gemcitabine, respectively (Fig. 39). 'siCHEK1-transfected' cells at the same two concentrations of gemcitabine, showed 57.8±4% and 47.1±2% survival, respectively. Similarly 'Untreated' and 'Mock-transfected' NSCLC cells

with loss of distal 11q (A549, 253T, 101-87T) showed 95 ± 2% and 67 ± 4%, and 88 ± 4% and 59.8±11.6% survival, respectively, at 5 and 10 nM gemcitabine (Fig. 40). 'siCHEK1-transfected' cells at the same two concentrations of gemcitabine showed 48 ± 9% and 28 ± 6% survival. The inhibition of *CHEK1* expression using siRNA-based knockdown resensitized HNSCC and NSCLC cells with loss of distal 11q to gemcitabine. Since the ATR-CHEK1 pathway is responsible for gemcitabine-induced damage response, *CHEK1* knockdown in NSCLC cells without loss of distal 11q also resulted in reduced survival in response to gemcitabine (Fig. 41). CALU-1 showed three-fold reduced survival at 5 nM and 10nM gemcitabine and H1299 showed ~two-fold reduced survival at the same two concentrations of gemcitabine. There was no significant difference in survival between the 'Untreated' and 'Mock-transfected' groups in these two cell lines. Hence, siRNA-based knockdown of *CHEK1*, unlike in combination with IR, did not exclusively resensitize tumor cells with loss of distal 11q to gemcitabine-induced damage. Instead, cells with or without loss of distal 11q showed increased sensitivity to DNA damage induced by gemcitabine.

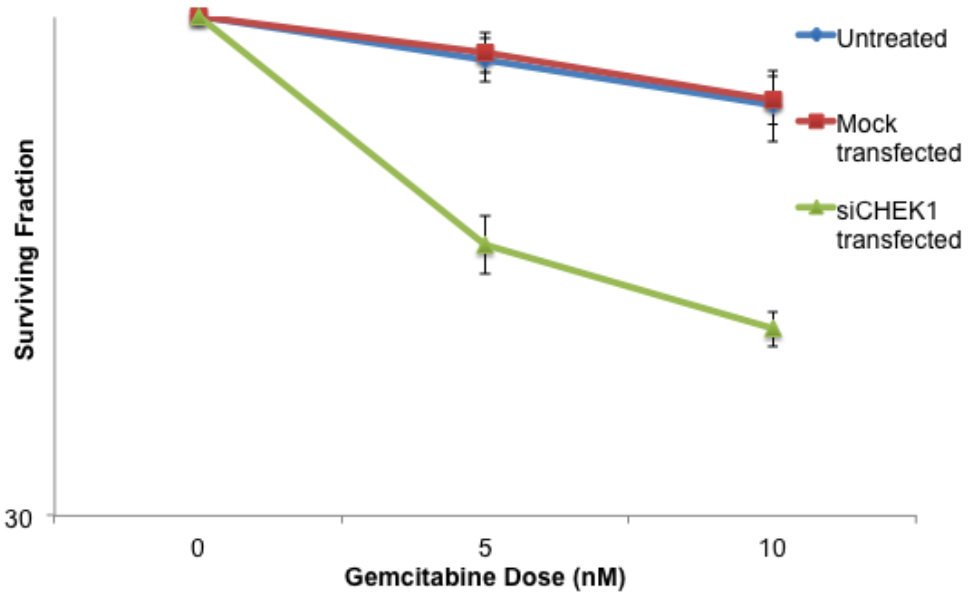

Figure 39. Clonogenic survival assay in response to gemcitabine after siRNA-based *CHEK1* knockdown in HNSCC cells with loss of distal 11q

The surviving fraction of cells at 0, 5 and 10 nM gemcitabine for the three conditions (untreated, mock-transfected and si*CHEK1*-transfected) is plotted with error bars (± SEM) on a logarithmic scale. HNSCC cells transfected with si*CHEK1* in the 'distal 11q loss' group (UPCI:SCC029B, 040, 131) showed two-fold decrease in survival at 5 and 10 nM compared to the untreated and mock-transfected cells.

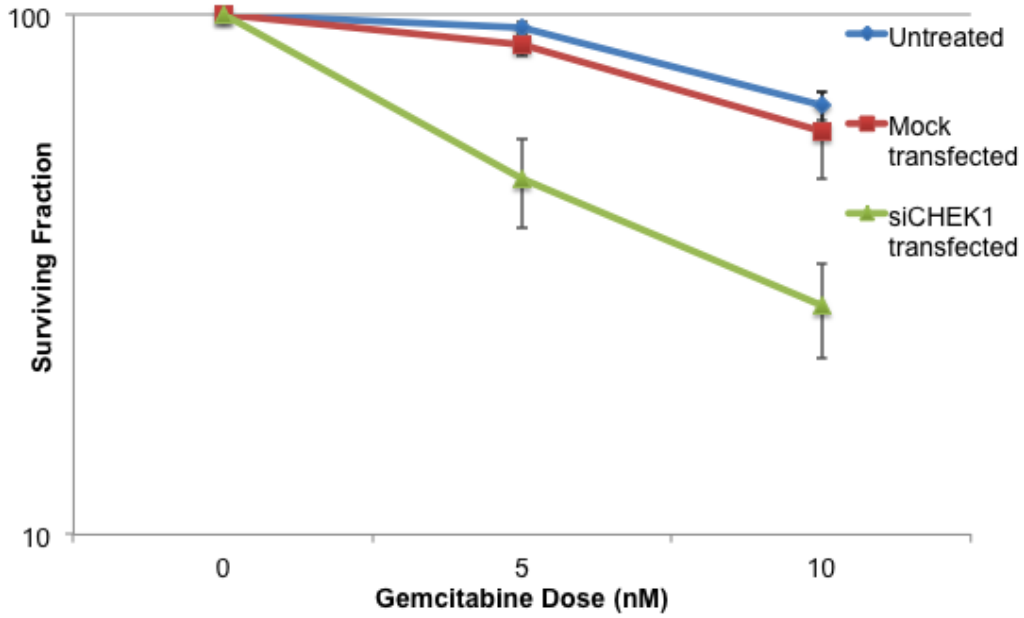

Figure 40. Clonogenic survival assay in response to gemcitabine after siRNA-based *CHEK1* knockdown in NSCLC cells with loss of distal 11q

The surviving fraction of cells at 0, 5 and 10 nM gemcitabine for the three conditions (untreated, mock-transfected and si*CHEK1*-transfected) is plotted with error bars (± SEM) on a logarithmic scale. NSCLC cells transfected with si*CHEK1* in the 'distal 11q loss' group (A549, 101-87T,

253T) showed two-fold decrease in survival at 5 and 10 nM compared to the untreated and mock-transfected cells.

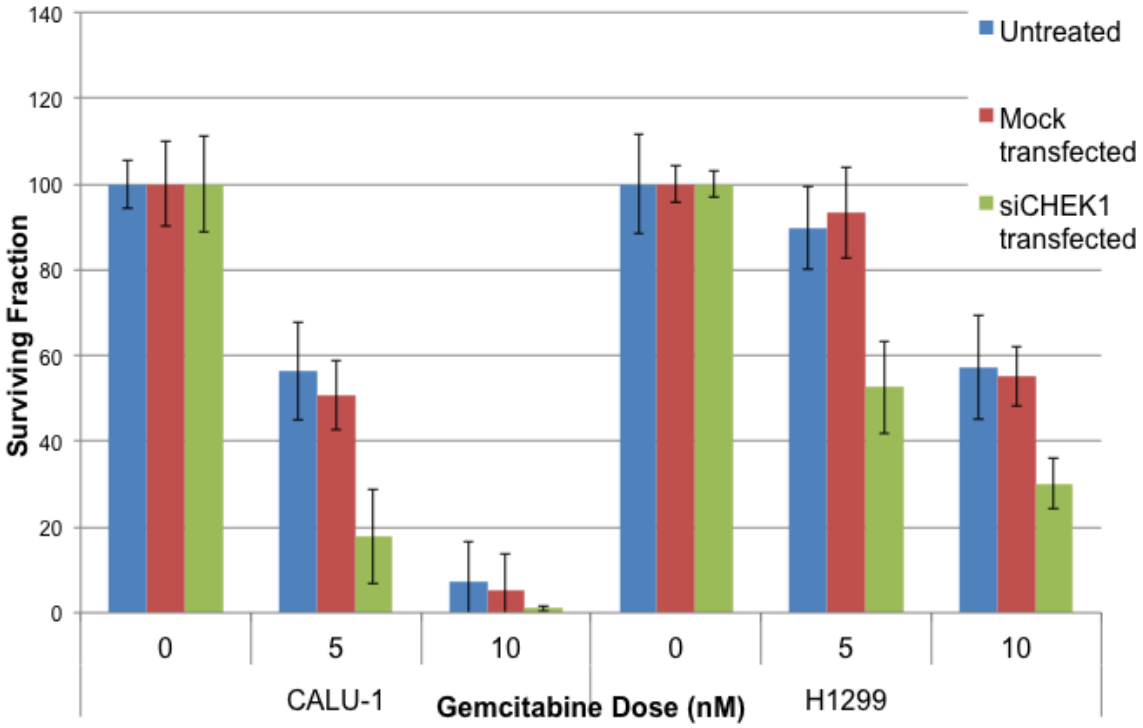

Figure 41. Clonogenic survival assay in response to gemcitabine after siRNA-based *CHEK1* knockdown in NSCLC cells without loss of distal 11q

The surviving fraction of cells at 0, 5 and 10 nM gemcitabine for the three conditions (untreated, mock-transfected and si*CHEK*- transfected) is plotted with error bars (± SEM) on a logarithmic scale. NSCLC cell line, CALU-1 (without distal 11q loss) transfected with si*CHEK1* showed three-fold decrease in survival at 5 and 10 nM compared to the untreated and mock-transfected cells. NSCLC cell line, H1299 (also without distal 11q loss) transfected with si*CHEK1* showed two-fold decrease in survival at 5 and 10 nM compared to the untreated and mock-transfected cells.

To assess the effect of inhibition of the ATR-CHEK1 pathway, *ATR* knockdown using siRNA was also carried out. HNSCC cells with loss of distal 11q showed two-fold decrease in survival at 5 nM gemcitabine and three-fold decrease at 10 nM gemcitabine (Fig. 42). NSCLC cells with loss of distal 11q showed three-fold decrease in survival at 5 nM gemcitabine and six-fold decrease at 10 nM gemcitabine (Fig. 43). NSCLC cells without loss of distal 11q (54T, CALU-1) in response to *ATR* knockdown and gemcitabine treatment showed three-fold decrease in survival at 5 nM gemcitabine and five-fold decrease at 10 nM gemcitabine (Fig. 44). There

was no significant difference in survival between 'Untreated' and 'Mock-transfected' groups in either HNSCC or NSCLC cells. Hence, siRNA-based inhibition of *CHEK1* and *ATR* increased the sensitivity of tumor cells to gemcitabine irrespective of their copy number of distal 11q.

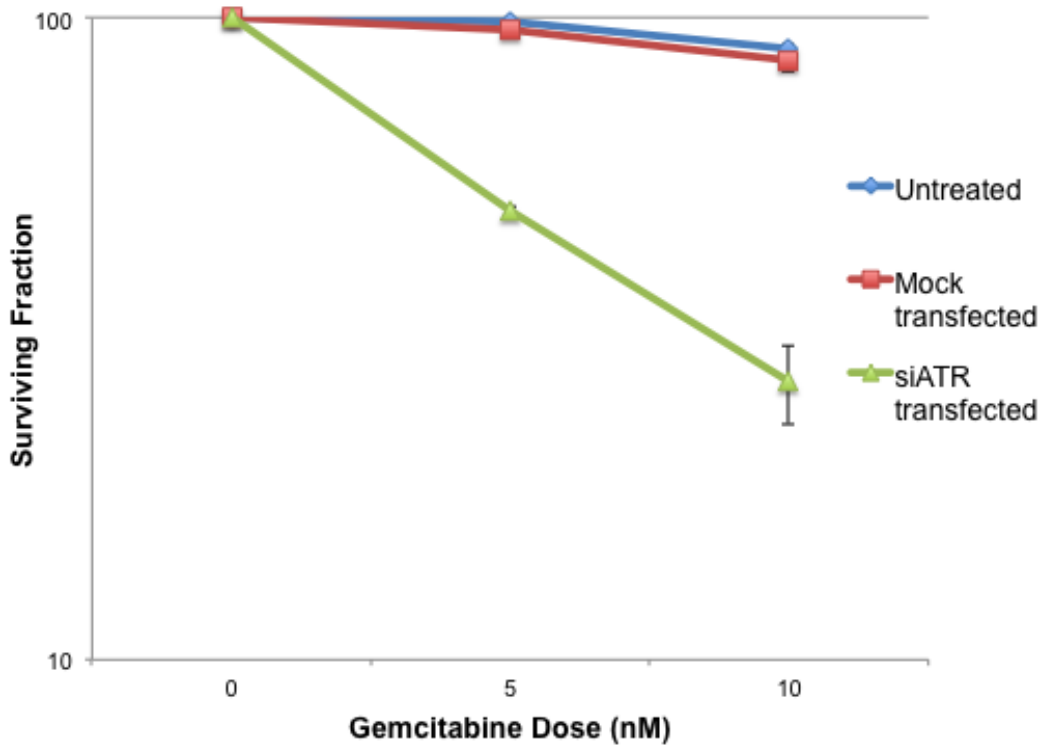

Figure 42. Clonogenic survival assay in response to gemcitabine after siRNA-based *ATR* knockdown in HNSCC cells with loss of distal 11q

The surviving fraction of cells at 0, 5 and 10 nM gemcitabine for the three conditions (untreated, mock-transfected and si*ATR*-transfected) is plotted with error bars (± SEM) on a logarithmic scale. HNSCC cells transfected with si*ATR* in the 'distal 11q loss' group (UPCI:SCC029B, 040, 131) showed two-fold decrease in survival at 5 nM and three-fold decrease at 10 nM compared to the untreated and mock-transfected cells.

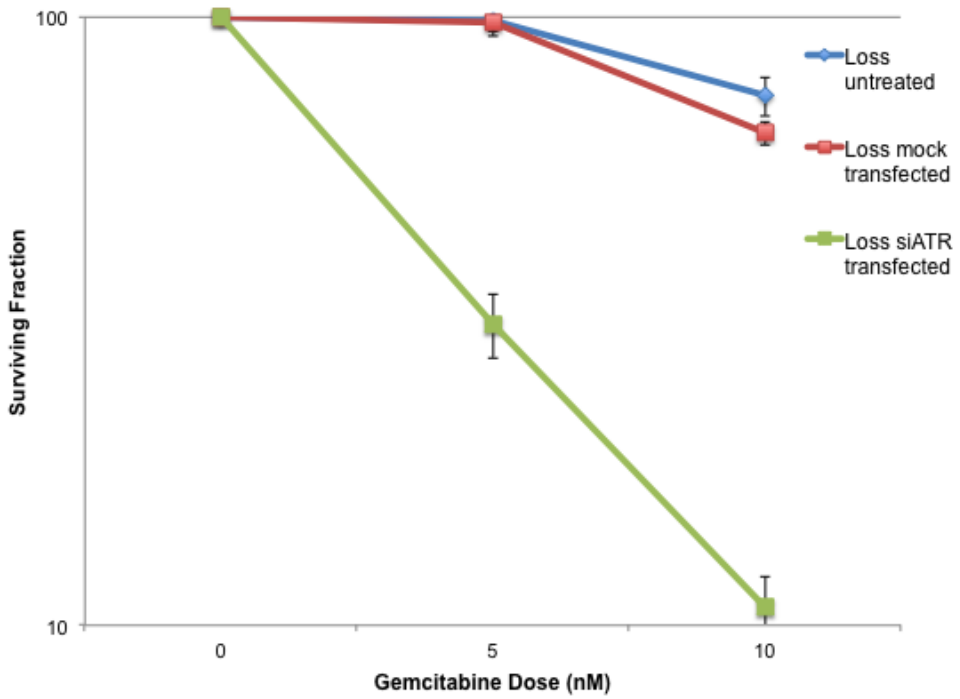

Figure 43. Clonogenic survival assay in response to gemcitabine after siRNA-based *ATR* knockdown in NSCLC cells with loss of distal 11q

The surviving fraction of cells at 0, 5 and 10 nM gemcitabine for the three conditions (untreated, mock-transfected and si*ATR*-transfected) is plotted with error bars (± SEM) on a logarithmic scale. NSCLC cells transfected with si*ATR* in the 'distal 11q loss' group (A549, 101-87T, 253T) showed three-fold decrease in survival at 5 nM and six-fold decrease at 10 nM compared to the untreated and mock-transfected cells.

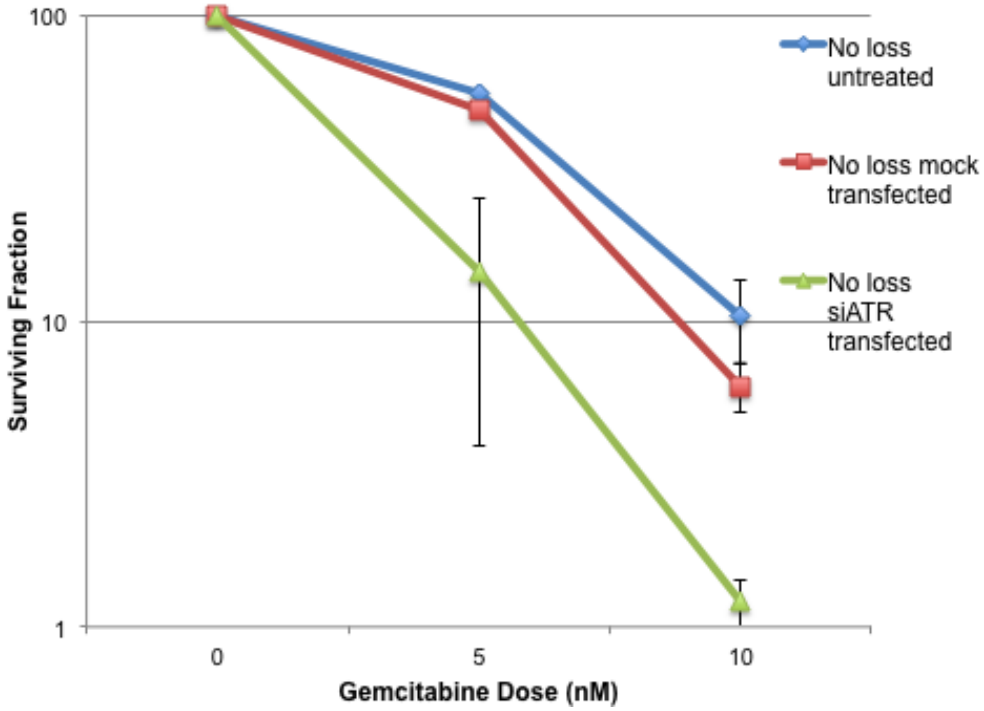

Figure 44. Clonogenic survival assay in response to gemcitabine after siRNA-based *ATR* knockdown in NSCLC cells without loss of distal 11q

The surviving fraction of cells at 0, 5 and 10 nM gemcitabine for the three conditions (untreated, mock-transfected and si*ATR*-transfected) is plotted with error bars (± SEM) on a logarithmic scale. NSCLC cells without distal 11q loss (CALU-1, 54T) showed three-fold decrease in survival at 5 nM and five-fold decrease at 10 nM compared to the untreated and mock-transfected cells.

Next, we treated HNSCC cell lines UPCI:SCC040, UPCI:SCC131 and UPCI:SCC066 with a combination of gemcitabine (5 and 10 nM) and PF-00477736 (360 nM) and evaluated the effect on cell survival. UPCI:SCC040 and UPCI:SCC131 (both with loss of distal 11q), when treated with the combination therapy resulted in approximately a two-fold decrease in survival compared to the cells treated with gemcitabine alone (Fig. 45). UPCI:SCC066 (no distal 11q loss) was highly sensitive to treatment with 360 nM SMI alone (~95% cell kill) and therefore, the effect of the combination therapy could not be assessed. All three OvC cell lines treated with combined therapy of gemcitabine (5 and 10 nM) and CHEK1 SMI (540 nM) showed decreased survival at both concentrations of gemcitabine (Fig. 46). The knockdown of CHEK1 resulted in

three-fold increased sensitivity of OvC cells to gemcitabine. Inhibition of the ATR-CHEK1 pathway either at the RNA or protein level was capable of increasing the sensitivity of HNSCC and NSCLC cells with and without loss of distal 11q to treatment with gemcitabine.

Hence, inhibition of the ATR-CHEK1 pathway either at the RNA or protein level was capable of increasing the sensitivity of HNSCC and NSCLC cells with and without loss of distal 11q to treatment with gemcitabine. These results indicate that the combination of gemcitabine and ATR-CHEK1 pathway disruption increases the efficacy of gemcitabine treatment in tumor cells.

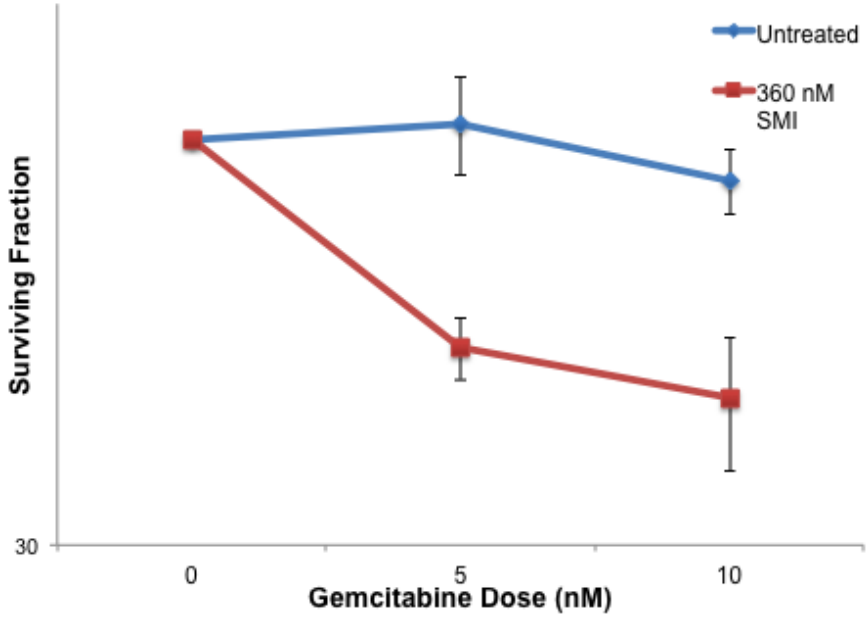

Figure 45. Clonogenic survival assay in response to gemcitabine after SMI-based CHEK1 knockdown in HNSCC cells

The surviving fraction of cells at 0, 5 and 10 nM gemcitabine for untreated and CHEK1 SMI treated is plotted with error bars (± SEM) on a logarithmic scale. Combined treatment of the SMI and IR in cells with distal 11q loss (UPCI:SCC131 and UPCI:SCC040) showed two-fold decrease in survival at 5 and 10 nM gemcitabine compared to cells treated only with gemcitabine.

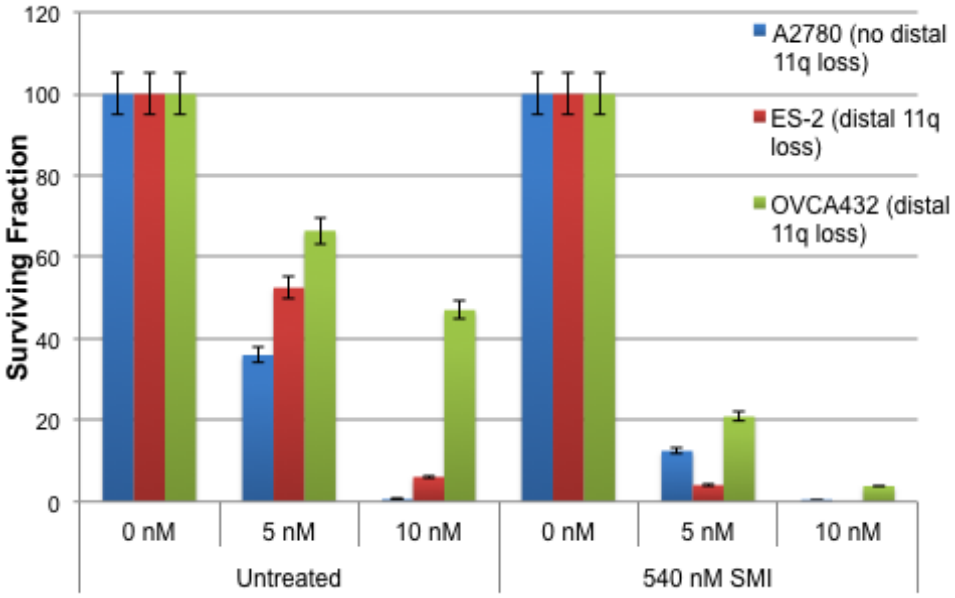

Figure 46. Clonogenic survival assay in response to gemcitabine after SMI-based CHEK1 knockdown in OvC cells

The surviving fraction of cells at 0, 5 and 10 nM gemcitabine for untreated and CHEK1 SMI treated is plotted with error bars (± SEM). Combined treatment of the SMI and IR in cells with (ES-2, OVCA432) and without (A2780) distal 11q loss showed decreased survival at 5 and 10 nM gemcitabine compared to cells treated only with gemcitabine.

4.0 DISCUSSION

4.1 LOSS OF DISTAL 11Q IN CARCINOMA CELLS

Although distal 11q copy number loss from chromosomal band 11q14 to 11qter has been reported in many types of tumors, its significance has not been investigated until our previous study (Parikh, et al. 2007). Our lab showed copy number loss of the region from 11q21 to 11q24 in about 25% of HNSCC, breast and ovarian primary tumors and a high frequency of loss in HNSCC cell lines (Parikh, et al. 2007). Our results showed that 30-35% of HNSCC, NSCLC and OvC cell lines had loss of copy number of the four genes, *MRE11A*, *ATM*, *H2AFX* and *CHEK1*, located on the distal portion of the long arm of chromosome 11. Of the 37 HNSCC cell lines for which FISH results were available for all four genes, 28 cell lines had copy number loss of at least two of the genes. Out of these 28 cell lines, 27 had copy number loss of *ATM* and 23 had copy number loss of *H2AFX*. Hence, copy number loss appears to be centered around chromosomal bands 11q22 to 11q23, in the vicinity of the *ATM* and *H2AFX* genes. In HNSCC cells, The Broad Institute TCGA and Tumorscape websites support our observations, showing *ATM* copy number loss in about 25% of all cancers and frequencies of loss as high as 55% in cutaneous melanomas and 48% in HNSCC. *ATM* copy number loss was also seen in 36% of bladder urothelial carcinomas, 32% of lung squamous cell carcinomas, 30% of ovarian serous cystadenocarcinomas, and between 18 and 28% of lung, stomach and rectal adenocarcinomas,

colorectal cancers, and hepatocellular carcinomas (Beroukhim, et al. 2010). Thus, based on the American Cancer Society statistics (Siegel, et al. 2013) and the *Tumorscape* frequencies, at least 330,000 of the 1,660,290 new cancer cases expected in the U.S. in 2013 may have distal 11q loss. Hence, distal 11q loss is a common defect observed in carcinoma cells. In our study, 30% of cell lines that were included in the 'Distal 11q loss' group had loss of all four genes. The primary mandate for this designation was that one of the genes that had loss of copy number had to be *ATM*. 'No distal 11q loss" group included cell lines that had a relative normal copy number of all four genes.

A number of other important genes are located on distal 11q and may also be lost cells with loss of distal 11q. Some of these genes are important members belonging to the caspase family and several genes involved in the ubiquitination pathway. The caspase pathway genes map to band 11q22.1-22.3 and 11q24.1. These genes include, three members of the caspase family *CASP1, CASP4* and *CASP5* and important regulators of the caspase pathway *BRCC2, CASP12P1, COP1, INCA* and *ICEBERG* (Broustas, et al. 2004). The increased survival of HNSCC, NSCLC and OvC cells with loss of distal 11q after IR may be due to loss of critical members of the caspase pathway and/or important regulators of this pathway. There are also members of the ubiquitination pathway on distal 11q, like *UBE4A* (11q23.3), *USP2* (11q23.3) and *USP28* (11q23.1) and these proteins play an important role in the stability and degradation of various other proteins. Thus, loss of distal 11q may impact the regulation of the ubiquitination pathway and alter the biochemical properties and half–life of different proteins. Since, the four critical DDR genes, *MRE11A, ATM, H2AFX* and *CHEK1*, are primarily involved in the repair and response to DSB and stalled replication forks, the main focus of the study was on the pathways regulated by these genes.

Previous results have shown that loss of distal 11q is associated with resistance to radiation therapy in HNSCC cell lines (Parikh, et al. 2007). The current results confirm and extend this finding in HNSCC cells and show that radioresistance is also associated with loss of distal 11q in NSCLC and OvC cells. AT cells, lacking a functional ATM protein are radiosensitive, whereas cancer cell lines with loss of distal 11q are radioresistant. AT cells do not have functional ATM protein, which is required 1 hour post-irradiation for cell survival (Choi, et al. 2010). Thus, they are radiosensitive. In contrast, tumor cells with distal 11q loss retain some ATM expression and that, based on our results, is sufficient to provide the cells the ability to 'repair' their DSB and survive IR. NSCLC cells with loss of distal 11q survived treatment with 2 Gy IR, five times per week for two weeks, which mimicked the treatment conditions in patients. In contrast, this same treatment was lethal in NSCLC cells without loss of distal 11q. The high frequency of tumors with distal 11q loss could explain the lack of efficacy of IR treatment observed in some cancer patients.

The intrinsic level of chromosomal instability observed in HNSCC cell lines with distal 11q loss is higher compared to normal keratinocytes or HNSCC cells without 11q loss (Parikh, et al. 2007). We also observed an increase in mitotic defects in HNSCC cells with distal 11q loss after treatment with IR compared to tumor cells without loss of distal 11q. Increased chromosomal instability is consistent with a diminished DDR to IR-induced damage in HNSCC cells with distal 11q loss. The DNA repair mechanism responsible for repairing IR-induced damage, especially in the S and G_2M phases of the cell cycle, has been shown to be HRR, confirmed when the effect of ATR and CHEK1 on radiosensitivity was shown to be independent of non-homologous end joining (NHEJ), but dependent on HRR (Wang, et al. 2004; Wang, et al. 2005). Even though HNSCC cells with loss of distal 11q arrest at the G_2M checkpoint after IR,

the observed increased accumulation of mitotic defects suggests repair by an error-prone repair mechanism that enables the cells to progress through mitosis without undergoing mitotic catastrophe. Also, loss of an intact DNA damage response is known to promote a mutator phenotype in somatic cells and leads to chromosomal instability (Gorgoulis, et al. 2005). Thus, the observation that loss of distal 11q leads to increased mitotic defects could contribute to a mutator phenotype effect in tumor cells. The "Mutator Phenotype Hypothesis," proposed by Loeb *et al*., states that cancer cells undergo changes which promote a very high level of background mutations and chromosomal abnormalities (Loeb, et al. 2008). Accumulation of mutations and other chromosomal abnormalities in tumor cells may provide a growth advantage to these cells. In contrast to HNSCC cells, NSCLC cells did not show a significant difference in frequency of mitotic defects. NSCLC cells with distal 11q loss did not have p53 signaling defects that result in loss of the G_1 checkpoint, like in HNSCC cells with distal 11q loss and defective p53 signaling. The presence of the G_1 checkpoint in NSCLC cells might result in the arrest of these cells at the G_1 checkpoint and subsequent repair of DNA. This could explain the lack of increased mitotic defects in NSCLC cells with distal 11q loss.

One of the other consequences of copy number loss of *ATM*, *MRE11A*, *H2AFX* and *CHEK1* is decreased expression of these genes, reduced γH2AX focus formation in response to radiation-induced DSBs, and chromosomal instability in HNSCC cell lines (Parikh, et al. 2007). In NSCLC cell lines, we observed that cells with loss of distal 11q had relatively lower *ATM* and *CHEK1* expression. CHEK1 protein expression in HNSCC and NSCLC cells with loss of distal 11q was also relatively lower than cells without distal 11q loss. Although reduced expression of ATM may be responsible for increased chromosomal instability through defective repair of damaged DNA, the retention of ATM expression provides these cells a survival advantage.

4.2 UPREGULATION OF THE ATR-CHEK1 PATHWAY

Our results showed that distal 11q loss is associated with decreased expression of *MRE11A*, *ATM* and *H2AFX*, which are important components of the ATM-CHEK2 DDR pathway (Parikh, et al. 2007). One might assume that the upregulation in ATR-CHEK1 pathway might be compensating for the decreased functioning of the ATM-CHEK2 pathway. It has been reported that in response to IR-induced DSB, both ATM and the MRN complex act upstream of ATR and CHEK1. ATR and CHEK1 are also involved in the signaling of DSB damage response and repair, but ATM is the primary protein involved in this process. ATR activation and recruitment to nuclear foci is delayed compared to ATM phosphorylation, and requires a functional MRN complex. The ATR-CHEK1 pathway is upregulated in IR-treated AT cells. Hence, a compensatory increase of the ATR-CHEK1 pathway following reduced ATM or MRE11A expression can be anticipated. The report that indicates that ATM expression is required for one hour after IR for cell survival also fits well with our hypothesis that the retention of a lowered ATM expression in our cells with distal 11q loss is responsible for increased survival after IR treatment. This residual ATM expression retained in cells with loss of distal 11q could play a role in the activation and recruitment of ATR, but the upregulated ATR-CHEK1 pathway subsequently initiates DDR. Despite copy number loss of the *CHEK1* gene, CHEK1 expression, especially after IR treatment is increased in tumor cells with distal 11q loss. CHEK1 expression is regulated by E2F transcription factors, and CHEK1 and E2F1 (transcriptional activator) expression are strongly correlated (Verlinden, et al. 2007). It has also been reported that E2F1 levels are higher in HNSCC cell lines from highly invasive tumors (Zhang, et al. 2000), and phosphorylation of E2F1 by ATM and CHEK2 results in protein stabilization (Inoue, et al. 2007). These findings show that transcriptional regulation of the *CHEK1* gene could be responsible for upregulation of

CHEK1 expression in tumor cell lines. This would explain the observed increase in CHEK1 expression in spite of copy number loss in HNSCC cell lines.

In response to IR, CHEK1 is phosphorylated on ser317 in an ATM-dependent manner (Gatei, et al. 2003; Wang, et al. 2012). This phosphorylation is necessary for the ser345 phosphorylation of CHEK1 that results in its activation. The early phosphorylation of ser345 of CHEK1 is ATR-dependent (Wang, et al. 2012), and that increased phosphorylation of ser345 is observed only in cells with distal 11q loss after IR treatment demonstrates upregulation of the ATR-CHEK1 pathway in these cells. In contrast, cells with or without loss of distal 11q have increased ATM-dependent phosphorylation of ser317 on CHEK1. This is consistent with our understanding that ATM expression after IR is required for cell survival.

Activated CHEK1 phosphorylates members of the CDC25 family resulting in their inhibition. We observed increased phosphorylation of CDC25C at ser216 after IR treatment in cells with distal 11q loss. CDC25 phosphatases are known to dephosphorylate cyclin-dependent kinases (CDK), thereby activating them, resulting in cell cycle progression (Uto, et al. 2004). Hence, inhibition of CDC25C phosphatase results in cell cycle arrest at the G_2M checkpoint. Thus, upregulation of the ATR-CHEK1 pathway is likely responsible for the G_2M arrest observed in HNSCC cells with distal 11q loss.

Like AT cells which lack ATM protein and have a compensatory upregulated ATR-CHEK1 pathway and prolonged G_2M arrest (Wang, et al. 2003), we observed upregulation of the ATR-CHEK1 pathway and cell cycle arrest in the S and G_2M phases of the cell cycle after IR in tumor cells with distal 11q loss. S phase arrest prevents replication of unrepaired DNA and the G_2M arrest prevents the entry of cells with DNA damage into mitosis, which would lead to mitotic catastrophe. Instead these cells seem to ‘repair’ the damaged DNA, enabling the cells to

survive, and resulting in decreased sensitivity to IR. The G_1 checkpoint is typically lost in a high percentage of HNSCC cells due to defective p53 signaling after DNA damage. This loss of the G_1 checkpoint in HNSCC leads to an increased number of cells with unrepaired DNA damage entering the S and the G_2M phases of the cell cycle. Upregulation of the ATR-CHEK1 pathway in HNSCC cells with distal 11q loss enhances the G_2M cell cycle checkpoints and these cells may be able to avoid TP53-independent cell death (PCC/MC) (Fragkos and Beard 2011) and may have a survival advantage as demonstrated by radioresistance in these cells. NSCLC cells with loss of distal 11q and an upregulated ATR-CHEK1 pathway did not arrest at G_2M like HNSCC cells. They did show a rapid increase in phosphorylation of CDC25C one hour after treatment with IR and this phosphorylation was reduced 16 hours after irradiation. Since all NSCLC cells with loss of distal 11q retained the G_1 checkpoint, this checkpoint might detect the damage before the G_2M checkpoint. CDC25C phosphorylation is also capable of arresting cells at the G_1 checkpoint and this arrest could also lead to enhanced DNA damage repair. Alternatively, since flow cytometry was done at 24 hours post-IR, the time point used for cell cycle analysis may not have been optimal. It has been reported that ATR overexpression in cancer cells increases the resistance of these cells to DNA damaging agents, like IR and these ATR-overexpressing cells tend to rapidly clear γH2AX foci after IR exposure due to enhanced DNA damage repair (Kim, et al. 2011). Presence of γH2AX foci is indicative of unrepaired DNA damage and rapid clearance would suggest that DNA damage was also rapidly repaired. This could explain the decreased CDC25C phosphorylation that was observed 16 h post-IR treatment in cells with distal 11q loss. To accurately pinpoint the mechanism by which the upregulated ATR-CHEK1 pathway confers a growth advantage on cells with loss of distal 11q, the DNA repair mechanisms used in these cells need to be characterized.

4.3 DNA DSB REPAIR MECHANISMS

DNA DSBs, in which both strands of the DNA are broken, are DNA lesions that if unrepaired could result in the loss of genome stability or cell death. The two DNA repair pathways thought to be involved in repair of double-strand breaks are NHEJ and HRR. NHEJ functions in all phases of the cell cycle; whereas the requirement of a sister chromatid restricts HRR to the S and G_2 phases of the cell cycle. Although inhibition of HRR and NHEJ sensitizes cells to radiation, cells with defective HRR are usually less sensitive to IR than cells with defective NHEJ. This could be attributed to the cell cycle phase limitation of HRR (Thompson 1996; Takagi, et al. 2010; Oike, et al. 2012). The importance of HRR as an IR-induced DSB-repair pathway has been shown by and by the drastic increase in radioresistance observed during late S/G_2 phase (Tamulevicius, et al. 2007). Eukaryotic HRR mutants show a high degree of radiosensitivity in late S/G_2 phase (Tamulevicius, et al. 2007). Since our biomarker-positive cells with *ATM* copy number loss tend to show increased S and late G_2M cell cycle arrest, we hypothesize that the mechanism of DSB repair that enables these cells to survive IR could be HRR. Cell cycle arrest combined with an upregulated ATR-CHEK1 pathway clearly points to possible involvement of HRR. It has been shown that decreased sensitivity to IR-induced DNA damage associated with increased ATR and CHEK1 functioning is independent of NHEJ (Wang, et al. 2004; Wang, et al. 2005). This could point to an ATR-CHEK1-regulated G_2/M checkpoint, facilitating HRR repair, which could protect the cells from IR-induced killing. Recently, however, studies have shown that decreased ATM function results in HRR defects in S-phase and a more prominent G_2 arrest (Kocher, et al. 2012). The HRR defects could be attributed to the requirement of ATM and Artemis for formation of single-stranded DNA (ssDNA) and for loading of RAD51 onto DNA ends (Beucher, et al. 2009). Since our biomarker-positive cells show decreased expression of

ATM, MRE11A and γH2AX, the efficiency of HRR could be compromised. Further, the loading of HRR proteins onto the DNA requires the dissociation of Ku proteins and the MRN complex facilitated by the MRE11 nuclease and CTP1 activity (Langerak, et al. 2011). On the other hand, since we suspect that the biomarker-positive, radioresistant cells may have properties of stem-like cells, the finding that NHEJ is responsible for DNA damage repair in human pleuripotent cells during late G_2 phase (Bogomazova, et al. 2011) points towards the possible choice of NHEJ in our biomarker-positive cells. A third DNA repair pathway gaining significant attention is microhomology-mediated end joining (MMEJ). MMEJ uses a region of DNA sequence homology about 5-25 bp in length to align the broken ends before ligation. This results in deletions flanking the original breakpoint, and hence MMEJ is frequently associated with deletions, translocations and other complex chromosomal abnormalities (Chen, et al. 1998; Welcker, et al. 2000; Yu and Gabriel 2003; Weinstock, et al. 2007). MMEJ is considered a Ku-independent repair mechanism that predominantly occurs in the S and G_2M phases of cell cycle, even in cells with an intact NHEJ pathway (Corneo, et al. 2007; Decottignies 2007; McVey and Lee 2008). Alternatively, Ku80 has been reported to enhance the activity of both NHEJ and MMEJ in response to DSBs, with lesser involvement in the latter (Katsura, et al. 2007). Our analysis of mitotic defects showed that tumor cells with distal 11q loss expressed more micronuclei and increased interphase bridge formation after treatment with IR compared to the tumor cells without distal 11q loss. Micronuclei and interphase bridges are known markers of genotoxic stress and chromosomal instability. This suggests that tumor cells with distal 11q loss use an error prone DNA repair mechanism. Hence, the repair process involved could be a combination of NHEJ and/or MMEJ, depending on the phase of cell cycle. Further studies are

warranted to clarify which of the three DNA repair pathways is responsible for survival of tumor cells with distal 11q loss after IR treatment.

4.4 CHEK1 INHIBITION

Our results show that distal 11q loss is associated with decreased DDR, radioresistance, an upregulated ATR-CHEK1 pathway, and loss of the G_1 checkpoint accompanied by G_2M arrest. Since the ATR-CHEK1 pathway appears to function as a compensatory mechanism for downregulated ATM-CHEK2 pathway, knocking it down with siRNA or a SMI should reverse the observed phenotype. The compensatory effect of the ATR-CHEK1 pathway in cells with loss of distal 11q was confirmed by the resensitization of tumor cells to IR-induced DNA damage after *ATR*, *CHEK1* and *RAD9A* knockdown using siRNA and CHEK1 inhibition using a SMI. The exclusive effect of this knockdown in cells with loss of distal 11q to all three of the genes, *ATR*, *CHEK1* and *RAD9A* points to the role played by the pathway as opposed to an individual protein. Inhibitions of *ATR*, *CHEK1* and *RAD9A* individually were not capable of replicating the radiosensitization effect in cells without loss of distal 11q. Hence, it can be said conclusively that an upregulated ATR-CHEK1 pathway through its regulation of one of the many DDR mechanisms, including control of cell cycle checkpoint, initiation of DNA repair and regulation of cell death, is responsible for the radioresistance phenotype.

Increased cell death observed in HNSCC cells with distal 11q loss appears to be due to synthetic lethality resulting from loss of the G_1 checkpoint and induced loss of the G_2M checkpoint by ATR-CHEK1 knockdown or inhibition. Synthetic lethality after loss of cell cycle checkpoints by CHEK1 inhibition and p53/p21 loss has been described earlier (Origanti, et al. 2013). Synthetic lethality-inducing drugs in the form of targeted CHEK1 SMIs are in clinical trials (NCT 00413686, NCT 00437203, NCT 00779584, NCT 01115790 and NCT 01139775) and several others are being developed (Shaheen, et al. 2011b). UCN-01 (7-hydroxystaurosporine), a potent first generation CHEK1 inhibitor abrogates the G_2M checkpoint

induced by DNA damaging agents (Busby, et al. 2000; Graves, et al. 2000). Another first generation CHEK1 inhibitor, LY2606318 is in clinical trials combined with gemcitabine or pemetrexed in non-small cell lung cancer (NCT01139775). The Merck CHEK1 inhibitor (MK8776/SCH900776) is available from the U.S. National Cancer Institute (NCI) Cancer Therapy Evaluation Program (CTEP) and is reportedly effective in combination with cytarabine in refractory AML (Karp, et al. 2012b; Schenk, et al. 2012b). A selective oral inhibitor is available for licensing from Sareum (Borst, et al. 2012b), and an inhibitor from Novartis (CHIR-124) appears to be an effective HCT-116 colon carcinoma radiosensitizer *in vitro* (Tao, et al. 2009). The inhibitor, AZD7762 has been combined with a variety of standard therapies effectively, but also has shown promise in triple negative breast cancers in combination with ribonucleotide reductase inhibitors (Bennett, et al. 2012). The second generation CHEK1 inhibitor, LY2606368 appears to function effectively as a stand-alone or monotherapy preclinically in cell lines and xenografts (McNeely, et al. 2011). A Lilly clinical trial is evaluating not only safety, toxicity, and dosage, but efficacy in advanced or metastatic cancer, squamous cell cancer of the head & neck or other organ sites (NCT01115790). PF-00477736 appears to be quite effective in sensitizing and killing radioresistant cells in our preclinical model and appears to enhance the antitumor activity of docetaxel (Bucher and Britten 2008). Knockdown of the ATR-CHEK1 pathway using siRNA or the Pfizer CHEK1 inhibitor resulted in resensitization of the cells with distal 11q loss to IR and cell death by mitotic catastrophe. Since CHEK1 inhibitors are being developed by several companies, our results suggest that distal 11q loss may be a useful companion diagnostic biomarker to select the subgroup of HNSCC and NSCLC patients expected to respond to combined radiation therapy and CHEK1 inhibition.

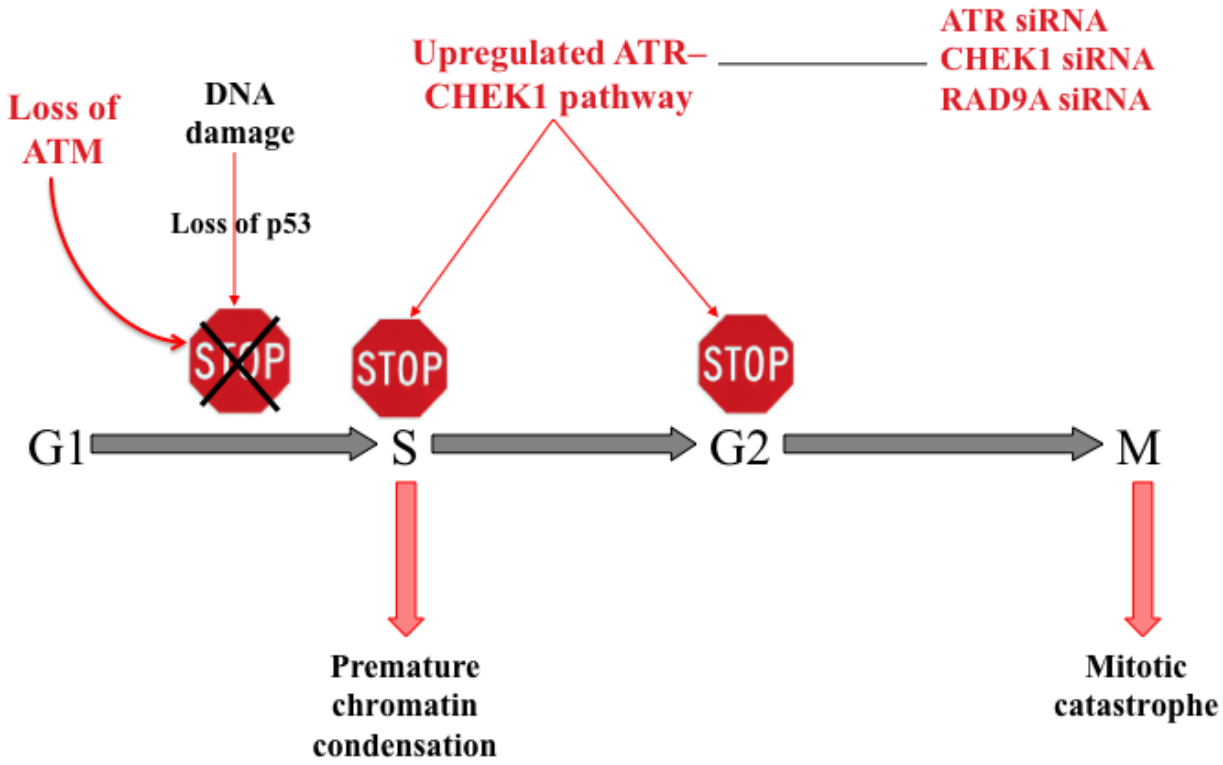

Figure 47. Model for resensitization of tumor cells to DNA damaging agents (adapted from Parikh et al. 2007)

Loss of p53 function combined with loss of ATM leads to loss of the G_1 cell cycle checkpoint in response to DNA damage in tumor cells. An upregulated ATR–CHEK1 pathway enhances the S and G_2M checkpoint arrest following DNA damage and protects cells with DNA damage from premature S phase entry and premature mitosis. Inhibition of the ATR–CHEK1 pathway using specific siRNA or a SMI can result in p53–independent forms of cell death (PCC or MC) in these cells.

4.5 LOSS OF DISTAL 11Q AND RESISTANCE TO GEMCITABINE

Based on our previous results that an upregulated ATR-CHK1 pathway resulted in radioresistance in tumor cells with loss of distal 11q, we hypothesized that an upregulated ATR-CHK1 pathway in tumor cells with distal 11q loss would result in reduced sensitivity to gemcitabine. Further, we hypothesized that knockdown of the ATR-CHK1 pathway would result in the resensitization of these cells to gemcitabine-induced DNA damage and increased tumor cell death. There was a statistically significant difference in survival after gemcitabine treatment between cells with and without loss of distal 11q loss, with the cells with loss of distal 11q showing reduced sensitivity to gemcitabine compared to cells without loss of distal 11q. Activity of the ATR-CHEK1 pathway in cells with loss of distal 11q assessed by total CHEK1 expression and phosphorylation of ser345 and ser317 sites on CHEK1 showed an upregulated ATR-CHEK1 pathway in response to gemcitabine. Cells without loss of distal 11q also showed an upregulated ATR-CHEK1 pathway in response to gemcitabine and a significant difference in ATR-CHEK1 upregulation was not observed between cells with and without loss. Hence, an upregulated ATR-CHEK1 pathway alone could not be responsible for the decreased sensitivity to gemcitabine observed in cells with loss of distal 11q. It has been reported that CHEK1 inhibition resulting in chemosensitization of cells requires inhibition of CHEK1-mediated RAD51 response to gemcitabine-induced replication stress (Parsels, et al. 2009). Also, the DDR to gemcitabine-induced damage requires functional ATM and MRN complex and the deficiency of these proteins increased the sensitivity of cells to gemcitabine (Ewald, et al. 2008). Hence, sensitivity to gemcitabine can be modified by alterations in the DDR and repair pathways in tumor cells. Further studies are warranted to clearly define the mechanism of decreased sensitivity to gemcitabine in tumor cells with loss of distal 11q. We observed that siRNA

knockdown of the ATR-CHEK1 pathway and SMI inhibition of CHEK1 signaling in HNSCC and NSCLC cell lines increase their sensitivity to treatment with gemcitabine. The resensitization to gemcitabine-induced damage by inhibition of the ATR-CHEK1 pathway was observed in cells with and without loss of distal 11q. Therefore, in response to gemcitabine-induced damage, our biomarker is a useful predictive marker of prognosis, as patients with our biomarker would be expected to have a worse prognosis after treatment with gemcitabine. Distal 11q loss could also be used as a companion diagnostic biomarker for inhibition of the ATR-CHEK1 pathway. Tumor cells with loss of distal 11q would require higher doses of gemcitabine in combination with SMI-induced inhibition of the ATR-CHEK1 pathway to attain similar levels of resensitization to gemcitabine treatment as the combination therapy in tumor cells without loss of distal 11q. This would improve the efficacy of gemcitabine in patients with our biomarker.

4.6 CONCLUSIONS

In conclusion, our results have shown that loss of copy number of genes on distal 11q is a common event in carcinoma cell lines and primary tumors. Our results have clearly shown that HNSCC cells with loss of distal 11q have a decreased DDR in response to IR, and HNSCC and NSCLC cells with loss of distal 11q have decreased sensitivity to treatment with IR. The ATR-CHEK1 pathway appears to function as a compensatory pathway and is upregulated in HNSCC and NSCLC cells with loss of distal 11q. In HNSCCs, upregulation of the ATR-CHEK1 pathway results in enhanced G_2M checkpoint control and cells with G_1 checkpoint loss arrest at the G_2M checkpoint. Knockdown of the ATR-CHEK1 pathway results in resensitization to IR. Since inhibition of CHEK1 using SMIs is being developed as a promising anti-tumor therapy, our results have substantial translational value. Distal 11q loss could be used as a biomarker predictive of decreased response to conventional radiation therapy. It could also be developed as a companion diagnostic to determine response to CHEK1 inhibition in combination with radiation or chemotherapy in the treatment of HNSCCs. HNSCC and NSCLC cells with distal 11q loss also show reduced sensitivity to gemcitabine compared to cells without loss of distal 11q. Since the ATR-CHEK1 pathway is primarily involved in DDR to gemcitabine-induced damage, cells with and without loss of distal 11q show upregulation of the ATR-CHEK1 pathway and knockdown of this pathway resensitizes the cells to gemcitabine, cells with distal 11q loss more than those without loss of distal 11q. Therefore, distal 11q loss could be a predictive marker for decreased response to gemcitabine and be used to select an appropriate dosage that will result in maximum efficacy of the combination therapy of gemcitabine and CHEK1 inhibition.

APPENDIX A

LIST OF BACTERIAL ARTIFICIAL CHROMOSOMES (BAC)

Gene name	BAC ID	Fluorescent tag
ATM	CTD2047A4	Spectrum Orange™
CHEK1	RP11-712D22	Spectrum Orange™
CCND1	RP11-699M19	Spectrum Aqua™
H2AFX	RP11-892K21	Spectrum Green™
MRE11A	RP11-685N10	Spectrum Orange™

All BACs used for FISH analysis were purchased from the Children's Hospital Oakland Research Institute (C.H.O.R.I.), Oakland, CA. Centromere enumeration probe for chromosome 11 was purchased from Abbott Molecular Inc., Des Plaines, IL.

APPENDIX B

SEQUENCES FOR ATR AND CHEK1 SIRNA

ATR and CHEK1 siRNAs were obtained from Dharmacon Inc. The individual sequences from the smartpool are outlined below:

ATR sequences:

GAACAACACUGCTGGUUUG	GAAGUCAUCUGUUCAUUAU
GAAAUAAGGUAGACUCAAU	CAACAUAAAUCCAAGAAGA

CHEK1 sequences:

UAAAGUACCACACAUCUUGUU	UAUUGGAUAUUGCCUUUCUU
AUAUGAUCAGGACAUGUGGUU	CCAUUGAUAGCCCAACUUCUU

CHEK1 SMALL MOLECULE INHIBITOR

PF-0077736, a potent, specific CHEK1 small molecule inhibitor (SMI) was a gift from Pfizer, Inc. (Groton, CT).

APPENDIX C

LIST OF ANTIBODIES USED FOR IMMUNOBLOTTING

Antibody	Type	Company	Concentration
Total p53 (D–01)	Mouse monoclonal	Santa Cruz	1:1000
Total p21	Mouse monoclonal	Santa Cruz	1:500
Total CHEK1	Mouse monoclonal	Santa Cruz	1:500
Total MRE11A	Goat polyclonal	Santa Cruz	1:1000
pCHEK1 (Ser317)	Rabbit polyclonal	Cell Signaling	1:1000
pCHEK1 (Ser 345)	Rabbit polyclonal	Cell Signaling	1:1000
pCDC25C(Ser 216)	Rabbit polyclonal	Cell Signaling	1:1000
α- Actinin	Mouse monoclonal	Santa Cruz	1:1000
Actin	Mouse monoclonal	Sigma	1:2000
Tubulin	Rabbit polyclonal	Santa Cruz	1:2000

BIBLIOGRAPHY

Abraham RT. 2001. Cell cycle checkpoint signaling through the ATM and ATR kinases. Genes Dev 15(17):2177-2196.

Abraham RT. 2004. PI 3-kinase related kinases: 'big' players in stress-induced signaling pathways. DNA Repair (Amst) 3(8-9):883-887.

Acilan C, Potter DM, Saunders WS. 2007. DNA repair pathways involved in anaphase bridge formation. Genes Chromosomes Cancer 46(6):522-531.

Adams KE, Medhurst AL, Dart DA, Lakin ND. 2006. Recruitment of ATR to sites of ionising radiation-induced DNA damage requires ATM and components of the MRN protein complex. Oncogene 25(28):3894-3904.

Akervall JA, Michalides RJ, Mineta H, Balm A, Borg A, Dictor MR, Jin Y, Loftus B, Mertens F, Wennerberg JP. 1997. Amplification of cyclin D1 in squamous cell carcinoma of the head and neck and the prognostic value of chromosomal abnormalities and cyclin D1 overexpression. Cancer 79(2):380-389.

Albertson DG. 2006. Gene amplification in cancer. Trends Genet 22(8):447-455.

Albertson DG, Collins C, McCormick F, Gray JW. 2003. Chromosome aberrations in solid tumors. Nat Genet 34(4):369-376.

Ambatipudi S, Gerstung M, Gowda R, Pai P, Borges AM, Schaffer AA, Beerenwinkel N, Mahimkar MB. 2011. Genomic profiling of advanced-stage oral cancers reveals chromosome 11q alterations as markers of poor clinical outcome. PLoS ONE 6(2):e17250.

Bakkenist CJ, Kastan MB. 2003. DNA damage activates ATM through intermolecular autophosphorylation and dimer dissociation. Nature 421(6922):499-506.

Bartek J, Lukas C, Lukas J. 2004. Checking on DNA damage in S phase. Nat Rev Mol Cell Biol 5(10):792-804.

Bennett CN, Tomlinson CC, Michalowski AM, Chu IM, Luger D, Mittereder LR, Aprelikova O, Shou J, Piwinica-Worms H, Caplen NJ, Hollingshead MG, Green JE. 2012. Cross-species genomic and functional analyses identify a combination therapy using a CHK1

inhibitor and a ribonucleotide reductase inhibitor to treat triple-negative breast cancer. Breast Cancer Res 14(4):R109.

Beroukhim R, Mermel CH, Porter D, Wei G, Raychaudhuri S, Donovan J, Barretina J, Boehm JS, Dobson J, Urashima M, Mc Henry KT, Pinchback RM, Ligon AH, Cho YJ, Haery L, Greulich H, Reich M, Winckler W, Lawrence MS, Weir BA, Tanaka KE, Chiang DY, Bass AJ, Loo A, Hoffman C, Prensner J, Liefeld T, Gao Q, Yecies D, Signoretti S, Maher E, Kaye FJ, Sasaki H, Tepper JE, Fletcher JA, Tabernero J, Baselga J, Tsao MS, Demichelis F, Rubin MA, Janne PA, Daly MJ, Nucera C, Levine RL, Ebert BL, Gabriel S, Rustgi AK, Antonescu CR, Ladanyi M, Letai A, Garraway LA, Loda M, Beer DG, True LD, Okamoto A, Pomeroy SL, Singer S, Golub TR, Lander ES, Getz G, Sellers WR, Meyerson M. 2010. The landscape of somatic copy-number alteration across human cancers. Nature 463(7283):899-905.

Beucher A, Birraux J, Tchouandong L, Barton O, Shibata A, Conrad S, Goodarzi AA, Krempler A, Jeggo PA, Lobrich M. 2009. ATM and Artemis promote homologous recombination of radiation-induced DNA double-strand breaks in G2. EMBO J 28(21):3413-3427.

Blasina A, Hallin J, Chen E, Arango ME, Kraynov E, Register J, Grant S, Ninkovic S, Chen P, Nichols T, O'Connor P, Anderes K. 2008. Breaching the DNA damage checkpoint via PF-00477736, a novel small-molecule inhibitor of checkpoint kinase 1. Mol Cancer Ther 7(8):2394-2404.

Bogomazova AN, Lagarkova MA, Tskhovrebova LV, Shutova MV, Kiselev SL. 2011. Error-prone nonhomologous end joining repair operates in human pluripotent stem cells during late G2. Aging (Albany NY) 3(6):584-596.

Borst GR, McLaughlin M, Kyula JN, Neijenhuis S, Khan A, Good J, Zaidi S, Powell NG, Meier P, Collins I, Garrett MD, Verheij M, Harrington KJ. 2012a. Targeted Radiosensitization by the Chk1 Inhibitor SAR-020106. International Journal of Radiation Oncology, Biology, Physics.

Borst GR, McLaughlin M, Kyula JN, Neijenhuis S, Khan A, Good J, Zaidi S, Powell NG, Meier P, Collins I, Garrett MD, Verheij M, Harrington KJ. 2012b. Targeted Radiosensitization by the Chk1 Inhibitor SAR-020106. Int J Radiat Oncol Biol Phys.

Boutros R, Dozier C, Ducommun B. 2006. The when and wheres of CDC25 phosphatases. Curr Opin Cell Biol 18(2):185-191.

Bray F, Ren JS, Masuyer E, Ferlay J. 2013. Global estimates of cancer prevalence for 27 sites in the adult population in 2008. Int J Cancer 132(5):1133-1145.

Broustas CG, Gokhale PC, Rahman A, Dritschilo A, Ahmad I, Kasid U. 2004. BRCC2, a novel BH3-like domain-containing protein, induces apoptosis in a caspase-dependent manner. J Biol Chem 279(25):26780-26788.

Brown EJ, Baltimore D. 2000. ATR disruption leads to chromosomal fragmentation and early embryonic lethality. Genes Dev 14(4):397-402.

Brown EJ, Baltimore D. 2003. Essential and dispensable roles of ATR in cell cycle arrest and genome maintenance. Genes Dev 17(5):615-628.

Brown LA, Kalloger SE, Miller MA, Shih Ie M, McKinney SE, Santos JL, Swenerton K, Spellman PT, Gray J, Gilks CB, Huntsman DG. 2008. Amplification of 11q13 in ovarian carcinoma. Genes Chromosomes Cancer 47(6):481-489.

Bucher N, Britten CD. 2008. G2 checkpoint abrogation and checkpoint kinase-1 targeting in the treatment of cancer. Br J Cancer 98(3):523-528.

Busby EC, Leistritz DF, Abraham RT, Karnitz LM, Sarkaria JN. 2000. The radiosensitizing agent 7-hydroxystaurosporine (UCN-01) inhibits the DNA damage checkpoint kinase hChk1. Cancer Res 60(8):2108-2112.

Byun TS, Pacek M, Yee MC, Walter JC, Cimprich KA. 2005. Functional uncoupling of MCM helicase and DNA polymerase activities activates the ATR-dependent checkpoint. Genes Dev 19(9):1040-1052.

Canman CE, Lim DS, Cimprich KA, Taya Y, Tamai K, Sakaguchi K, Appella E, Kastan MB, Siliciano JD. 1998. Activation of the ATM kinase by ionizing radiation and phosphorylation of p53. Science 281(5383):1677-1679.

Carmichael J. 1998. The role of gemcitabine in the treatment of other tumours. Br J Cancer 78 Suppl 3:21-25.

Cavenee WK, White RL. 1995. The genetic basis of cancer. Sci Am 272(3):72-79.

Chen C, Umezu K, Kolodner RD. 1998. Chromosomal rearrangements occur in S. cerevisiae rfa1 mutator mutants due to mutagenic lesions processed by double-strand-break repair. Mol Cell 2(1):9-22.

Chen M, Hough AM, Lawrence TS. 2000. The role of p53 in gemcitabine-mediated cytotoxicity and radiosensitization. Cancer Chemother Pharmacol 45(5):369-374.

Choi S, Gamper AM, White JS, Bakkenist CJ. 2010. Inhibition of ATM kinase activity does not phenocopy ATM protein disruption: implications for the clinical utility of ATM kinase inhibitors. Cell Cycle 9(20):4052-4057.

Coco Martin JM, Balkenende A, Verschoor T, Lallemand F, Michalides R. 1999. Cyclin D1 overexpression enhances radiation-induced apoptosis and radiosensitivity in a breast tumor cell line. Cancer Res 59(5):1134-1140.

Corneo B, Wendland RL, Deriano L, Cui X, Klein IA, Wong SY, Arnal S, Holub AJ, Weller GR, Pancake BA, Shah S, Brandt VL, Meek K, Roth DB. 2007. Rag mutations reveal robust alternative end joining. Nature 449(7161):483-486.

Cortez D, Guntuku S, Qin J, Elledge SJ. 2001. ATR and ATRIP: partners in checkpoint signaling. Science 294(5547):1713-1716.

Crul M, van Waardenburg RC, Bocxe S, van Eijndhoven MA, Pluim D, Beijnen JH, Schellens JH. 2003. DNA repair mechanisms involved in gemcitabine cytotoxicity and in the interaction between gemcitabine and cisplatin. Biochem Pharmacol 65(2):275-282.

Cuadrado M, Martinez-Pastor B, Murga M, Toledo LI, Gutierrez-Martinez P, Lopez E, Fernandez-Capetillo O. 2006. ATM regulates ATR chromatin loading in response to DNA double-strand breaks. J Exp Med 203(2):297-303.

D'Amours D, Jackson SP. 2002. The Mre11 complex: at the crossroads of dna repair and checkpoint signalling. Nat Rev Mol Cell Biol 3(5):317-327.

de Klein A, Muijtjens M, van Os R, Verhoeven Y, Smit B, Carr AM, Lehmann AR, Hoeijmakers JH. 2000. Targeted disruption of the cell-cycle checkpoint gene ATR leads to early embryonic lethality in mice. Curr Biol 10(8):479-482.

Decottignies A. 2007. Microhomology-mediated end joining in fission yeast is repressed by pku70 and relies on genes involved in homologous recombination. Genetics 176(3):1403-1415.

Derheimer FA, Kastan MB. 2010. Multiple roles of ATM in monitoring and maintaining DNA integrity. FEBS Lett 584(17):3675-3681.

Dickson MA, Hahn WC, Ino Y, Ronfard V, Wu JY, Weinberg RA, Louis DN, Li FP, Rheinwald JG. 2000. Human keratinocytes that express hTERT and also bypass a p16(INK4a)-enforced mechanism that limits life span become immortal yet retain normal growth and differentiation characteristics. Mol Cell Biol 20(4):1436-1447.

Druker BJ, Tamura S, Buchdunger E, Ohno S, Segal GM, Fanning S, Zimmermann J, Lydon NB. 1996. Effects of a selective inhibitor of the Abl tyrosine kinase on the growth of Bcr-Abl positive cells. Nat Med 2(5):561-566.

Edelmann J, Holzmann K, Miller F, Winkler D, Buhler A, Zenz T, Bullinger L, Kuhn MW, Gerhardinger A, Bloehdorn J, Radtke I, Su X, Ma J, Pounds S, Hallek M, Lichter P, Korbel J, Busch R, Mertens D, Downing JR, Stilgenbauer S, Dohner H. 2012. High-resolution genomic profiling of chronic lymphocytic leukemia reveals new recurrent genomic alterations. Blood 120(24):4783-4794.

Elbashir SM, Harborth J, Lendeckel W, Yalcin A, Weber K, Tuschl T. 2001. Duplexes of 21-nucleotide RNAs mediate RNA interference in cultured mammalian cells. Nature 411(6836):494-498.

Ewald B, Sampath D, Plunkett W. 2007. H2AX phosphorylation marks gemcitabine-induced stalled replication forks and their collapse upon S-phase checkpoint abrogation. Mol Cancer Ther 6(4):1239-1248.

Ewald B, Sampath D, Plunkett W. 2008. ATM and the Mre11-Rad50-Nbs1 complex respond to nucleoside analogue-induced stalled replication forks and contribute to drug resistance. Cancer Res 68(19):7947-7955.

Fenech M, Kirsch-Volders M, Natarajan AT, Surralles J, Crott JW, Parry J, Norppa H, Eastmond DA, Tucker JD, Thomas P. 2011. Molecular mechanisms of micronucleus, nucleoplasmic bridge and nuclear bud formation in mammalian and human cells. Mutagenesis 26(1):125-132.

Ferlay J, Shin HR, Bray F, Forman D, Mathers C, Parkin DM. 2010. GLOBOCAN 2008 v1.2, cancer Incidence and Mortality Worldwide: IARC CancerBase No.10. In: Cancer IAfRo, editor. Lyon, France: International Agency for Research on Cancer.

Fernandez-Capetillo O, Lee A, Nussenzweig M, Nussenzweig A. 2004. H2AX: the histone guardian of the genome. DNA Repair (Amst) 3(8-9):959-967.

Ferrari E, Lucca C, Foiani M. 2010. A lethal combination for cancer cells: synthetic lethality screenings for drug discovery. Eur J Cancer 46(16):2889-2895.

Fracchiolla NS, Pruneri G, Pignataro L, Carboni N, Capaccio P, Boletini A, Buffa R, Neri A. 1997. Molecular and immunohistochemical analysis of the bcl-1/cyclin D1 gene in laryngeal squamous cell carcinomas: correlation of protein expression with lymph node metastases and advanced clinical stage. Cancer 79(6):1114-1121.

Fragkos M, Beard P. 2011. Mitotic catastrophe occurs in the absence of apoptosis in p53-null cells with a defective G1 checkpoint. PLoS One 6(8):e22946.

Furgason JM, Bahassi el M. 2013. Targeting DNA repair mechanisms in cancer. Pharmacol Ther 137(3):298-308.

Gagou ME, Zuazua-Villar P, Meuth M. 2010. Enhanced H2AX phosphorylation, DNA replication fork arrest, and cell death in the absence of Chk1. Mol Biol Cell 21(5):739-752.

Galmarini CM, Clarke ML, Falette N, Puisieux A, Mackey JR, Dumontet C. 2002. Expression of a non-functional p53 affects the sensitivity of cancer cells to gemcitabine. Int J Cancer 97(4):439-445.

Garon EB, Finn RS, Hosmer W, Dering J, Ginther C, Adhami S, Kamranpour N, Pitts S, Desai A, Elashoff D, French T, Smith P, Slamon DJ. 2010. Identification of common predictive markers of in vitro response to the Mek inhibitor selumetinib (AZD6244; ARRY-142886) in human breast cancer and non-small cell lung cancer cell lines. Mol Cancer Ther 9(7):1985-1994.

Gatei M, Sloper K, Sorensen C, Syljuasen R, Falck J, Hobson K, Savage K, Lukas J, Zhou BB, Bartek J, Khanna KK. 2003. Ataxia-telangiectasia-mutated (ATM) and NBS1-dependent phosphorylation of Chk1 on Ser-317 in response to ionizing radiation. J Biol Chem 278(17):14806-14811.

Gautschi O, Ratschiller D, Gugger M, Betticher DC, Heighway J. 2007. Cyclin D1 in non-small cell lung cancer: a key driver of malignant transformation. Lung Cancer 55(1):1-14.

George RE, Attiyeh EF, Li S, Moreau LA, Neuberg D, Li C, Fox EA, Meyerson M, Diller L, Fortina P, Look AT, Maris JM. 2007. Genome-wide analysis of neuroblastomas using high-density single nucleotide polymorphism arrays. PLoS One 2(2):e255.

Gibcus JH, Kok K, Menkema L, Hermsen MA, Mastik M, Kluin PM, van der Wal JE, Schuuring E. 2007. High-resolution mapping identifies a commonly amplified 11q13.3 region containing multiple genes flanked by segmental duplications. Hum Genet 121(2):187-201.

Golding SE, Rosenberg E, Valerie N, Hussaini I, Frigerio M, Cockcroft XF, Chong WY, Hummersone M, Rigoreau L, Menear KA, O'Connor MJ, Povirk LF, van Meter T, Valerie K. 2009. Improved ATM kinase inhibitor KU-60019 radiosensitizes glioma cells, compromises insulin, AKT and ERK prosurvival signaling, and inhibits migration and invasion. Mol Cancer Ther 8(10):2894-2902.

Gollin SM. 2001. Chromosomal alterations in squamous cell carcinomas of the head and neck: window to the biology of disease. Head Neck 23(3):238-253.

Gollin SM. 2005. Mechanisms leading to chromosomal instability. Semin Cancer Biol 15(1):33-42.

Gorgoulis VG, Vassiliou LV, Karakaidos P, Zacharatos P, Kotsinas A, Liloglou T, Venere M, Ditullio RA, Jr., Kastrinakis NG, Levy B, Kletsas D, Yoneta A, Herlyn M, Kittas C, Halazonetis TD. 2005. Activation of the DNA damage checkpoint and genomic instability in human precancerous lesions. Nature 434(7035):907-913.

Graves PR, Yu L, Schwarz JK, Gales J, Sausville EA, O'Connor PM, Piwnica-Worms H. 2000. The Chk1 protein kinase and the Cdc25C regulatory pathways are targets of the anticancer agent UCN-01. J Biol Chem 275(8):5600-5605.

Greenman C, Wooster R, Futreal PA, Stratton MR, Easton DF. 2006. Statistical analysis of pathogenicity of somatic mutations in cancer. Genetics 173(4):2187-2198.

Ha PK, Califano JA, 3rd. 2002. The molecular biology of laryngeal cancer. Otolaryngol Clin North Am 35(5):993-1012.

Hanahan D, Weinberg RA. 2000. The hallmarks of cancer. Cell 100(1):57-70.

Hanahan D, Weinberg RA. 2011. Hallmarks of cancer: the next generation. Cell 144(5):646-674.

Harnden DG. 1994. The nature of ataxia-telangiectasia: problems and perspectives. Int J Radiat Biol 66(6 Suppl):S13-19.

Hekmat-Nejad M, You Z, Yee MC, Newport JW, Cimprich KA. 2000. Xenopus ATR is a replication-dependent chromatin-binding protein required for the DNA replication checkpoint. Curr Biol 10(24):1565-1573.

Heron M, Hoyert DL, Murphy SL, Xu J, Kochanek KD, Tejada-Vera B. 2009. Deaths: final data for 2006. Natl Vital Stat Rep 57(14):1-134.

Hirao A, Cheung A, Duncan G, Girard PM, Elia AJ, Wakeham A, Okada H, Sarkissian T, Wong JA, Sakai T, De Stanchina E, Bristow RG, Suda T, Lowe SW, Jeggo PA, Elledge SJ, Mak TW. 2002. Chk2 is a tumor suppressor that regulates apoptosis in both an ataxia telangiectasia mutated (ATM)-dependent and an ATM-independent manner. Mol Cell Biol 22(18):6521-6532.

Hoeijmakers JH. 2009. DNA damage, aging, and cancer. N Engl J Med 361(15):1475-1485.

Hsu LC, Huang X, Seasholtz S, Potter DM, Gollin SM. 2006. Gene amplification and overexpression of protein phosphatase 1alpha in oral squamous cell carcinoma cell lines. Oncogene 25(40):5517-5526.

Huang X, Gollin SM, Raja S, Godfrey TE. 2002. High-resolution mapping of the 11q13 amplicon and identification of a gene, TAOS1, that is amplified and overexpressed in oral cancer cells. Proc Natl Acad Sci U S A 99(17):11369-11374.

Huertas P. 2010. DNA resection in eukaryotes: deciding how to fix the break. Nat Struct Mol Biol 17(1):11-16.

Inoue Y, Kitagawa M, Taya Y. 2007. Phosphorylation of pRB at Ser612 by Chk1/2 leads to a complex between pRB and E2F-1 after DNA damage. EMBO J 26(8):2083-2093.

Izzo JG, Papadimitrakopoulou VA, Li XQ, Ibarguen H, Lee JS, Ro JY, El-Naggar A, Hong WK, Hittelman WN. 1998. Dysregulated cyclin D1 expression early in head and neck tumorigenesis: in vivo evidence for an association with subsequent gene amplification. Oncogene 17(18):2313-2322.

Janku F, Stewart DJ, Kurzrock R. 2010. Targeted therapy in non-small-cell lung cancer--is it becoming a reality? Nat Rev Clin Oncol 7(7):401-414.

Jemal A, Bray F, Center MM, Ferlay J, Ward E, Forman D. 2011. Global cancer statistics. CA Cancer J Clin 61(2):69-90.

Jiang K, Pereira E, Maxfield M, Russell B, Goudelock DM, Sanchez Y. 2003. Regulation of Chk1 includes chromatin association and 14-3-3 binding following phosphorylation on Ser-345. J Biol Chem 278(27):25207-25217.

Jin C, Jin Y, Gisselsson D, Wennerberg J, Wah TS, Stromback B, Kwong YL, Mertens F. 2006. Molecular cytogenetic characterization of the 11q13 amplicon in head and neck squamous cell carcinoma. Cytogenet Genome Res 115(2):99-106.

Jin Y, Hoglund M, Jin C, Martins C, Wennerberg J, Akervall J, Mandahl N, Mitelman F, Mertens F. 1998. FISH characterization of head and neck carcinomas reveals that amplification of band 11q13 is associated with deletion of distal 11q. Genes Chromosomes Cancer 22(4):312-320.

Jin Y, Jin C, Wennerberg J, Hoglund M, Mertens F. 2002. Cyclin D1 amplification in chromosomal band 11q13 is associated with overrepresentation of 3q21-q29 in head and neck carcinomas. Int J Cancer 98(3):475-479.

Karnitz LM, Flatten KS, Wagner JM, Loegering D, Hackbarth JS, Arlander SJ, Vroman BT, Thomas MB, Baek YU, Hopkins KM, Lieberman HB, Chen J, Cliby WA, Kaufmann SH. 2005. Gemcitabine-induced activation of checkpoint signaling pathways that affect tumor cell survival. Mol Pharmacol 68(6):1636-1644.

Karp JE, Thomas BM, Greer JM, Sorge C, Gore SD, Pratz KW, Smith BD, Flatten KS, Peterson K, Schneider P, Mackey K, Freshwater T, Levis MJ, McDevitt MA, Carraway HE, Gladstone DE, Showel MM, Loechner S, Parry DA, Horowitz JA, Isaacs R, Kaufmann SH. 2012a. Phase I and Pharmacologic Trial of Cytosine Arabinoside with the Selective Checkpoint 1 Inhibitor Sch 900776 in Refractory Acute Leukemias. Clinical Cancer Research.

Karp JE, Thomas BM, Greer JM, Sorge C, Gore SD, Pratz KW, Smith BD, Flatten KS, Peterson K, Schneider P, Mackey K, Freshwater T, Levis MJ, McDevitt MA, Carraway HE, Gladstone DE, Showel MM, Loechner S, Parry DA, Horowitz JA, Isaacs R, Kaufmann SH. 2012b. Phase I and pharmacologic trial of cytosine arabinoside with the selective checkpoint 1 inhibitor Sch 900776 in refractory acute leukemias. Clin Cancer Res 18(24):6723-6731.

Kastan MB, Bartek J. 2004. Cell-cycle checkpoints and cancer. Nature 432(7015):316-323.

Kastan MB, Zhan Q, el-Deiry WS, Carrier F, Jacks T, Walsh WV, Plunkett BS, Vogelstein B, Fornace AJ, Jr. 1992. A mammalian cell cycle checkpoint pathway utilizing p53 and GADD45 is defective in ataxia-telangiectasia. Cell 71(4):587-597.

Katsura Y, Sasaki S, Sato M, Yamaoka K, Suzukawa K, Nagasawa T, Yokota J, Kohno T. 2007. Involvement of Ku80 in microhomology-mediated end joining for DNA double-strand breaks in vivo. DNA Repair (Amst) 6(5):639-648.

Keith CT, Schreiber SL. 1995. PIK-related kinases: DNA repair, recombination, and cell cycle checkpoints. Science 270(5233):50-51.

Kim YM, Lee YM, Park SY, Pyo H. 2011. Ataxia telangiectasia and Rad3-related overexpressing cancer cells induce prolonged G(2) arrest and develop resistance to ionizing radiation. DNA Cell Biol 30(4):219-227.

Kinner A, Wu W, Staudt C, Iliakis G. 2008. Gamma-H2AX in recognition and signaling of DNA double-strand breaks in the context of chromatin. Nucleic Acids Res 36(17):5678-5694.

Kitagawa R, Kastan MB. 2005. The ATM-dependent DNA damage signaling pathway. Cold Spring Harb Symp Quant Biol 70:99-109.

Kocher S, Rieckmann T, Rohaly G, Mansour WY, Dikomey E, Dornreiter I, Dahm-Daphi J. 2012. Radiation-induced double-strand breaks require ATM but not Artemis for homologous recombination during S-phase. Nucleic Acids Res.

Langerak P, Mejia-Ramirez E, Limbo O, Russell P. 2011. Release of Ku and MRN from DNA ends by Mre11 nuclease activity and Ctp1 is required for homologous recombination repair of double-strand breaks. PLoS Genet 7(9):e1002271.

Lavin MF, Shiloh Y. 1997. The genetic defect in ataxia-telangiectasia. Annu Rev Immunol 15:177-202.

Levine AJ. 1997. p53, the cellular gatekeeper for growth and division. Cell 88(3):323-331.

Li M, Fang X, Baker DJ, Guo L, Gao X, Wei Z, Han S, van Deursen JM, Zhang P. 2010. The ATM-p53 pathway suppresses aneuploidy-induced tumorigenesis. Proc Natl Acad Sci U S A 107(32):14188-14193.

Liu Q, Guntuku S, Cui XS, Matsuoka S, Cortez D, Tamai K, Luo G, Carattini-Rivera S, DeMayo F, Bradley A, Donehower LA, Elledge SJ. 2000. Chk1 is an essential kinase that is regulated by Atr and required for the G(2)/M DNA damage checkpoint. Genes Dev 14(12):1448-1459.

Loeb LA, Bielas JH, Beckman RA. 2008. Cancers exhibit a mutator phenotype: clinical implications. Cancer Res 68(10):3551-3557; discussion 3557.

Lord CJ, Ashworth A. 2012. The DNA damage response and cancer therapy. Nature 481(7381):287-294.

Lovejoy CA, Cortez D. 2009. Common mechanisms of PIKK regulation. DNA Repair (Amst) 8(9):1004-1008.

Lukas C, Melander F, Stucki M, Falck J, Bekker-Jensen S, Goldberg M, Lerenthal Y, Jackson SP, Bartek J, Lukas J. 2004a. Mdc1 couples DNA double-strand break recognition by Nbs1 with its H2AX-dependent chromatin retention. EMBO J 23(13):2674-2683.

Lukas J, Lukas C. 2013. Molecular biology. Shielding broken DNA for a quick fix. Science 339(6120):652-653.

Lukas J, Lukas C, Bartek J. 2004b. Mammalian cell cycle checkpoints: signalling pathways and their organization in space and time. DNA Repair (Amst) 3(8-9):997-1007.

Lundberg AS, Weinberg RA. 1999. Control of the cell cycle and apoptosis. Eur J Cancer 35(4):531-539.

Ma Z, Yao G, Zhou B, Fan Y, Gao S, Feng X. 2012. The Chk1 inhibitor AZD7762 sensitises p53 mutant breast cancer cells to radiation in vitro and in vivo. Mol Med Report. 6(4):897-903.

Maemondo M, Inoue A, Kobayashi K, Sugawara S, Oizumi S, Isobe H, Gemma A, Harada M, Yoshizawa H, Kinoshita I, Fujita Y, Okinaga S, Hirano H, Yoshimori K, Harada T, Ogura T, Ando M, Miyazawa H, Tanaka T, Saijo Y, Hagiwara K, Morita S, Nukiwa T. 2010. Gefitinib or chemotherapy for non-small-cell lung cancer with mutated EGFR. N Engl J Med 362(25):2380-2388.

Mailand N, Falck J, Lukas C, Syljuasen RG, Welcker M, Bartek J, Lukas J. 2000. Rapid destruction of human Cdc25A in response to DNA damage. Science 288(5470):1425-1429.

Massague J. 2004. G1 cell-cycle control and cancer. Nature 432(7015):298-306.

McNeely S, Burke T, DurlandBusbice S, Barnard D, Marshall M, Bence A. 2011. LY2606368, a second generation Chk1 inhibitor, inhibits growth of ovarian carcinoma xenografts either as monotherapy or in combination with standard-of-care agents. Molecular Cancer Therapeutics 10(11):A108.

McVey M, Lee SE. 2008. MMEJ repair of double-strand breaks (director's cut): deleted sequences and alternative endings. Trends Genet 24(11):529-538.

Merlin T, Brandner G, Hess RD. 1998. Cell cycle arrest in ovarian cancer cell lines does not depend on p53 status upon treatment with cytostatic drugs. Int J Oncol 13(5):1007-1016.

Mermel CH, Schumacher SE, Hill B, Meyerson ML, Beroukhim R, Getz G. 2011. GISTIC2.0 facilitates sensitive and confident localization of the targets of focal somatic copy-number alteration in human cancers. Genome Biol 12(4):R41.

Merry C, Fu K, Wang J, Yeh IJ, Zhang Y. 2010. Targeting the checkpoint kinase Chk1 in cancer therapy. Cell Cycle 9(2):279-283.

Michalides RJ, van de Brekel M, Balm F. 2002. Defects in G1-S cell cycle control in head and neck cancer: a review. Head Neck 24(7):694-704.

Michalides RJ, van Veelen NM, Kristel PM, Hart AA, Loftus BM, Hilgers FJ, Balm AJ. 1997. Overexpression of cyclin D1 indicates a poor prognosis in squamous cell carcinoma of the head and neck. Arch Otolaryngol Head Neck Surg 123(5):497-502.

Mirzoeva OK, Petrini JH. 2003. DNA replication-dependent nuclear dynamics of the Mre11 complex. Mol Cancer Res 1(3):207-218.

Mitchell C, Park M, Eulitt P, Yang C, Yacoub A, Dent P. 2010. Poly(ADP-ribose) polymerase 1 modulates the lethality of CHK1 inhibitors in carcinoma cells. Mol Pharmacol 78(5):909-917.

Miyamoto R, Uzawa N, Nagaoka S, Hirata Y, Amagasa T. 2003. Prognostic significance of cyclin D1 amplification and overexpression in oral squamous cell carcinomas. Oral Oncol 39(6):610-618.

Morgan MA, Parsels LA, Zhao L, Parsels JD, Davis MA, Hassan MC, Arumugarajah S, Hylander-Gans L, Morosini D, Simeone DM, Canman CE, Normolle DP, Zabludoff SD, Maybaum J, Lawrence TS. 2010. Mechanism of radiosensitization by the Chk1/2 inhibitor AZD7762 involves abrogation of the G2 checkpoint and inhibition of homologous recombinational DNA repair. Cancer Res 70(12):4972-4981.

Morgan SE, Kastan MB. 1997. p53 and ATM: cell cycle, cell death, and cancer. Adv Cancer Res 71:1-25.

Myers JS, Cortez D. 2006. Rapid activation of ATR by ionizing radiation requires ATM and Mre11. J Biol Chem 281(14):9346-9350.

Nabhan C, Krett N, Gandhi V, Rosen S. 2001. Gemcitabine in hematologic malignancies. Curr Opin Oncol 13(6):514-521.

Nam EA, Cortez D. 2011. ATR signalling: more than meeting at the fork. Biochem J 436(3):527-536.

Nghiem P, Park PK, Kim Y, Vaziri C, Schreiber SL. 2001. ATR inhibition selectively sensitizes G1 checkpoint-deficient cells to lethal premature chromatin condensation. Proc Natl Acad Sci U S A 98(16):9092-9097.

Niida H, Katsuno Y, Banerjee B, Hande MP, Nakanishi M. 2007. Specific role of Chk1 phosphorylations in cell survival and checkpoint activation. Mol Cell Biol 27(7):2572-2581.

O'Driscoll M, Ruiz-Perez VL, Woods CG, Jeggo PA, Goodship JA. 2003. A splicing mutation affecting expression of ataxia-telangiectasia and Rad3-related protein (ATR) results in Seckel syndrome. Nat Genet 33(4):497-501.

Oike T, Ogiwara H, Torikai K, Nakano T, Yokota J, Kohno T. 2012. Garcinol, a Histone Acetyltransferase Inhibitor, Radiosensitizes Cancer Cells by Inhibiting Non-Homologous End Joining. Int J Radiat Oncol Biol Phys.

Origanti S, Cai SR, Munir AZ, White LS, Piwnica-Worms H. 2013. Synthetic lethality of Chk1 inhibition combined with p53 and/or p21 loss during a DNA damage response in normal and tumor cells. Oncogene 32(5):577-588.

Pan Y, Ren KH, He HW, Shao RG. 2009. Knockdown of Chk1 sensitizes human colon carcinoma HCT116 cells in a p53-dependent manner to lidamycin through abrogation of a G2/M checkpoint and induction of apoptosis. Cancer Biol Ther 8(16):1559-1566.

Pandita TK, Lieberman HB, Lim DS, Dhar S, Zheng W, Taya Y, Kastan MB. 2000. Ionizing radiation activates the ATM kinase throughout the cell cycle. Oncogene 19(11):1386-1391.

Pandita TK, Westphal CH, Anger M, Sawant SG, Geard CR, Pandita RK, Scherthan H. 1999. Atm inactivation results in aberrant telomere clustering during meiotic prophase. Mol Cell Biol 19(7):5096-5105.

Parikh RA, White JS, Huang X, Schoppy DW, Baysal BE, Baskaran R, Bakkenist CJ, Saunders WS, Hsu LC, Romkes M, Gollin SM. 2007. Loss of distal 11q is associated with DNA repair deficiency and reduced sensitivity to ionizing radiation in head and neck squamous cell carcinoma. Genes Chromosomes Cancer 46(8):761-775.

Parrilla-Castellar ER, Arlander SJ, Karnitz L. 2004. Dial 9-1-1 for DNA damage: the Rad9-Hus1-Rad1 (9-1-1) clamp complex. DNA Repair (Amst) 3(8-9):1009-1014.

Parsels LA, Morgan MA, Tanska DM, Parsels JD, Palmer BD, Booth RJ, Denny WA, Canman CE, Kraker AJ, Lawrence TS, Maybaum J. 2009. Gemcitabine sensitization by checkpoint kinase 1 inhibition correlates with inhibition of a Rad51 DNA damage response in pancreatic cancer cells. Mol Cancer Ther 8(1):45-54.

Peasland A, Wang LZ, Rowling E, Kyle S, Chen T, Hopkins A, Cliby WA, Sarkaria J, Beale G, Edmondson RJ, Curtin NJ. 2011. Identification and evaluation of a potent novel ATR inhibitor, NU6027, in breast and ovarian cancer cell lines. Br J Cancer 105(3):372-381.

Plunkett W, Huang P, Searcy CE, Gandhi V. 1996. Gemcitabine: preclinical pharmacology and mechanisms of action. Semin Oncol 23(5 Suppl 10):3-15.

Reaper PM, Griffiths MR, Long JM, Charrier JD, Maccormick S, Charlton PA, Golec JM, Pollard JR. 2011. Selective killing of ATM- or p53-deficient cancer cells through inhibition of ATR. Nat Chem Biol 7(7):428-430.

Reshmi SC, Roychoudhury S, Yu Z, Feingold E, Potter D, Saunders WS, Gollin SM. 2007. Inverted duplication pattern in anaphase bridges confirms the breakage-fusion-bridge (BFB) cycle model for 11q13 amplification. Cytogenet Genome Res 116(1-2):46-52.

Riballo E, Kuhne M, Rief N, Doherty A, Smith GC, Recio MJ, Reis C, Dahm K, Fricke A, Krempler A, Parker AR, Jackson SP, Gennery A, Jeggo PA, Lobrich M. 2004. A pathway of double-strand break rejoining dependent upon ATM, Artemis, and proteins locating to gamma-H2AX foci. Mol Cell 16(5):715-724.

Rieger J, Durka S, Streffer J, Dichgans J, Weller M. 1999. Gemcitabine cytotoxicity of human malignant glioma cells: modulation by antioxidants, BCL-2 and dexamethasone. Eur J Pharmacol 365(2-3):301-308.

Riesterer O, Matsumoto F, Wang L, Pickett J, Molkentine D, Giri U, Milas L, Raju U. 2011. A novel Chk inhibitor, XL-844, increases human cancer cell radiosensitivity through promotion of mitotic catastrophe. Investigational New Drugs 29(3):514-522.

Rotman G, Shiloh Y. 1998. ATM: from gene to function. Hum Mol Genet 7(10):1555-1563.

Sanchez Y, Wong C, Thoma RS, Richman R, Wu Z, Piwnica-Worms H, Elledge SJ. 1997. Conservation of the Chk1 checkpoint pathway in mammals: linkage of DNA damage to Cdk regulation through Cdc25. Science 277(5331):1497-1501.

Savitsky K, Bar-Shira A, Gilad S, Rotman G, Ziv Y, Vanagaite L, Tagle DA, Smith S, Uziel T, Sfez S, Ashkenazi M, Pecker I, Frydman M, Harnik R, Patanjali SR, Simmons A, Clines GA, Sartiel A, Gatti RA, Chessa L, Sanal O, Lavin MF, Jaspers NG, Taylor AM, Arlett CF, Miki T, Weissman SM, Lovett M, Collins FS, Shiloh Y. 1995. A single ataxia telangiectasia gene with a product similar to PI-3 kinase. Science 268(5218):1749-1753.

Saxena N, Lahiri SS, Hambarde S, Tripathi RP. 2008. RAS: target for cancer therapy. Cancer Invest 26(9):948-955.

Schenk EL, Koh BD, Flatten KS, Peterson KL, Parry D, Hess AD, Smith BD, Karp JE, Karnitz LM, Kaufmann SH. 2012a. Effects of Selective Checkpoint Kinase 1 Inhibition on Cytarabine Cytotoxicity in Acute Myelogenous Leukemia Cells In Vitro. Clinical Cancer Research 18(19):5364-5373.

Schenk EL, Koh BD, Flatten KS, Peterson KL, Parry D, Hess AD, Smith BD, Karp JE, Karnitz LM, Kaufmann SH. 2012b. Effects of selective checkpoint kinase 1 inhibition on cytarabine cytotoxicity in acute myelogenous leukemia cells in vitro. Clin Cancer Res 18(19):5364-5373.

Schraml P, Kononen J, Bubendorf L, Moch H, Bissig H, Nocito A, Mihatsch MJ, Kallioniemi OP, Sauter G. 1999. Tissue microarrays for gene amplification surveys in many different tumor types. Clin Cancer Res 5(8):1966-1975.

Shaheen M, Allen C, Nickoloff JA, Hromas R. 2011a. Synthetic lethality: exploiting the addiction of cancer to DNA repair. Blood 117(23):6074-6082.

Shaheen M, Allen C, Nickoloff JA, Hromas R. 2011b. Synthetic lethality: exploiting the addiction of cancer to DNA repair. Blood 117(23):6074-6082.

Sharma SV, Bell DW, Settleman J, Haber DA. 2007. Epidermal growth factor receptor mutations in lung cancer. Nat Rev Cancer 7(3):169-181.

Shi Z, Azuma A, Sampath D, Li YX, Huang P, Plunkett W. 2001. S-Phase arrest by nucleoside analogues and abrogation of survival without cell cycle progression by 7-hydroxystaurosporine. Cancer Res 61(3):1065-1072.

Shiloh Y. 1995. Ataxia-telangiectasia: closer to unraveling the mystery. Eur J Hum Genet 3(2):116-138.

Shiloh Y. 2003. ATM and related protein kinases: safeguarding genome integrity. Nat Rev Cancer 3(3):155-168.

Shiloh Y. 2006. The ATM-mediated DNA-damage response: taking shape. Trends Biochem Sci 31(7):402-410.

Shiloh Y, Lehmann AR. 2004. Maintaining integrity. Nat Cell Biol 6(10):923-928.

Shuster MI, Han L, Le Beau MM, Davis E, Sawicki M, Lese CM, Park NH, Colicelli J, Gollin SM. 2000. A consistent pattern of RIN1 rearrangements in oral squamous cell carcinoma cell lines supports a breakage-fusion-bridge cycle model for 11q13 amplification. Genes Chromosomes Cancer 28(2):153-163.

Siegel R, Naishadham D, Jemal A. 2012. Cancer statistics, 2012. CA Cancer J Clin 62(1):10-29.

Siegel R, Naishadham D, Jemal A. 2013. Cancer statistics, 2013. CA Cancer J Clin 63(1):11-30.

Smalley KS. 2010. PLX-4032, a small-molecule B-Raf inhibitor for the potential treatment of malignant melanoma. Curr Opin Investig Drugs 11(6):699-706.

Solit DB, Garraway LA, Pratilas CA, Sawai A, Getz G, Basso A, Ye Q, Lobo JM, She Y, Osman I, Golub TR, Sebolt-Leopold J, Sellers WR, Rosen N. 2006. BRAF mutation predicts sensitivity to MEK inhibition. Nature 439(7074):358-362.

Sorensen CS, Syljuasen RG, Falck J, Schroeder T, Ronnstrand L, Khanna KK, Zhou BB, Bartek J, Lukas J. 2003. Chk1 regulates the S phase checkpoint by coupling the physiological turnover and ionizing radiation-induced accelerated proteolysis of Cdc25A. Cancer Cell 3(3):247-258.

Stracker TH, Theunissen JW, Morales M, Petrini JH. 2004. The Mre11 complex and the metabolism of chromosome breaks: the importance of communicating and holding things together. DNA Repair (Amst) 3(8-9):845-854.

Stucki M, Clapperton JA, Mohammad D, Yaffe MB, Smerdon SJ, Jackson SP. 2005. MDC1 directly binds phosphorylated histone H2AX to regulate cellular responses to DNA double-strand breaks. Cell 123(7):1213-1226.

Stucki M, Jackson SP. 2004. MDC1/NFBD1: a key regulator of the DNA damage response in higher eukaryotes. DNA Repair (Amst) 3(8-9):953-957.

Swarts DR, Claessen SM, Jonkers YM, van Suylen RJ, Dingemans AM, de Herder WW, de Krijger RR, Smit EF, Thunnissen FB, Seldenrijk CA, Vink A, Perren A, Ramaekers FC, Speel EJ. 2011. Deletions of 11q22.3-q25 are associated with atypical lung carcinoids and poor clinical outcome. Am J Pathol 179(3):1129-1137.

Takagi M, Sakata K, Someya M, Tauchi H, Iijima K, Matsumoto Y, Torigoe T, Takahashi A, Hareyama M, Fukushima M. 2010. Gimeracil sensitizes cells to radiation via inhibition of homologous recombination. Radiother Oncol 96(2):259-266.

Tamulevicius P, Wang M, Iliakis G. 2007. Homology-directed repair is required for the development of radioresistance during S phase: interplay between double-strand break repair and checkpoint response. Radiat Res 167(1):1-11.

Tao Y, Leteur C, Yang C, Zhang P, Castedo M, Pierre A, Golsteyn RM, Bourhis J, Kroemer G, Deutsch E. 2009. Radiosensitization by Chir-124, a selective CHK1 inhibitor: effects of p53 and cell cycle checkpoints. Cell Cycle 8(8):1196-1205.

Thompson LH. 1996. Evidence that mammalian cells possess homologous recombinational repair pathways. Mutat Res 363(2):77-88.

Tibbetts RS, Brumbaugh KM, Williams JM, Sarkaria JN, Cliby WA, Shieh SY, Taya Y, Prives C, Abraham RT. 1999. A role for ATR in the DNA damage-induced phosphorylation of p53. Genes Dev 13(2):152-157.

Uto K, Inoue D, Shimuta K, Nakajo N, Sagata N. 2004. Chk1, but not Chk2, inhibits Cdc25 phosphatases by a novel common mechanism. EMBO J 23(16):3386-3396.

Uziel T, Lerenthal Y, Moyal L, Andegeko Y, Mittelman L, Shiloh Y. 2003. Requirement of the MRN complex for ATM activation by DNA damage. EMBO J 22(20):5612-5621.

Venkatesha VA, Parsels LA, Parsels JD, Zhao L, Zabludoff SD, Simeone DM, Maybaum J, Lawrence TS, Morgan MA. 2012. Sensitization of pancreatic cancer stem cells to gemcitabine by Chk1 inhibition. Neoplasia 14(6):519–525.

Verlinden L, Vanden Bempt I, Eelen G, Drijkoningen M, Verlinden I, Marchal K, De Wolf-Peeters C, Christiaens MR, Michiels L, Bouillon R, Verstuyf A. 2007. The E2F-regulated gene Chk1 is highly expressed in triple-negative estrogen receptor /progesterone receptor /HER-2 breast carcinomas. Cancer Res 67(14):6574-6581.

Wang H, Hu B, Liu R, Wang Y. 2005. CHK1 affecting cell radiosensitivity is independent of non-homologous end joining. Cell Cycle 4(2):300-303.

Wang H, Powell SN, Iliakis G, Wang Y. 2004. ATR affecting cell radiosensitivity is dependent on homologous recombination repair but independent of nonhomologous end joining. Cancer Res 64(19):7139-7143.

Wang J, Han X, Zhang Y. 2012. Autoregulatory mechanisms of phosphorylation of checkpoint kinase 1. Cancer Res 72(15):3786-3794.

Wang X, Khadpe J, Hu B, Iliakis G, Wang Y. 2003. An overactivated ATR/CHK1 pathway is responsible for the prolonged G2 accumulation in irradiated AT cells. J Biol Chem 278(33):30869-30874.

Ward IM, Chen J. 2001. Histone H2AX is phosphorylated in an ATR-dependent manner in response to replicational stress. J Biol Chem 276(51):47759-47762.

Ward IM, Wu X, Chen J. 2001. Threonine 68 of Chk2 is phosphorylated at sites of DNA strand breaks. J Biol Chem 276(51):47755-47758.

Warmerdam DO, Kanaar R. 2010. Dealing with DNA damage: relationships between checkpoint and repair pathways. Mutat Res 704(1-3):2-11.

Weinberg RA. 1996. How cancer arises. Sci Am 275(3):62-70.

Weinstock DM, Brunet E, Jasin M. 2007. Formation of NHEJ-derived reciprocal chromosomal translocations does not require Ku70. Nat Cell Biol 9(8):978-981.

Welcker AJ, de Montigny J, Potier S, Souciet JL. 2000. Involvement of very short DNA tandem repeats and the influence of the RAD52 gene on the occurrence of deletions in Saccharomyces cerevisiae. Genetics 156(2):549-557.

White JS, Choi S, Bakkenist CJ. 2008. Irreversible chromosome damage accumulates rapidly in the absence of ATM kinase activity. Cell Cycle 7(9):1277-1284.

White JS, Weissfeld JL, Ragin CC, Rossie KM, Martin CL, Shuster M, Ishwad CS, Law JC, Myers EN, Johnson JT, Gollin SM. 2007. The influence of clinical and demographic risk factors on the establishment of head and neck squamous cell carcinoma cell lines. Oral Oncol 43(7):701-712.

Wilkerson PM, Reis-Filho JS. 2013. the 11q13-q14 amplicon: Clinicopathological correlations and potential drivers. Genes Chromosomes Cancer 52(4):333-355.

Wilsker D, Petermann E, Helleday T, Bunz F. 2008. Essential function of Chk1 can be uncoupled from DNA damage checkpoint and replication control. Proc Natl Acad Sci U S A 105(52):20752-20757.

Yoo SS, Carter D, Turner BC, Sasaki CT, Son YH, Wilson LD, Glazer PM, Haffty BG. 2000. Prognostic significance of cyclin D1 protein levels in early-stage larynx cancer treated with primary radiation. Int J Cancer 90(1):22-28.

Yu X, Gabriel A. 2003. Ku-dependent and Ku-independent end-joining pathways lead to chromosomal rearrangements during double-strand break repair in Saccharomyces cerevisiae. Genetics 163(3):843-856.

Zabludoff SD, Deng C, Grondine MR, Sheehy AM, Ashwell S, Caleb BL, Green S, Haye HR, Horn CL, Janetka JW, Liu D, Mouchet E, Ready S, Rosenthal JL, Queva C, Schwartz GK, Taylor KJ, Tse AN, Walker GE, White AM. 2008. AZD7762, a novel checkpoint kinase inhibitor, drives checkpoint abrogation and potentiates DNA-targeted therapies. Mol Cancer Ther 7(9):2955-2966.

Zhang SY, Liu SC, Johnson DG, Klein-Szanto AJ. 2000. E2F-1 gene transfer enhances invasiveness of human head and neck carcinoma cell lines. Cancer Res 60(21):5972-5976.

Zou L, Elledge SJ. 2003. Sensing DNA damage through ATRIP recognition of RPA-ssDNA complexes. Science 300(5625):1542-1548.